

UNCLASSIFIED
AD 437575

DEFENSE DOCUMENTATION CENTER
FOR
SCIENTIFIC AND TECHNICAL INFORMATION
CAMERON STATION, ALEXANDRIA, VIRGINIA



UNCLASSIFIED

NOTICE: When government or other drawings, specifications or other data are used for any purpose other than in connection with a definitely related government procurement operation, the U. S. Government thereby incurs no responsibility, nor any obligation whatsoever; and the fact that the Government may have formulated, furnished, or in any way supplied the said drawings, specifications, or other data is not to be regarded by implication or otherwise as in any manner licensing the holder or any other person or corporation, or conveying any rights or permission to manufacture, use or sell any patented invention that may in any way be related thereto.

64-12

437575

AMRL-TDR-64-20

437575

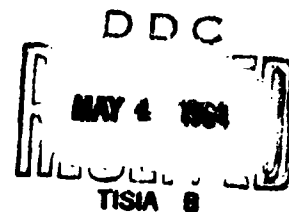
**A THEORETICAL STUDY OF SPACE EQUIVALENT
THERMAL CONDITIONS AND THEIR APPLICABILITY**

TECHNICAL DOCUMENTARY REPORT No. AMRL-TDR-64-20

MARCH 1964

BIOMEDICAL LABORATORY
AEROSPACE MEDICAL RESEARCH LABORATORIES
AEROSPACE MEDICAL DIVISION
AIR FORCE SYSTEMS COMMAND
WRIGHT-PATTERSON AIR FORCE BASE, OHIO

Contract Monitor: W. C. Kaufman, Maj, USAF
Project No. 7164, Task No. 716409



(Prepared under Contract No. AF 33(657)-11346 by
T. A. Auxier

Wenner-Gren Aeronautical Research Laboratory
Kentucky Research Foundation, University of Kentucky)

NOTICES

When US Government drawings, specifications, or other data are used for any purpose other than a definitely related government procurement operation, the government thereby incurs no responsibility nor any obligation whatsoever; and the fact that the government may have formulated, furnished, or in any way supplied the said drawings, specifications, or other data is not to be regarded by implication or otherwise, as in any manner licensing the holder or any other person or corporation, or conveying any rights or permission to manufacture, use, or sell any patented invention that may in any way be related thereto.

Qualified requesters may obtain copies from the Defense Documentation Center (DDC), Cameron Station, Alexandria, Virginia. Orders will be expedited if placed through the librarian or other person designated to request documents from DDC (formerly ASTIA).

Do not return this copy. Retain or destroy.

Stock quantities available at Office of Technical Services, Department of Commerce, Washington 25, D. C. Price per copy is \$2.50.

Change of Address

Organizations receiving reports via the 6570th Aerospace Medical Research Laboratories automatic mailing lists should submit the addressograph plate stamp on the report envelope or refer to the code number when corresponding about change of address.

FOREWORD

This study was initiated by the Biomedical Laboratory of the 6570th Aerospace Medical Research Laboratories, Aerospace Medical Division, Wright-Patterson Air Force Base, Ohio. The research was conducted by the Wenner-Gren Aeronautical Research Laboratory, University of Kentucky, Lexington, Kentucky under Contract No. AF 33(657-11346). Mr. T. A. Auxier, Research Associate, was the principal investigator for the Wenner-Gren Aeronautical Research Laboratory. Major W. C. Kaufman of the Biophysics Branch, Biomedical Laboratory, 6570th Aerospace Medical Research Laboratories was the contract monitor. The work was performed in support of Project No. 7164 and Task No. 716409, was started in May 1963 and was completed in January 1964.

The author acknowledges the help and suggestions of Dr. James F. Thorpe, Professor, Department of Mechanical Engineering, University of Kentucky; and Mr. A. W. Mayne, Jr., student assistant.

ABSTRACT

Radiation heat transfer calculations are made for a cylindrical model of a 50th percentile "suited" space man in 7 space configurations: (1) deep space probe, (2) a point 136 miles from the bright side of the moon, (3) a point 136 miles from the surface of the dark side of the moon, (4) a point 500 miles from the surface of the bright side of the earth, (5) a point 500 miles from the surface of the dark side of the earth, (6) a 500 mile circular earth orbit and (7) a 136 mile circular moon orbit. Similarly, radiation heat transfer calculations are made for the same space man model in four hypothetical chamber configurations I, II, III and IV. The space results are superimposed on the chamber results in order to determine equivalent temperatures for simulating the given space conditions. For instance, depending on the space suit absorptance, the required chamber III temperature for simulating the deep space probe can vary from 260 R to 1150 R. With these results the capabilities of the AMRL thermal chamber for simulating any one of the seven space configurations are determined.

PUBLICATION REVIEW

This technical documentary report is approved.

Wayne H. McCandless
WAYNE H. McCANDLESS
Technical Director
Biomedical Laboratory

TABLE OF CONTENTS

	PAGE
INTRODUCTION.	1
THEORY AND METHOD OF SOLUTION	3
SHAPE FACTORS	17
THE EARTH-MOON-SUN ENVIRONMENT.	20
SPACE MAN MODEL	24
SPACE CONFIGURATIONS A, B, C, D, E, F AND G	26
HYPOTHETICAL CHAMBER CONFIGURATIONS I, II, III AND IV.	52
COMPARISON OF SPACE CONFIGURATIONS A, B, C, D AND E WITH CHAMBER CONFIGURATION III.	70
SUMMATION OF MAJOR CONCLUSIONS.	80
RECOMMENDATIONS	81
REFERENCES.	83
APPENDIX I.	87
APPENDIX II	89
APPENDIX III.	93
APPENDIX IV	95
APPENDIX V.	99
APPENDIX VI	103

LIST OF SYMBOLS

- E - Total emissive power (Btu/Hr ft²)
- σ - Stefan-Boltzmann constant (0.1714×10^{-8} Btu/Hr ft²R⁴)
- I - Radiation intensity
- d ω - Differential solid angle
- $I_{b\lambda}$ - Radiation intensity of a blackbody radiator as a function of wavelength
- $E_{b\Delta\lambda}$ - Monochromatic emissive power of a blackbody (Btu/Hr ft²)
- λ - Wavelength in microns
- T - Absolute temperature (R)
- C_1 - 1.1870×10^8 Btu μ^4 /ft² Hr
- C_2 - 2.5896×10^4 R μ
- Z_e - Distance from the surface of the earth measured in earth radii
- Z_m - Distance from the surface of the moon measured in moon radii
- E_{nb} - Emissive power of a non-blackbody radiator
- ϵ_λ - Spectral hemispherical emittance
- ϵ_t - Total hemispherical emittance
- ϵ_g - Greybody emittance
- α - Absorptivity
- ϵ_a - Average emissivity for a given wavelength band
- α_a - Average absorptivity for a given wavelength band
- α_λ - Spectral absorptivity
- Q - Net radiation heat transfer
- A - Area
- F - Geometrical shape factor
- ϵ_s - Satellite emissivity

- W - Weight of differential element
- C_p - Specific heat of differential element
- $\frac{dT_s}{dt}$ - Rate of change of T_s with time
- P_t - Internal generated heat
- Q_c - Heat conducted along the satellite wall to the differential
- Q_i - Internal heat radiation
- h_c - Natural convection heat transfer film coefficient
- T_a - Air temperature inside the thermal simulator
- Q_{con} - Net heat transferred by convection
- ϵ_w - Emittance of chamber walls
- E_{g1} - Total radiation leaving a grey surface A
- α_c - Absorptivity of space suit in the thermal chambers

LIST OF ILLUSTRATIONS

Figure	Page
1. Radiation intensity vector notation	4
2. Monochromatic intensity of radiation for blackbody and greybody radiators at 2700 R versus wavelength.	9
3. Monochromatic absorptance or emittance versus wavelength for white tile and anodised aluminum.	9
4. Geometry for mechanical shapefactor integration	19
5. The earth's orbit	21
6. The moon's orbit.	22
7. Cylindrical model of a "suited" man	25
8. Space configurations A, B, C, D and E	27
9. Space configuration F. Space man in orbit about the moon.	28
10. Space configuration G. Space man in orbit about the earth	29
11. Variation of the total heat absorbed by the cylindrical model with respect to the distance from the surface of the earth.	32
12. Variation of the total heat absorbed by the cylindrical model with respect to the distance from the surface of the earth's albedo.	33
13. Variation of the heat absorbed due to the moon's emitted energy and albedo for the cylindrical model with respect to the distance of the model from the surface of the moon	34
14. Average absorptance and reflectance for aluminized nylon cloth at different wavelengths	35
15. Total heat absorbed by the cylindrical model versus chamber I wall temperature.	54
16. Total heat absorbed by the cylindrical model in chamber II versus the wall temperature of chamber II.	56
17. Total heat absorbed by the cylindrical model in chamber III versus the wall temperature of chamber III.	59

	Page
18. The ratio of the heat transferred by convection to the heat absorbed by radiation versus the absorptance of the space suit.	62
19. The ratio of the heat transferred by convection to the heat absorbed by radiation at chamber pressures of 1.0, 0.1 and 0.01 atmospheres versus space suit absorptance. .	63
20. The ratio of the heat transfered by convection to the heat absorbed by radiation at chamber pressures of 1.0, 0.1 and 0.01 atmospheres versus space suit absorptance. .	64
21. The ratio of the heat transferred by convection to the heat absorbed by radiation at chamber pressures of 1.0, 0.1 and 0.01 atmospheres versus space suit absorptance. .	66
22. The total heat absorbed by the cylindrical model in chamber IV versus the wall temperature of chamber IV. . .	68
23. Comparison of the heat absorbed by the cylindrical model in chamber III with the heat absorbed by the model in space configuration A.	71
24. Comparison of the heat absorbed by the cylindrical model in chamber III with the heat absorbed by the model in space configuration B.	72
25. Comparison of the heat absorbed by the cylindrical model in chamber III with the heat absorbed by the model in space configuration C	73
26. Comparison of the heat absorbed by the cylindrical model in chamber III with the heat absorbed by the model in space configuration D.	74
27. Comparison of the heat absorbed by the cylindrical model in chamber III with the heat absorbed by the model in space configuration E	75
28. Space man model based on a system of cylinders.	82
29. Properties of dry air at atmospheric pressure	91

LIST OF TABLES

Table	Page
1. The variation in shape factor F for chamber walls with an emittance of 1.0 and 0.94	15
2. Radiative heat absorbed (btu/hr) by the cylindrical model in space configuration A.	36
3. Radiative heat absorbed (btu/hr) by the cylindrical model in space configuration B.	37
4. Radiative heat absorbed (btu/hr) by the cylindrical model in space configuration C.	38
5. Radiative heat absorbed (btu/hr) by the cylindrical model in space configuration D.	39
6. Radiative heat absorbed (btu/hr) by the cylindrical model in space configuration E.	40
7. Heat absorbed by the cylindrical model in space configuration F	41
8. Heat absorbed by the cylindrical model in space configuration G	46
9. Radiative heat absorbed by the cylindrical model in chamber I.	53
10. Radiative heat absorbed by the cylindrical model in chamber II	55
11. Radiative heat absorbed by the cylindrical model in chamber III.	58
12. Natural convection film coefficients for flow over a horizontal cylinder using various environmental and surface temperatures at a barometric pressure of 1.0 atmospheres.	60
13. Natural convection film coefficients for flow over a horizontal cylinder using various environmental and surface temperatures at a barometric pressure of 0.1 atmospheres.	60

	Page
14. Natural convection film coefficients for flow over a horizontal cylinder using various environmental surface temperatures at a barometric pressure of 0.01 atmospheres.	61
15. Radiative heat absorbed by the cylindrical model in chamber IV.	67
16. Specific heat of dry air at various pressures and temperatures.	90
17. Density of dry air at various pressures and temperatures.	90
18. Radiative heat absorbed by the cylindrical model in space configurations A, B, C, D and E for special cases (1), (2), (3) and (4)	100
19. Special case 1F; Earth orbit analysis	100
20. Equivalent chamber temperature for space configurations A, B, C, D and E.	101

INTRODUCTION

Various theoretical investigations have been made of the thermal condition of satellites, space suits and space men in a variety of space configurations. For instance, Irvine and Cramer (ref. 14) have conducted a thermal analysis of space suits in earth orbit and of non-uniform suit temperatures for space suits in earth orbit. Correale and Guy (ref. 12) show that the total heat absorbed by a "suited man" on the solar side of the moon is approximately 400 btu/hr. Schmidt and Hanawalt (ref. 39) show that satellite skin temperatures for an earth orbiting satellite vary from approximately 400 F to -200 F depending on the orbit attitude and the thermal radiation properties of the orbiting vehicle.

Similar studies have been conducted, both theoretically and experimentally, with human subjects in space suits, flying suits and "shirt sleeve" attire during laboratory imposed thermal environments. For example, McCutchan (ref. 34) provided a graphical computation of human thermal tolerance time in terms of body storage index (btu/hr) and tolerance time (hr) where body storage index is defined as a function of thermal chamber properties. On the theoretical side, Iberall's hypothesis (ref. 26) points to the number of degrees of freedom that must be involved in the thermoregulation of the human body as an inconstant heat source and the specific non-linear characteristics of the system. He concludes that a resistance model to clothing, space suits, etc., is possible only as an ohmic relation among time-averaged equilibrium values and for a specific mode of operation of the system.

Finally, Kaufman (ref. 29) has determined the thermal tolerance time of "shirt sleeve" crews in a thermal environment in which the temperature was varied from 115 F to 130 F at humidities of 10 to 20 mm of hg water vapor pressure. He found that human tolerance time ranged from 8 to 2 hours. However, in all cases a common link between theoretical space and laboratory environments and human tolerance time in these environments is missing. Therefore, the purpose of this investigation is to provide a link between space and laboratory thermal environments and human tolerance time in these environments. Specifically, the following questions are asked:

- (1) Is it theoretically possible to conduct human experimentation in ventilated space suits under less than space-equivalent conditions and extrapolate the results to a specific space condition?
- (2) Is it feasible to perform these experiments in the Aerospace Medical Research Laboratories Environmental Test Facility (AMRL)?

- (3) If the capabilities of the environmental test facility are inadequate, what are the minimum conditions required?

THEORY AND METHOD OF SOLUTION

Blackbody Radiation (ref. 24, ref. 30, ref. 31)

A blackbody radiator is defined as a diffuse radiator (intensity is independent of direction) which emits at any specified body temperature the maximum possible amount of thermal radiation at all wavelengths. Moreover, it absorbs all incident radiation and transmits none. Kirchhoff's law as applied to blackbody radiation concludes that no surface can absorb or emit more radiation than a blackbody surface. Furthermore, the total emissive power of a blackbody is given by the Stefan-Boltzmann equation as

$$E = \sigma T^4$$

where E is the total emissive power in btu/hr ft^2 , σ is the Stefan-Boltzmann constant ($0.1714 \times 10^{-8} \text{ btu/hr ft}^2 \text{ R}^4$) and T is the absolute temperature of the body.

The radiation intensity I is the energy radiated from a body within a unit solid angle in a given direction by a unit surface element projected on a plane perpendicular to the radiation direction. Refer to figure 1.

$$I_{1-2} = \frac{dq_{1-2}}{dA_1 \cos \theta_1 d\omega_{1-2}}$$

$d\omega_{1-2}$ - the solid angle subtended by dA_2 with respect to the center of dA_1

$$d\omega_{1-2} = \frac{dA_2 \cos \theta_2}{L_{1-2}^2}$$

dq_{1-2} - the portion of the radiation from dA_1 intercepted by dA_2

Lambert's cosine law states that the rate at which radiant energy is emitted from a blackbody source is independent of direction, or the surface of the source has the same flux density in all directions. Mathematically, where I is the time rate per unit area of the source,

$$I_\theta = I \cos \theta$$

per unit solid angle, at which radiant energy is emitted from an infinitesimal element of blackbody surface into a minute solid angle around the normal to the element of surface and I_θ is the corresponding

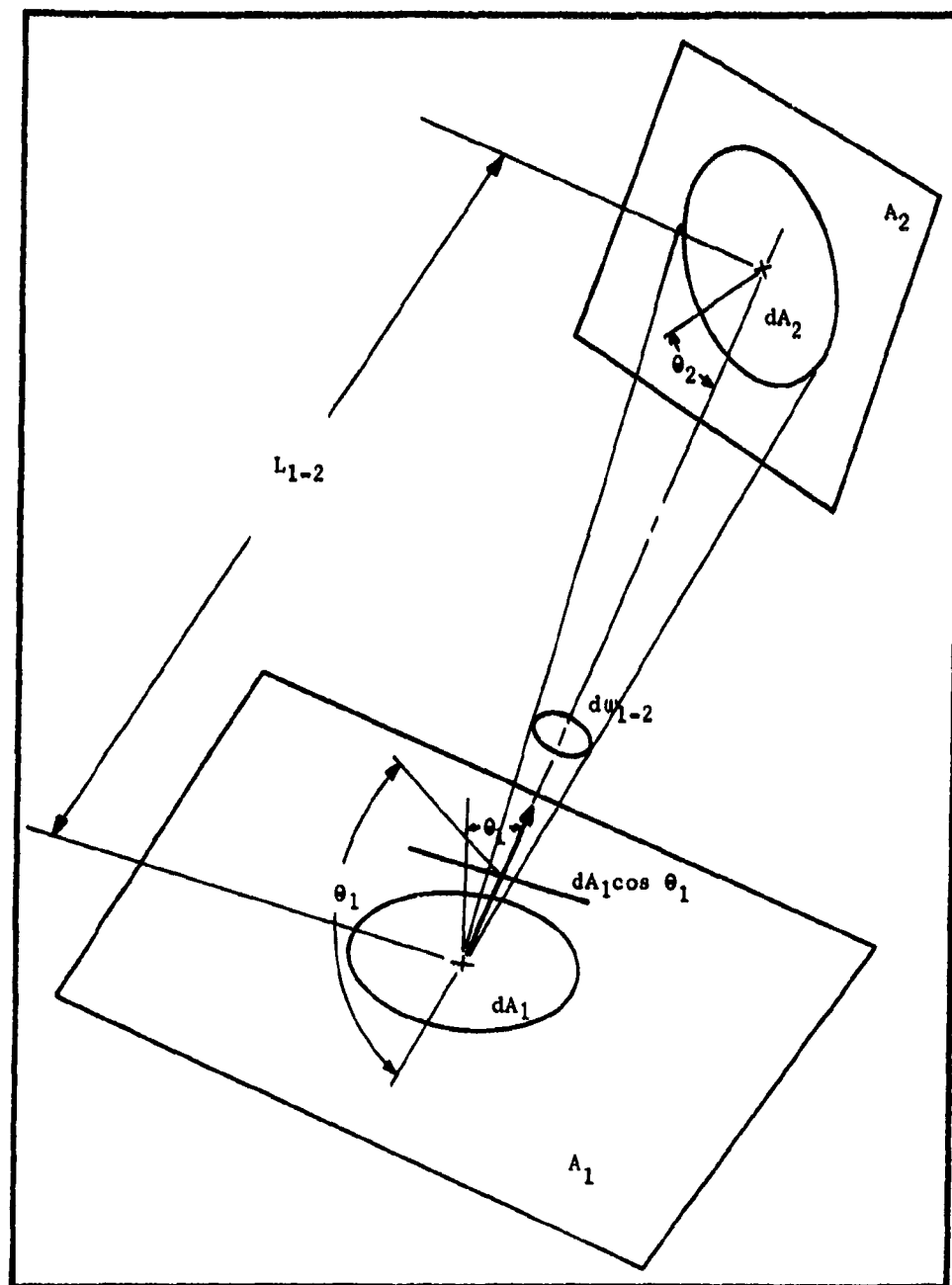


Figure 1. Radiation intensity vector notation.

rate of emission in a direction making angle θ with the normal. Consequently, the rate of emission of radiant energy from a blackbody of given area in a direction making angle θ with its normal is proportional to the projection of that area upon a plane normal to the direction in question: that is, it is proportional to the $\cos \theta$ (ref. 24). Thus, the corresponding rate of emission per unit of projected area is

$$\frac{I_{\theta}}{\cos \theta}$$

This means that an emitting area $A' = 1/\cos \theta$ is necessary in order to have one unit projected area in that direction, or the rate of radiant energy I_p in the specified direction per unit projected area of surface is

$$I_p = I_{\theta} A' = I$$

I_p is called the radiance of the blackbody.

Furthermore, when a hemisphere of radius unity is placed over the area dA_1 , the solid angle subtended by any portion dA_2 of the area of the hemisphere with respect to dA_1 is numerically equal to dA_2 . If E_1 is the total rate of radiative emission by the area dA_1 , then

$$E_1 = \int_{A_2} I_{\theta} \cos \theta_1 d\omega_1 = 2\pi I_1 \int_0^{\pi/2} \cos \theta_1 \sin \theta_1 d\theta_1 = \pi I_1$$

Whereas, the Stefan-Boltzmann equation represents the total radiant energy emitted by a blackbody in all directions of a hemispherical space per unit area and time for all wavelengths, Planck's quantum theory gives the radiation intensity and emissive power as a function of wavelength. Specifically,

$$I_{b\lambda} = \frac{\frac{C_1}{\pi}}{\lambda^5 (e^{C_2/\lambda T} - 1)}$$

$$E_{b\lambda} = \frac{C_1}{\lambda^5 (e^{C_2/\lambda T} - 1)}$$

$E_{b\lambda}$ - monochromatic emissive power of a blackbody (btu/hr ft²)

λ - wavelength (μ)

T - absolute temperature (R)

e - napierian base of logarithms

C_1 - 1.1870×10^8 btu μ^4/ft^2 hr

C_2 - 2.5896×10^4 R μ

Comparison of the equations of Planck and the Stefan-Boltzmann equation for blackbody radiation shows that

$$E = \int_0^{\infty} E_b \lambda d\lambda = C_1 \int_0^{\infty} \frac{d\lambda}{\lambda^5 (e^{C_2/\lambda T} - 1)}$$

$$E = \frac{C_1 \pi^4}{15 C_2^4} T^4 = \sigma T^4$$

where $\sigma = \frac{C_1 \pi^4}{15 C_2^4}$ (see appendix III).

In a manner similar to the derivation above, Livingston (ref. 33) shows that the band emissive power of blackbody source functions can be described in terms of blackbody radiation as follows. Given that

$$E_{b\lambda} d\lambda = \frac{C_1}{\lambda^5 (e^{C_2/\lambda T} - 1)} d\lambda$$

Then, the emissive power over a band of wavelengths is

$$E_{b\Delta\lambda} = \int_{\lambda_1}^{\lambda_2} E_{b\lambda} d\lambda = \int_{\lambda_1}^{\lambda_2} \frac{C_1}{\lambda^5 (e^{C_2/\lambda T} - 1)} d\lambda$$

Let $x = \frac{C_2}{\lambda T}$

Then,

$$E_{b\Delta x} = \sigma T^4 \int_{x_1}^{x_2} \frac{15}{\pi^4} \frac{y^3}{e^y - 1} dy$$

where y is a dummy variable. Let

$$f(x) = \frac{15}{\pi^4} \int_x^{\infty} y^3 (e^y - 1)^{-1} dy$$

$$E_{b\Delta x} = \sigma T^4 [f(x_2) - f(x_1)] x_1 = \frac{C_2}{\lambda_1 T} ; x_2 = \frac{C_2}{\lambda_2 T}$$

Thus, Livingston states that the fraction of radiation emitted by a source in a desired wavelength band is determined by the values of

$f(x)$ between the two limits of the wavelength band and lists the following source functions for the sun, earth and moon (in btu/hr ft²).

The Sun

$$E_{b\Delta x} = 444 [f(x_2) - f(x_1)]$$

$$x = \frac{2.51}{\lambda(\mu)}$$

The Earth

The earth's thermal radiation observed at a distance Z from the earth (measured in earth radii) is

$$E_{b\Delta x} = \frac{66.3}{Z_e^2} [f(x_2) - f(x_1)]$$

$$x = \frac{51.5}{\lambda(\mu)}$$

The earth's albedo flux measured at a distance Z from the earth (measured in earth radii) is

$$E_{b\Delta x} = \frac{37.7}{Z_e^2} [(\pi - \psi_e) \cos \psi_e + \sin \psi_e] [f(x_2) - f(x_1)]$$

$$x = \frac{2.51}{\lambda(\mu)}$$

ψ_e is the angle subtended at the earth between the sun and an imaginary observer.

The Moon

The moon's thermal radiation observed at a distance Z (measured in moon radii) from the moon is

$$E_{b\Delta x} = \frac{412}{Z_m^2} \left[\frac{1 + \cos \psi_m}{2} \right] [f(x_2) - f(x_1)] ; \quad x = \frac{36.4}{\lambda(\mu)}$$

The moon's albedo flux measured at a distance Z (measured in moon radii) from the moon is

$$E_{b\Delta x} = \frac{31}{Z_m^2} [(\pi - \psi_m) \cos \psi_m + \sin \psi_m] [f(x_2) - f(x_1)] ; \quad x = \frac{2.51}{\lambda(\mu)}$$

where ψ_m is the angle between the sun and the vehicle as seen from the moon.

Non-Blackbody Radiation (ref. 24, ref. 28, ref. 29, ref. 30, ref. 31)

A real surface always radiates less than a blackbody surface at the same temperature. Specifically, the intensity of radiation of a non-blackbody may be expressed as a fractional ratio of the intensity of radiation of a blackbody at the same temperature and is defined as the emittance ϵ of the body. Furthermore, the magnitude of the emittance is dependent on the composition, size, shape and surface properties of the body in question, the temperature of the body and the wavelength or the wavelength band for which the ratio applies. Thus, in order to denote the emittance of a surface at various wavelengths, the spectral hemispherical emittance ϵ_λ is defined as the emittance of a non-blackbody at a given wavelength λ . Consequently, the total emissive power E_{nb} of a non-blackbody is

$$E_{nb} = \int_0^\infty \epsilon_\lambda E_\lambda d\lambda = C_1 \int_0^\infty \frac{\epsilon_\lambda d\lambda}{\lambda^5 (e^{C_2/\lambda T} - 1)} = \epsilon_t \sigma T^4$$

where ϵ_t is the total hemispherical emittance. Also, a greybody radiator is defined as a non-blackbody radiator for which the emittance $\epsilon_\lambda = \epsilon_g$ is constant over all wavelengths, and the shape of a spectroradiometric curve for a greybody surface is similar to that of a blackbody surface at the same temperature except that the height is reduced by the numerical value of the emittance (see fig. 2).

Suppose, now, that two small bodies B_1 and B_2 with surface areas A_1 and A_2 are placed in a large evacuated enclosure which is perfectly insulated from its surroundings. A net radiation exchange between the bodies and the enclosure walls exists until both bodies and the walls have reached the same temperature. Then, the rate at which each body emits radiation must equal the rate at which it absorbs radiation. Kreith shows that if E is the rate of emission from the enclosure walls on each of the bodies, and α_1 and α_2 are the absorptances and E_1 and E_2 are the emissive powers of B_1 and B_2 respectively,

$$A_1 E \alpha_1 = A_1 E_1 \quad ; \quad A_2 E \alpha_2 = A_2 E_2$$

or

$$\frac{E_1}{\alpha_1} = \frac{E_2}{\alpha_2} = \frac{E}{\alpha} = \frac{E_b}{1}$$

$$\frac{\frac{E}{E_b}}{\alpha} = 1$$

However, $\frac{E}{E_b} = \epsilon$. Thus, $\alpha = \epsilon$, or at thermal equilibrium the

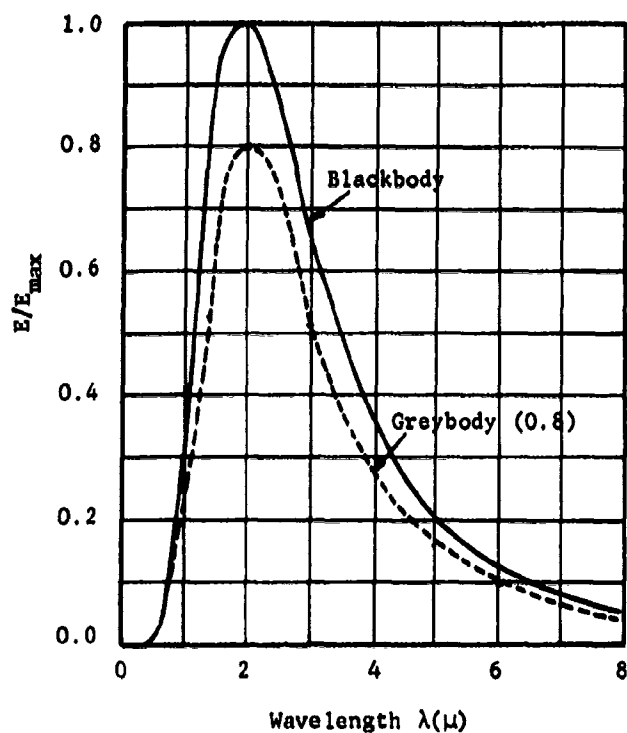


Figure 2. Monochromatic intensity of radiation for blackbody and greybody radiators at 2700 R versus wavelength.

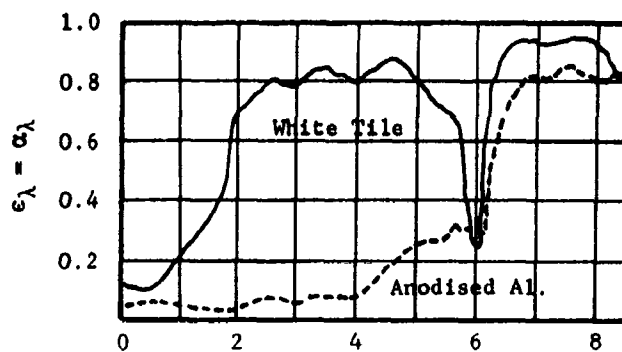


Figure 3. Monochromatic absorptance or emittance versus wavelength for white tile and anodised aluminum.

the absorptance and the emittance of a body are equal. Again, for graybody radiators, α_λ and ϵ_λ are constant over the entire wavelength spectrum; consequently, $\alpha = \epsilon$ irrespective of the temperatures of the emitter and receiver.

In contrast to graybody radiation suppose $\alpha = \epsilon$ vary with wavelength such that the absorptance and emittance are equal only at a given wavelength and temperature. For example, the variation of α_λ and ϵ_λ for two real surfaces, anodised aluminum and white tile, is given in figure 3. α_λ and ϵ_λ are not constant. Thus, Kreith suggests that for radiation heat transfer calculations with real surfaces such as anodised aluminum on white tile, use an average emittance (ϵ_a) or absorptance (α_a) for the wavelength band in which the bulk of the radiation is received or emitted. He further suggests that in order to evaluate α_a and ϵ_a correctly for a real surface, α_a should be chosen to correspond to the wavelength spectrum of the thermal energy source and ϵ_a corresponding to the actual temperature of the body.

Suppose two blackbody environments A and B are maintained at reference temperatures T_a and T_b and

- (1) that T_a is greater than T_b
- (2) that a diffusely radiating body C is enclosed in environment A
- (3) that a vacuum and/or non-absorbing medium exists between the enclosed body and the environment.

Three particular problems are evident, namely the net heat exchange between the enclosed body and the environment when the enclosed body is considered

- (1) a blackbody radiator
- (2) a graybody radiator
- (3) a non-blackbody radiator

Christiansen's equation for the net heat transfer by radiation from an enclosed graybody to its grey enclosure is

$$Q_{\text{net}} = \frac{1}{1 + \epsilon_1 \left(\frac{1}{\epsilon_2} - 1 \right) \frac{A_1}{A_2}} \epsilon_1 \sigma A_1 (T_1^4 - T_2^4)$$

where subscripts (1) refer to the body in question and subscripts (2) refer to the enclosure in question. If the environment or enclosure is a blackbody enclosure,

$$Q_{\text{net}} = \epsilon_1 \sigma A_1 (T_1^4 - T_2^4)$$

or

$$E_{\text{net}} = \frac{Q_{\text{net}}}{A_1} = \epsilon_1 \sigma (T_1^4 - T_2^4)$$

Christiansen's equation then applies to cases (1) and (2); however, if the surface or body in question is a non-blackbody surface, the relationship between any two areas A_1 and A_2 applies only at a given wavelength λ or, in other words, Q_{net} is now a function of λ . Thus,

$$Q_{\text{net}} = \int_0^{\infty} \frac{E_{\lambda 1} - E_{\lambda 2}}{(1 + \epsilon_{\lambda 1}) + \frac{A_1}{A_2} \left(\frac{1}{\epsilon_{\lambda 2}} - 1 \right)} d\lambda$$

It is possible to simplify the calculations for non-blackbody surfaces if, for example, $\epsilon_{\lambda 1}$ and $\epsilon_{\lambda 2}$ have constant values from $\lambda = 0$ to $\lambda = K$ and from $\lambda = K$ to $\lambda = \infty$. In this case the integral may be broken into two parts and Christiansen's equation may be used for a direction analysis. Although the enclosed body is non-black over the entire radiation spectrum, it is considered grey over the spectral bands, that is, from $\lambda = 0$ to $\lambda = K$ and from $\lambda = K$ to $\lambda = \infty$. The energy fluxes emitted by the environments A and B are then

$$E_a = \frac{Q_a}{A_a} = \sigma T_a^4$$

$$E_b = \frac{Q_b}{A_b} = \sigma T_b^4$$

When the enclosed body is in environment A, the incident energy on the body is the same as the energy emitted by environment A. Furthermore, the radiating body will absorb a certain amount of the incident radiation depending on whether it is defined by case 1, case 2 or case 3. For example, if the body is a blackbody; if the body is a greybody

$$Q_{\text{absorbed}} = A_{\text{body}} E_a$$

$$Q_{\text{absorbed}} = A_{\text{body}} \epsilon_{\text{body}} E_a, \text{ respectively.}$$

The body will emit a certain amount of energy to the environment dependent on its emittance and its temperature. If the body is a blackbody,

$$Q_{\text{emitted}} = A_{\text{body}} \sigma T_{\text{body}}^4$$

If the body is a greybody,

$$Q_{\text{emitted}} = A_{\text{body}} \epsilon_{\text{body}} \sigma T_{\text{body}}^4$$

If the body is non-black,

$$Q_{\lambda \text{ emitted}} = A_{\text{body}} \epsilon_{\lambda \text{ body}} \sigma T_{\text{body}}^4$$

Let environment A denote a satellite earth orbit in which the external sources of energy are (1) solar radiation, (2) the earth's emitted energy and (3) the earth's albedo. The heat transfer equation governing the instantaneous heat balance on a surface element of the earth orbit space vehicle is

$$Wc_p dx \frac{dT_s}{dt} = F_s S \alpha_s + F_r R \alpha_r + F_e \alpha_e E_e + P_t + Q_c + Q_i - \sigma \epsilon_s T_s^4$$

Wd_x - weight of the element

C_p - specific heat of the element

$\frac{dT_s}{dt}$ - rate of change of element surface temperature with time

$F_s S \alpha_s$ - absorbed solar radiation

$F_r R \alpha_r$ - absorbed earth reflection

$F_e E_e \alpha_e$ - absorbed earth emission

$\sigma \epsilon_s T_s^4$ - radiation emitted by the satellite

P_t - internal generated heat

Q_c - heat conducted along the satellite wall to the element in question

Q_i - internal heat radiation

Let environment B (ref. 37) denote a thermal simulator or chamber with the following properties:

- (1) The internal radiation area of the chamber is very large.
- (2) The internal chamber pressure is 0 atmospheres.
- (3) The chamber walls are diffuse blackbody radiators.
- (4) There are no internal radiation sources available except the subject and the chamber walls.
- (5) Any external heat transfer to an enclosed surface by conduction is negligible.
- (6) The interior of the chamber is a non-absorbing medium.

The heat balance on the same element in the thermal simulator (environment B) is

$$WC_p dx \frac{dT_s}{dt} = \sigma F(T_w^4 - T_s^4) + P_t + Q_c + Q_i \quad (2)$$

where F is the geometrical configuration factor and T_w is the wall temperature of the thermal simulator. All other remaining terms of equation (2) are identical with those of equation (1).

Exact temperature simulation requires, then, that at any time the general solutions and boundary conditions of equations (1) and (2) must be the same, or

$$WC_p \frac{dT_s}{dt} (1) = WC_p \frac{dT_s}{dt} (2)$$

and

$$\sigma F(T_w^4 - T_s^4) + P_t + Q_c + Q_i = F_s S \alpha_s + F_r R \alpha_r + F_e E_e \alpha_e + P_t + Q_c + Q_i - \sigma \epsilon_s T_s^4 \quad (3)$$

Thus, the P_t , Q_c and Q_i terms can be canceled since the initial conditions for both configurations are assumed to be the same, or

$$\sigma F(T_w^4 - T_s^4) = F_s S \alpha_s + F_r R \alpha_r + F_e E_e \alpha_e - \sigma \epsilon_s T_s^4 \quad (4)$$

If equation (4) can be satisfied, the space environment A can be successfully simulated in environment B. From Christiansen's equation

$$F = \frac{\epsilon_s}{1 + \epsilon_s \left(\frac{1}{\epsilon_w} - 1 \right)} \frac{A}{A_w}$$

where ϵ_s is the emittance of the enclosed body. However, since environment A is a blackbody environment, $\epsilon_w = 1$ and $F = \epsilon_s$. Thus, equation (4) can be revised as follows:

$$\sigma \epsilon_s T_w^4 = F_s S \alpha_s + F_r R \alpha_r + F_e E_e \alpha_e \quad (5)$$

Equation (5) indicates that the temperature history of environment B depends only on the time history of the external radiation absorbed by the vehicle in the given space configuration (A) and its surface properties. Thus, in order to simulate space environments in this theoretical laboratory environment it is not necessary to evaluate the complex internal heat transfer terms of equations (1) and (2). However, two primary simulator requirements must be satisfied:

- (1) The simulator walls must be blackbody radiators.

- (2) The simulator must be maintained at a complete vacuum.

The chamber walls of the AMRL facility are not blackbody radiators, and the internal chamber pressure varies between finite limits. Thus, revise environment B as follows:

- (1) Let $\epsilon_w = \epsilon_w = 0.94$ (greybody radiator).
 (2) Let the internal chamber pressure vary between finite limits.

Hence, for the revised version of environment B, two heat transfer mechanisms are employed for transferring heat to the surface element in question, namely heat transfer by radiation and heat transfer by convection. Also, since ϵ_w is now 0.94 instead of 1.0, the shape factor F is not necessarily equal to ϵ_s . Refer again to Christiansen's equation.

$$F = \frac{\epsilon_s}{1 + \epsilon_s \left(\frac{1}{\epsilon_w} - 1 \right) \frac{A}{A_w}} \quad (6)$$

Let $\frac{A}{A_w}$ equal 0.1 and ϵ_w equal 0.94.

$$F = \frac{\epsilon_s}{1 + 0.0064 \epsilon_s}$$

From table 1 ($\epsilon_w = 0.94$) F varies from 0.9936 ($\epsilon_s = 1.0$) to 0.04998 ($\epsilon_s = 0.05$). The difference between F based on $\epsilon_w = .94$ and F based on $\epsilon_w = 1.0$ varies from 0.64% ($\epsilon_s = 1.0$) to a minimum of 0.03% at $\epsilon_s = 0.05$. It is concluded that greybody thermal environments with $\epsilon_w = \epsilon_w$ for at least values of 0.94 and greater can be considered blackbody radiators. Of course, referring again to equation (6), F is approximately equal to ϵ_s if the ratio of A/A_w is very small regardless of the value of ϵ_w . However, the ratio of $A/A_w = 0.1$ was selected since it is a representative value for the AMRL thermal chamber.

Convection heat transfer is introduced into the analysis by adding the convection term, $Q_{con} = h_c(T_a - T_s)$, into equation 5.

$$\sigma \epsilon T_w^4 + h_c(T_a - T_s) = F_s S \alpha_s + F_r R \alpha_r + F_e E \alpha_e \quad (7)$$

where Q_{con} is the net heat transferred by convection and T_a is the air temperature inside the thermal simulator.

Introduction of the convection term upsets the simulation equation since it now contains a quantity which represents the net heat gained or lost due to convection. One obvious simplification is to reduce the pressure in the chamber to a point where Q_{con} is negligible when compared to the heat absorbed by radiation. Equation (7) is then effectively reduced to equation (5).

TABLE 1

THE VARIATION IN SHAPE FACTOR F FOR CHAMBER
WALLS WITH AN EMITTANCE OF 1.0 AND 0.94

Emittance	F(Greybody Radiator)	F(Blackbody Radiator)	Percent Variation
1.0	0.9936	1.0	0.642
0.9	0.8948	0.9	0.579
0.8	0.7959	0.8	0.510
0.7	0.6969	0.7	0.450
0.6	0.5977	0.6	0.38
0.5	0.4984	0.5	0.32
0.4	0.3990	0.4	0.26
0.3	0.2994	0.3	0.19
0.2	0.1997	0.2	0.13
0.1	0.0999	0.1	0.06
0.05	0.04998	0.05	0.03

Thus, in order to utilize this concept for comparing spatial and laboratory thermal conditions it is necessary to stipulate the incident absorbed thermal radiation on a space man in various space configurations and to compare these absorbed heat loads with incident absorbed thermal loads which can be produced by the AMRL facility or at least by representative models of the AMRL facility. Specifically, incident absorbed heat calculations are calculated for a cylindrical model of a 50th percentile suited man in the following space configurations:

- (A) Deep space probe
- (B) A point 136 miles from the surface of the bright side of the moon
- (C) A point 136 miles from the surface of the dark side of the moon
- (D) A point 500 miles from the surface of the bright side of the earth
- (E) A point 500 miles from the surface of the dark side of the earth
- (F) A 500 mile circular earth orbit
- (G) A 136 mile circular moon orbit

Assume, now, that a man in a space suit in any one of the space configurations above will move about, turn around, etc., in an attempt to prevent over-heating or cooling of his body in such a manner that the average rate of thermal radiation on the space suit is constant. In this case a blackbody environment at the appropriate uniform temperature can simulate the given space condition. For a non-turning space man, at least two separate thermal energy fields are necessary. Specifically, incident absorbed heat load calculations are made for four hypothetical chambers I, II, III and IV. Chambers I and III apply to a turning or spinning space man and chambers II and IV apply to a non-turning space man. These chambers are then used to determine the limitations of the space simulation and/or human tolerance to space capabilities of the AMRL thermal chamber.

SHAPE FACTORS

The intensity of blackbody radiation in a non-absorbing medium between two areas, A_1 and A_2 , is a vector quantity whose magnitude has been defined previously as

$$|I_{1-2}| = \frac{dq_{1-2} L_{1-2}^2}{dA_1 dA_2 \cos \theta_1 \cos \theta_2}$$

or

$$dq_{1-2} = \frac{|I_{1-2}| dA_1 dA_2 \cos \theta_1 \cos \theta_2}{L_{1-2}^2}$$

and

$$E_{1-2} = \pi I_{1-2}$$

Let E_{g1} be defined as the total radiation leaving a greybody surface A_1 per unit time

$$E_{g1} = \frac{dQ_1}{dA_1}$$

where dQ_1 is the total radiation. The rate of radiative heat transfer from a greybody dA_1 to dA_2 is

$$dq_{1-2} = E_{g1} d(A_1 F_{12})$$

Similarly, the rate of radiative heat transfer from dA_2 to dA_1 is

$$dq_{2-1} = E_{g2} d(A_2 F_{21})$$

where

$$d(A_1 F_{12}) = d(A_2 F_{21}) = \frac{\cos \theta_1 \cos \theta_2}{\pi L_{1-2}^2} dA_1 dA_2$$

Combining these two equations

$$dq_{1-2} = \frac{(E_{g1} - E_{g2}) \cos \theta_1 \cos \theta_2 dA_1 dA_2}{\pi L_{1-2}^2}$$

For uniformly irradiated finite areas, the net rate of radiative heat transfer is

$$q_{1-2} = E_{g1} - E_{g2} \int_{A_1} \int_{A_2} \frac{\cos \theta_1 \cos \theta_2}{\pi L_{1-2}^2} dA_1 dA_2$$

Since

$$\int_{A_1} \int_{A_2} \frac{\cos \theta_1 \cos \theta_2}{\pi L_{1-2}^2} dA_1 dA_2 = A_1 F_{12} \quad ,$$

$$q_{1-2} = A_1 F_{12} (E_{g1} - E_{g2})$$

or

$$q_{1-2} = A_1 F_{12} \sigma (T_1^4 - T_2^4)$$

F_{12} is defined as the shape factor based on area A_1 , and F_{21} is defined as the shape factor based on area A_2 . In more general notation $A_1 F_{12}$ is given as $A_1 F_{1j}$ and is defined as the "effective area".

Kreith further shows that the shape factor of a surface element dA_1 with respect to a finite surface A_2 at a distance L_{1-2} from the surface element is

$$F_{1-2} = \frac{1}{\pi} \int_{A_2} \cos \theta_1 d\omega_1$$

which referring to figure 4 reduces to

$$F_{1-2} = \frac{A_2''}{\pi R^2}$$

F_{1-2} - shape factor

θ_1 - angle between the normal to dA_1 and the line of sight from dA_1 to A_2

$d\omega_1$ - unit solid angle subtended by an element of A_2 , dA_2 at dA_1

A_2 - finite area in question

dA_1 - surface element

H - a fictitious hemisphere of radius R

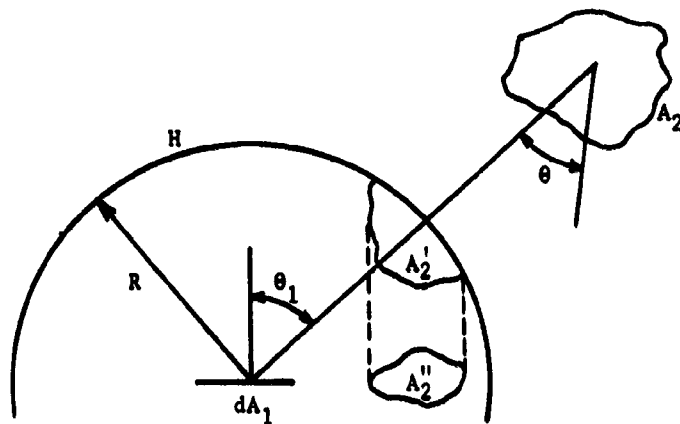


Figure 4. Geometry for mechanical shape factor integration.

- θ_z - angle between L_{1-2} and the normal to A_2
- L_{1-2} - distance from dA_1 to A_2
- A_2' - area subtended on the surface hemisphere by the solid angle
- ω_1 - solid angle subtended at dA_1 by A_2
- A_2'' - area obtained by normal projection of A_2 on the base of the hemisphere

Let the hemisphere denote a diffuse thermal radiation source and/or reflector and let A_2 denote the area of a body at a distance L from the hemisphere. By determining A_2'' graphically, mechanically or optically, the shape factor for numerical heat transfer calculations between the body and the source can be computed. Specifically, Belasco (ref. 1) gives the shape factors for a cylindrical model versus distance from the surface of the earth for the earth's albedo and the earth's emitted energy. For this report, shape factors for the earth's emitted energy, the earth's albedo, the moon's emitted energy and the moon's albedo with regard to the cylindrical model are included in the heat transfer calculations and are not given as separate information. See figures 11, 12 and 13 for the variation of the earth's and moon's albedo etc. absorbed by the space man as a function of the distance from the space man to the surface of the earth or moon.

THE EARTH-SUN ENVIRONMENT

Dynamics of the earth-moon-sun system (ref. 2)

In the earth-moon-sun system the earth rotates in an elliptic path (perihelion 91.3×10^6 miles; aphelion 94.5×10^6 miles) about the sun with an average distance between centers of 92.88×10^6 miles, and the moon rotates in an elliptic path about the earth with an average distance between centers of 238,856 miles (perigee 221,463 miles; apogee 252,710 miles). During the orbit of the earth about the sun (see figure 5), the equatorial plane of the earth is at an angle of $23^\circ 7'$ with respect to the plane of the ecliptic. Also, the plane of the earth-moon system about its barycenter is inclined to the plane of the ecliptic by $5^\circ 9'$ (see figure 6). The points where the moon's orbit meets the ecliptic plane are called its "nodes", and the ascending node denotes motion from south to north while the descending node denotes motion from north to south. When the ascending node coincides with the vernal equinox, the angle between the moon's orbit and the earth's equator is a maximum of $28^\circ 36'$. When the descending node of the lunar orbit coincides with the vernal equinox, the angle between the moon's and earth's equators is $18^\circ 18'$. The moon's equator is tilted with respect to its orbit by $6^\circ 41'$.

Thermal properties of the earth-moon-sun system

The Sun (ref. 30). Inspection of the sun's solar distribution curve shows that it is closely approximated by a blackbody radiator at a temperature of 10,400 R and that 95% of its total energy is transmitted at wavelengths less than 2.5 microns. Kreith gives a detailed table of the sun's radiation intensity versus wavelength at an atmospheric pressure of zero atmospheres and at the average earth to sun distance of 92.88×10^6 miles. He concludes that the solar constant at the earth is $442 \text{ btu/hr ft}^2 \pm 9 \text{ btu/hr ft}^2$.

The Earth. The earth's radiation effects are (1) the earth's albedo and (2) the earth's emitted energy. The earth's albedo is usually given as 0.4 ± 0.1 and its spectral distribution is assumed to be the same as the sun's incident energy. As far as the earth's emitted energy is concerned, a rather wide variation in analysis exists. Kreith suggests that the earth is a blackbody radiator at an equivalent blackbody temperature of 455 R. On the other hand, Livingston suggests that the earth's blackbody temperatures are 516 R in the sunlight and 499 R in the shadow for an average blackbody temperature of 504 R. For calculating the terrestrial radiation, Belasco used yet another blackbody temperature of 450 R. Kuiper (ref. 32) also lists the earth's blackbody temperature as 450 R. Consequently, for these calculations the earth is assumed to approximate a

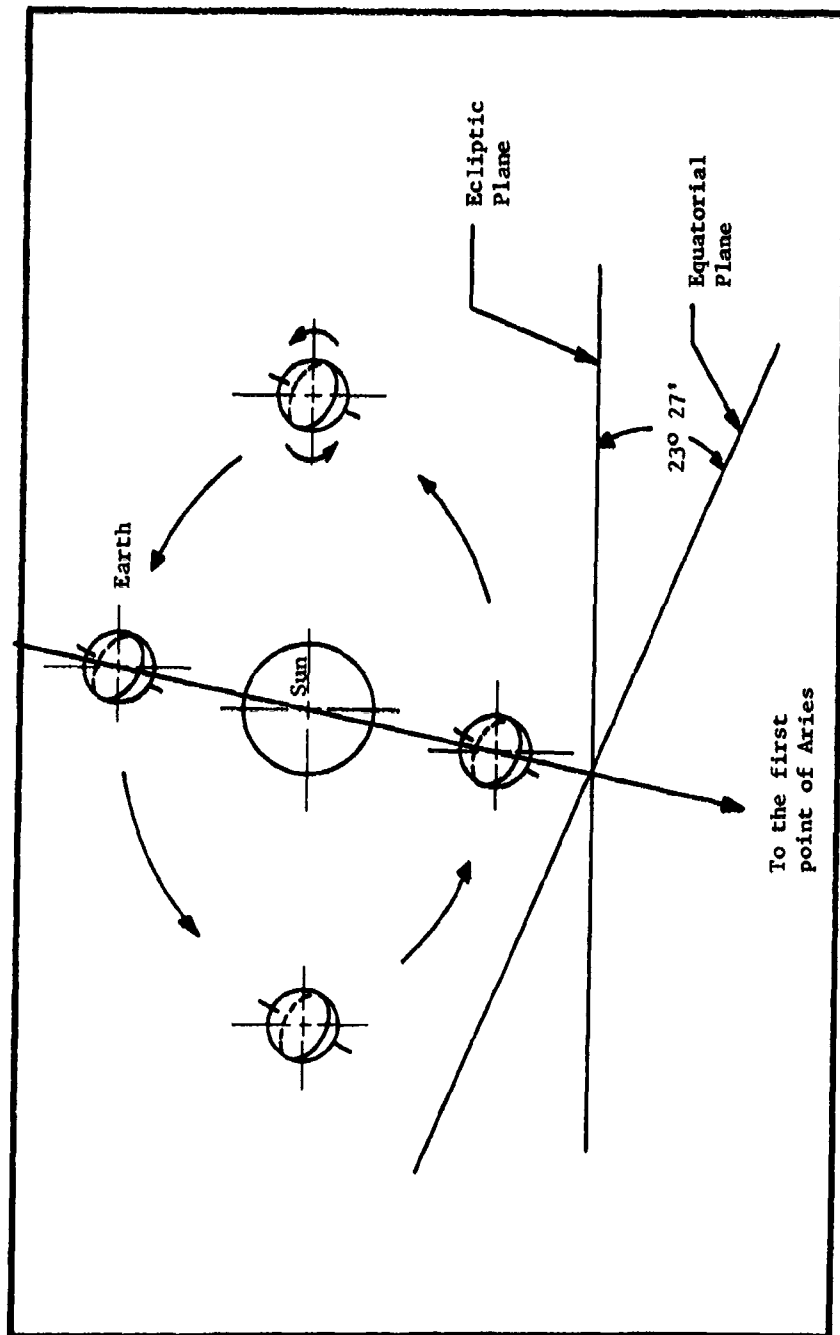


Figure 5. The earth's orbit.

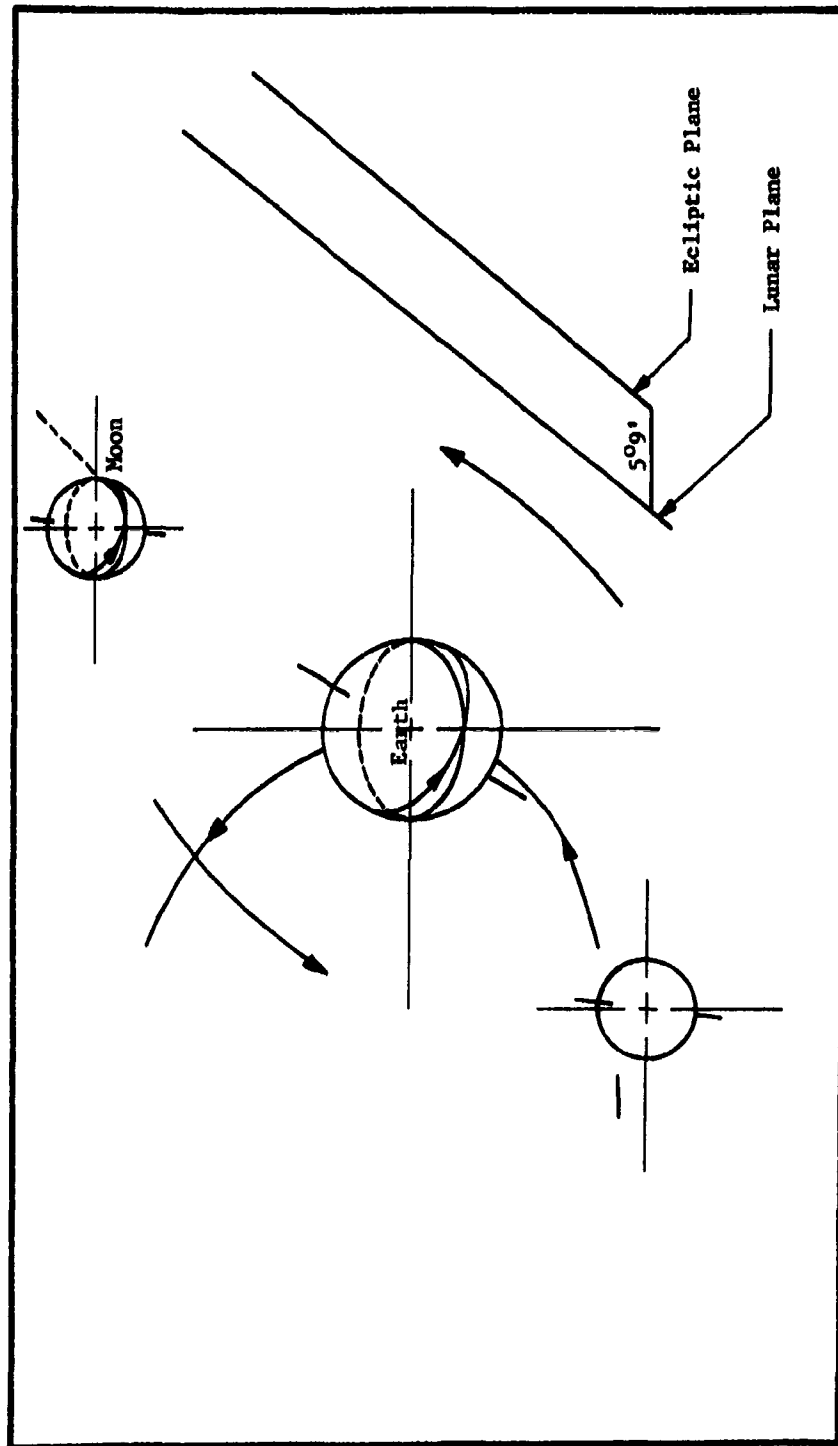


Figure 6. The moon's orbit.

A blackbody radiator at a temperature of 450 R with the major portion of the emitted energy transmitted at wavelengths between 4 and 32 microns.

The Moon. (ref. 2, ref. 32, ref. 42, ref. 45). The moon is subjected to a wide variety of temperatures varying from 710 R at subsolar to 210 R during the middle of the lunar night since the relatively slow spin of the moon allows it to acquire different "equilibrium" temperatures at distinct lunar locations. Consequently, the bright side of the moon is assumed a blackbody radiator at a temperature of 710 R, while the dark side of the moon is assumed a blackbody radiator at a temperature of 210 R. These values for the temperature of the light and dark sides of the moon are confirmed by Livingston who lists temperatures of 713 R and 210 R. Furthermore, based on these temperatures, the major part of the moon's emitted energy is transmitted at wavelengths between 2.8 and 27 microns and 9.5 and 90 microns for the solar and dark sides of the moon, respectively.

Correale and guy suggest that the moon's albedo at or near the moon's surface is 0.07. Kuiper gives a value for the moon's albedo of 0.073. For these calculations the moon's albedo is assumed to be 0.073 and spectrally is assumed to exhibit the same properties as the sun's incident solar energy.

SPACE MAN MODEL

Dunkle (ref. 17) shows that the surface area of a "standard" man without a space suit is 22.5 ft^2 and that the effective radiation area of the same man is 18.51 ft^2 . He attributes this decrease in area of 17% to the fact that there is radiation heat transfer between certain areas of the body such as the arms, legs or neck. Belasco (ref. 1) states that the surface area of a 50th percentile suited man is 22.5 ft^2 . Consequently, based on Dunkle's analysis the effective radiation area of a 50th percentile suited space man is approximately 20 ft^2 .

The applicable model used for these investigations is based on the cylindrical model adapted by Belasco with one major exception: Belasco based the dimensions of his model on the surface area of a 50th percentile man while for these investigations the dimensions of the model are based on the effective radiation area of 20 ft^2 . Specifically, the model is 5.84 ft by 1.13 ft (diameter) with a projected area of 6.56 ft^2 (see fig. 7).

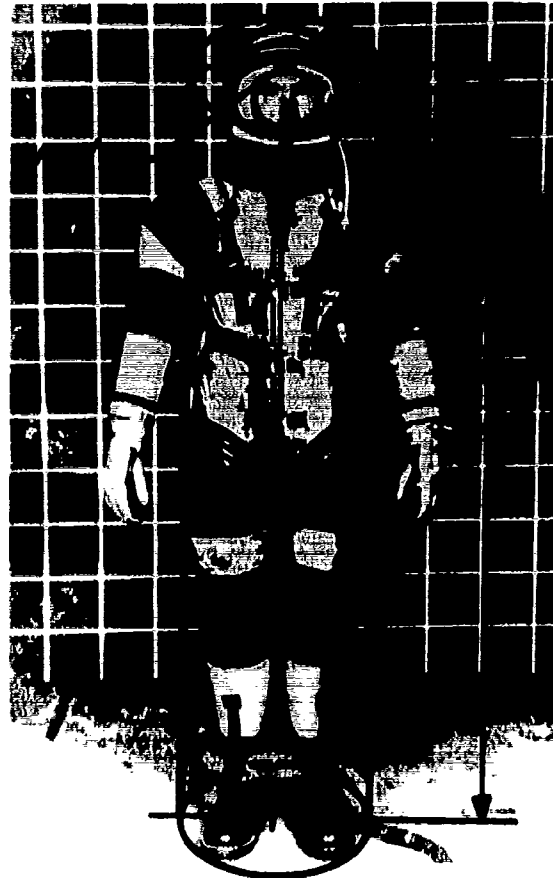


Figure 7. Cylindrical model of a "suited" man.

SPACE CONFIGURATIONS

Configuration A (Deep Space Probe). The space man is considered at least 100,000 miles from either the moon or the earth with no other radiation sources available except the sun (see fig. 8). Moreover, any change in the "mean" man to sun distance is considered negligible when compared to the "mean" earth to sun distance. The effective solar constant is 442 btu/hr ft², and the area over which the solar energy acts is the applicable projected area of the man. The presence of a space capsule is neglected.

Configuration B (Solar Side of the Moon) defines the hottest possible point in a moon orbit when the orbit is at an angle of zero degrees with respect to the moon-sun centerline (see fig. 8). Specifically, the space man is suspended at a point 136 miles from the surface of the moon on the moon-sun centerline. The presence of a space capsule is neglected.

Configuration C (Dark Side of the Moon). The space man is suspended 136 miles from the moon's surface in the umbra region on the projected moon-sun centerline and is at the coldest possible point in a moon orbit when the orbit is at an angle of zero degrees with respect to the moon-sun centerline (see fig. 8). The presence of a space capsule is neglected.

Configuration D (Solar Side of Earth) defines the hottest possible point in an earth orbit when the orbit is at an angle of zero degrees with respect to the earth-sun centerline (see fig. 8). Specifically, the space man is suspended at a point 500 miles from the surface of the earth on the earth-sun centerline. The presence of a space capsule is neglected.

Configuration E (Dark Side of the Earth). The space man is suspended 500 miles in the umbra region from the surface of the earth on the projected earth-sun centerline (see fig. 8). He is at the coldest possible point in an earth orbit when the orbit is at an angle of zero degrees with respect to the earth-sun centerline. The presence of a space capsule is neglected.

Configuration F (Moon Orbit) is the moon orbit outlined in space configuration B (see fig. 9).

Configuration G (Earth Orbit) is the earth orbit outlined in space configuration D (see fig. 10).

Analytically, the total heat loads absorbed (Q_{absorbed}) by the space man in each of the space configurations A through G are

$$(1) \quad Q_A = \alpha_s S A_p + \alpha_{bs} E_{bs} A_s$$

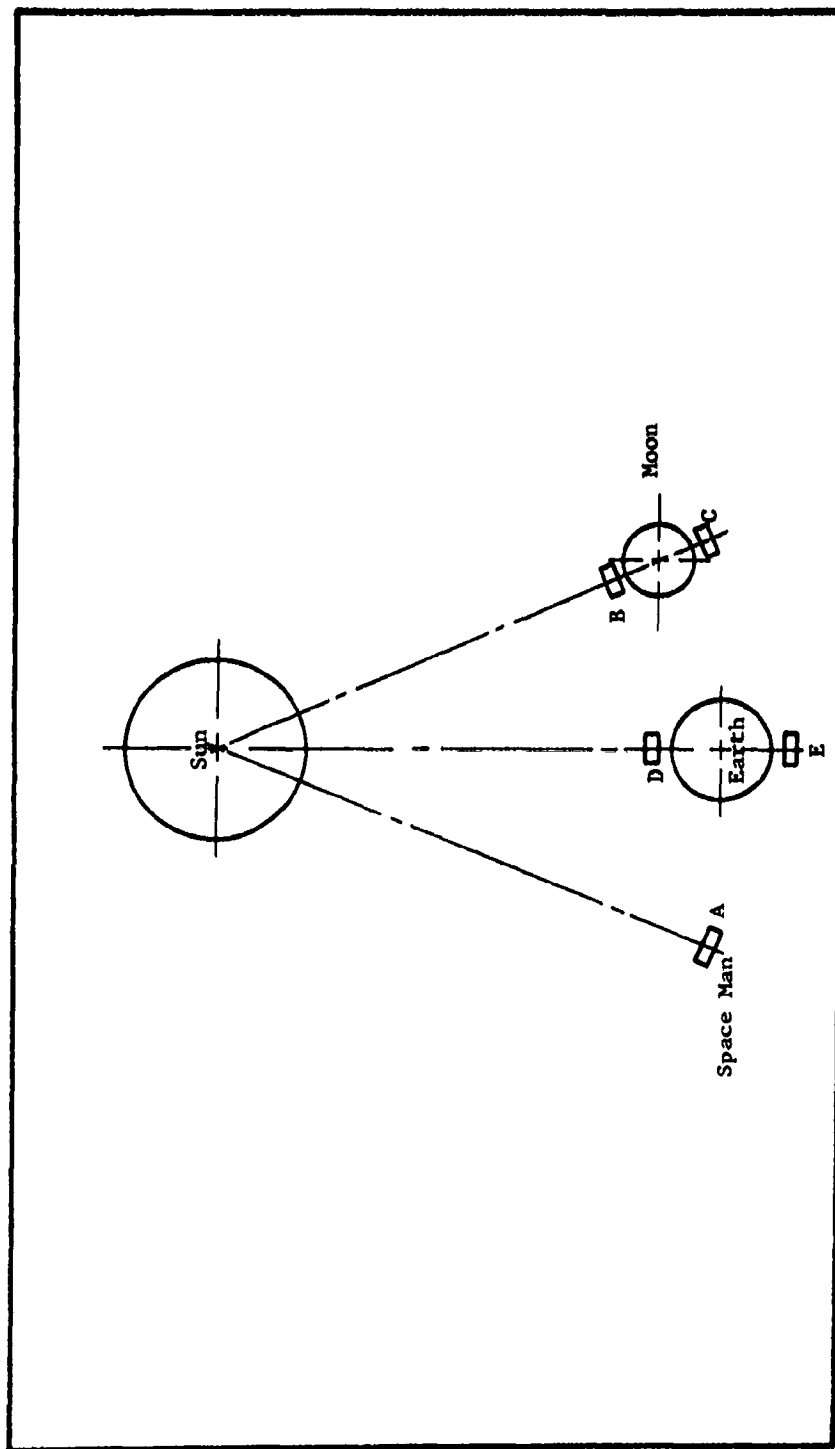


Figure 8. Space configurations A, B, C, D and E.

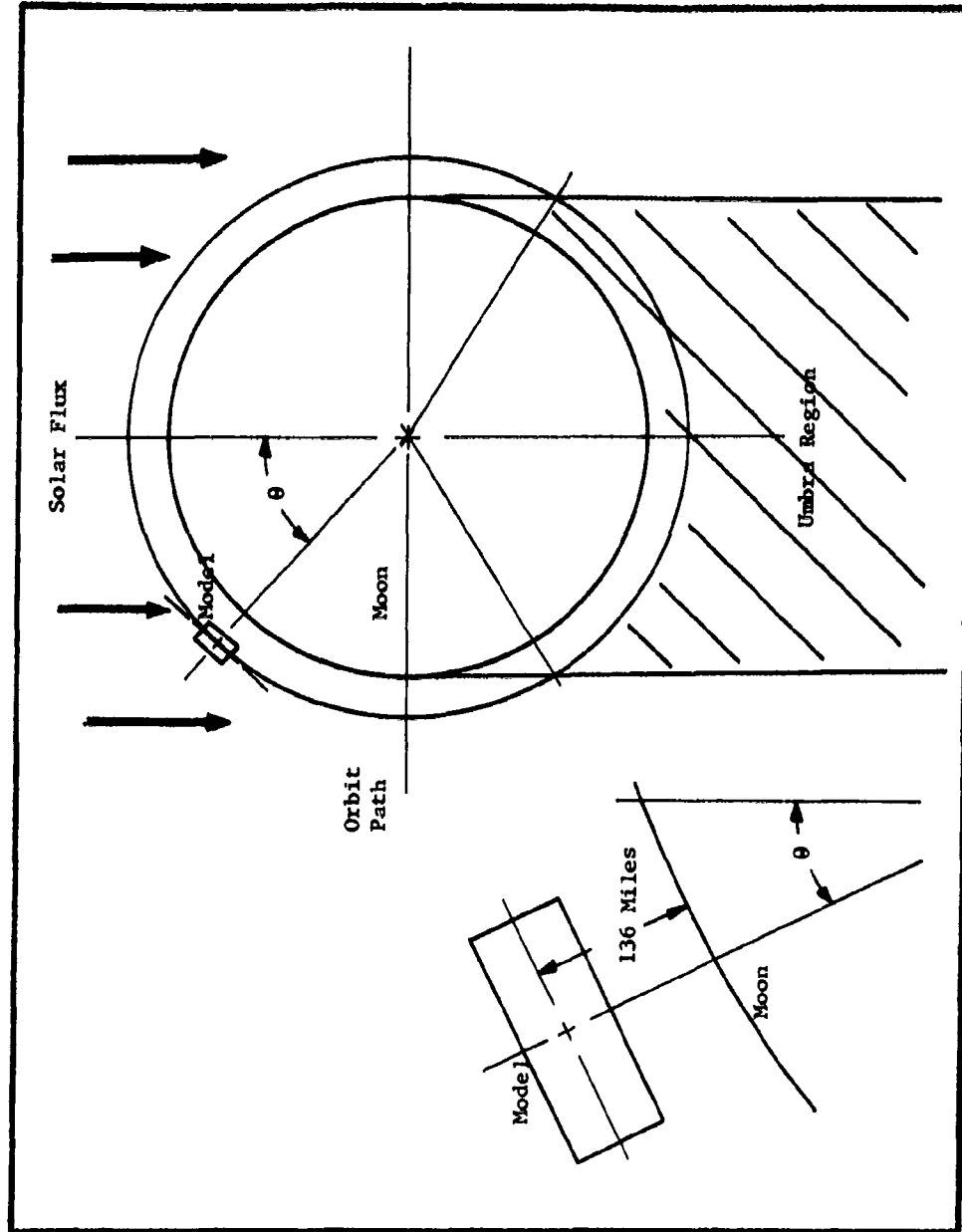


Figure 9. Space configuration F. Space man in orbit about the moon.

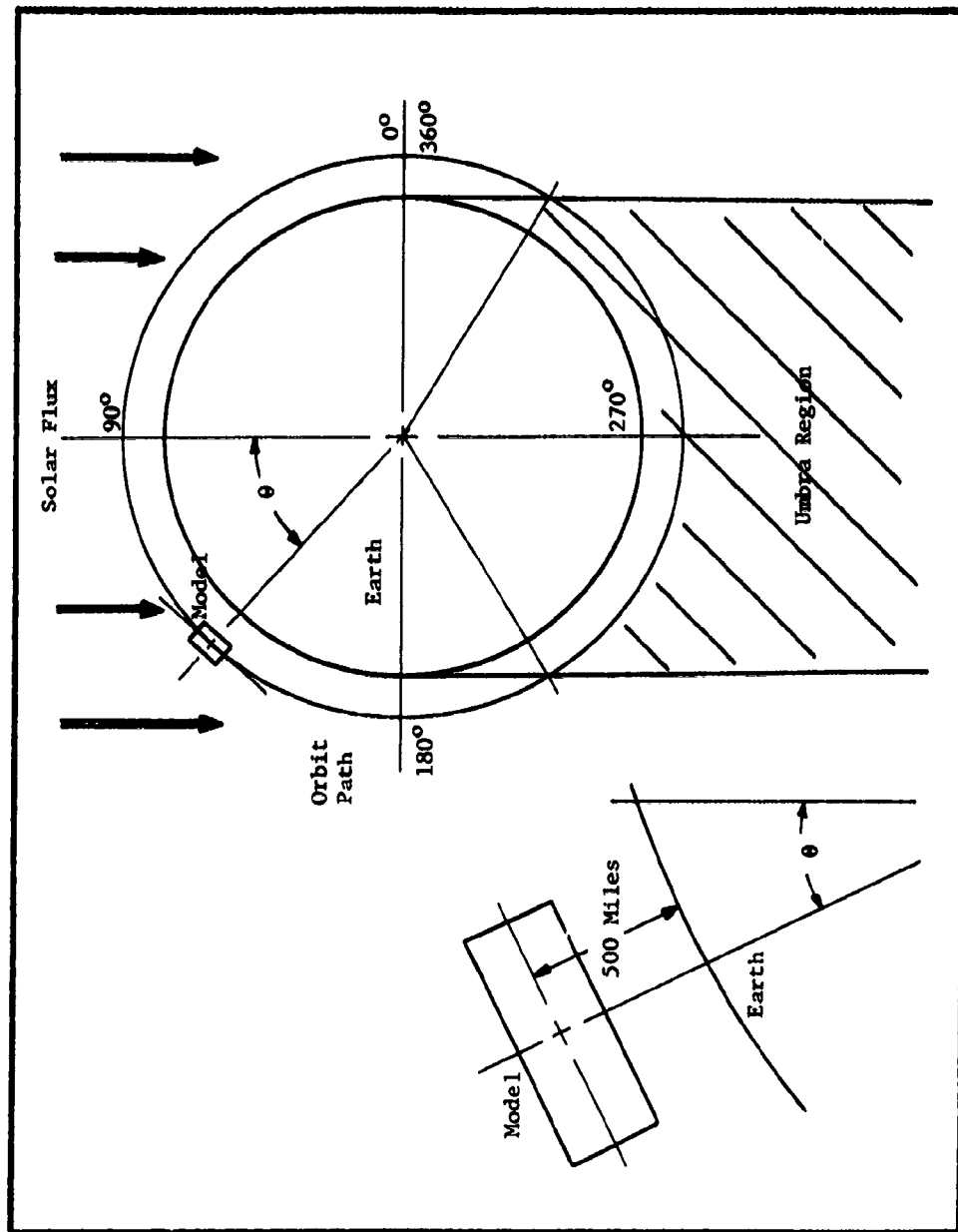


Figure 10. Space configuration G. Space man in orbit about the Earth.

$$(2) \quad Q_b = \alpha_s S A_p + \alpha_{ma} F_{ma} R_m A_p + \alpha_{me} F_{me} E_{me} A_p$$

$$(3) \quad Q_c = \alpha_{me} F_{me} E_{me} A_p + \alpha_{bs} A_s E_{bs}$$

$$(4) \quad Q_d = \alpha_s S A_p + \alpha_{ee} F_{ee} E_{ee} A_p + \alpha_{ea} F_{ea} R_e A_p$$

$$(5) \quad Q_e = \alpha_{ee} F_{ee} E_{ee} A_p + \alpha_{bs} E_{bs} A_s$$

$$(6) \quad Q_f = \alpha_s S [A_p \cos \theta + A_e \sin \theta]_{30}^{210} + A_p [F_{me} \alpha_{me} E_{ms}]_0^{180} + A_p [F_{me} \alpha_{me} E_{md}]_{180}^{360} \\ + A_p [\alpha_{ma} F_{ma} R_m]_0^{180}$$

$$(7) \quad Q_g = \alpha_s S [A_p \cos \theta + A_e \sin \theta]_{30}^{210} + A_p [\alpha_{ee} E_{es} F_{ee}]_0^{360} \\ + \alpha_{ea} F_{ea} R_e A_p]_0^{180}$$

α_s - space suit absorptance based on the sun as the energy source

S - solar constant

A_p - projected area of the space man

α_{bs} - space suit absorptance based on the energy spectrum of black space

E_{bs} - energy emitted by the black space environment

A_s - surface area of the space man

α_{ma} - space suit absorptance based on the energy spectrum of the moon's albedo

F_{ma} - shape factor for the moon's albedo

R_m - moon's albedo

α_{me} - space suit absorptance based on the temperature of the moon

F_{me} - emitted energy shape factor for the moon

E_{ms}, E_{md} - emitted energy of the moon

α_{ee} - space suit absorptance based on the earth's temperature

E_{ee} - emitted energy of the earth

α_{ea} - space suit absorptance based on the energy spectrum of the earth's albedo

F_{ea} - earth's albedo shape factor

R_e - earth's albedo

F_{ee} - emitted energy shape factor for the earth

Black space calculations are neglected for space configurations D, E, F and G and the heat absorbed by the space man due to the moon's and earth's emitted energy and albedo is given as a function of distance to the space man from the surface of the moon and earth in figures 11, 12 and 13. These results are then combined with equations 1, 2, 3, 4, 5, 6 and 7 to yield values of heat absorbed by the space man in terms of btu/hr. Moreover, in analyzing equations 1, 2, 3, 4, 5, 6 and 7 it is necessary to know the thermal radiation properties of the space suit in question. An initial assumption is:

Assume that the space suit is a diffuse greybody radiator.

Belasco based his analysis on the greybody assumption and suggested that an absorptance and/or emittance of 0.12 is somewhat representative of a typical space suit. His assumption is substantiated by fig. 14 which shows that the average reflectance for aluminized nylon cloth from 0.6 to 2.25 microns is essentially constant and that the average absorptance is approximately 0.12. Consider the space configurations. For calculations of the incident absorbed thermal radiation during the deep space probe, Belasco's assumption is probably valid since the heat absorbed due to the incident solar flux is transmitted primarily at wavelengths between 0.3 and 2.5 microns and since the incident energy absorbed due to black space is very small. Furthermore, analysis of configuration B shows that the assumption for the heat absorbed due to the solar flux and albedo flux is again feasible, but consider the moon's emitted energy. In this case the major portion of the absorbed energy is transmitted within a wavelength band of 2.8 to 27 microns. Consequently, there is no justification for assuming that the absorptance of the suit is 0.12 when subjected to these higher wavelength radiations. As a matter of fact, the average absorptance versus wavelength for aluminized cloth in the range of 2 to 9 microns (ref. 22) increases to about 0.3 (see fig. 14).

Thus, absorptance and emittance of probable space suit surfaces versus wavelength, say from 0.3 μ to 70 μ is essential for an exact thermal analysis. A review of the literature shows that this information is, in general, inaccessible. Therefore, the following procedure is adopted for the remainder of the report. Total heat load calculations are made for space configurations A, B, C, D, E, F and G in which the average absorptance for a given space suit is broken into two categories: (1) absorptance (α_s) based on short wavelength radiation or radiation transmitted at wavelengths less than 4 μ and (2) absorptance (α_h) based on higher wavelength radiation or radiation at wavelengths greater than 4 μ . The results of these calculations are then given in tabular form in terms of total heat absorbed by the space man (see Tables 2, 3, 4, 5, 6, 7 and 8) as α_s and α_h vary from values of 1.0 to 0.05.

These tables are used as follows:

Suppose that the absorptance and/or emittance for a given space suit is 0.12. Then, in order to determine the heat absorbed by the space man in

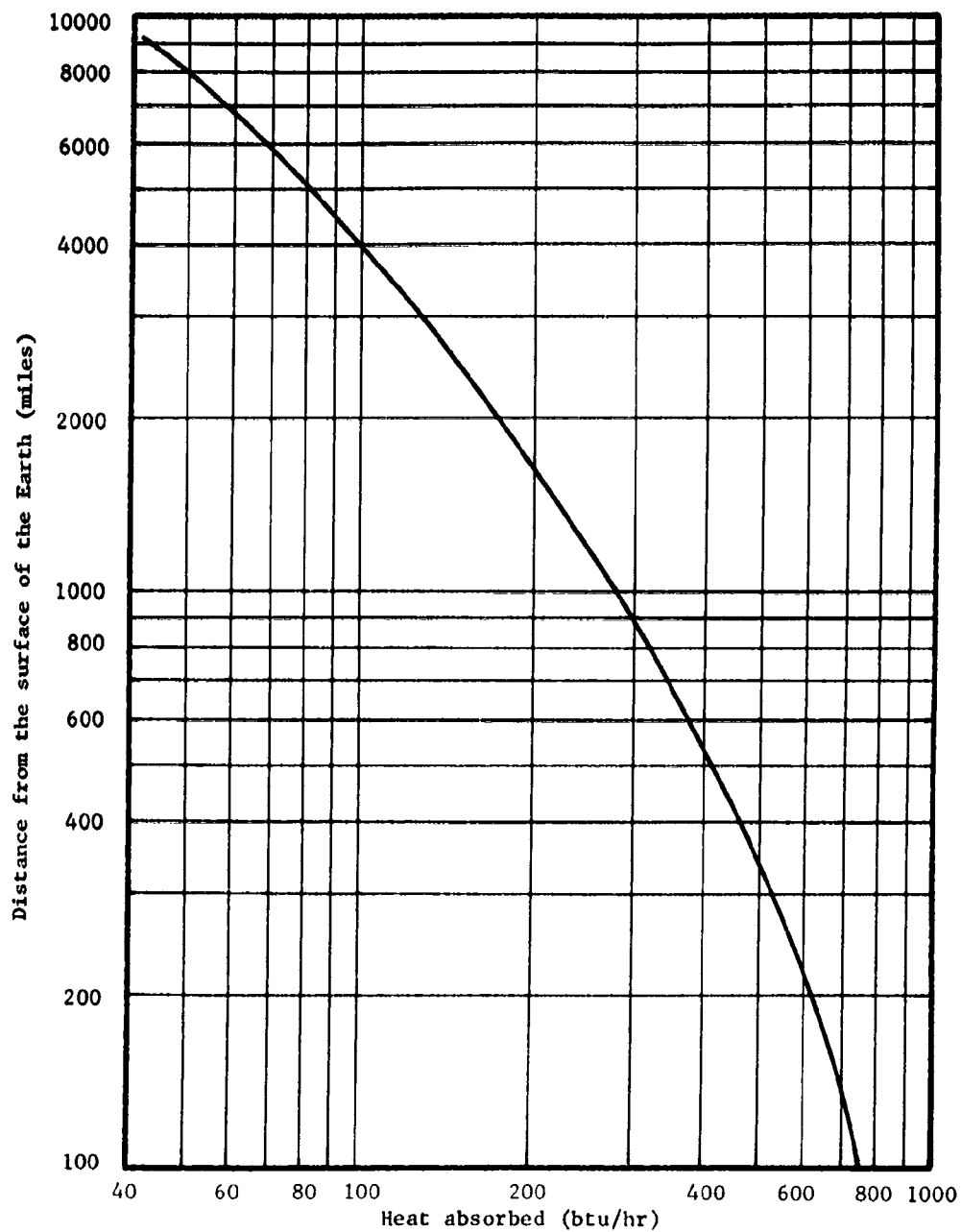


Figure 11. Variation of the Total heat absorbed by the cylindrical model with respect to the distance from the surface of the earth.

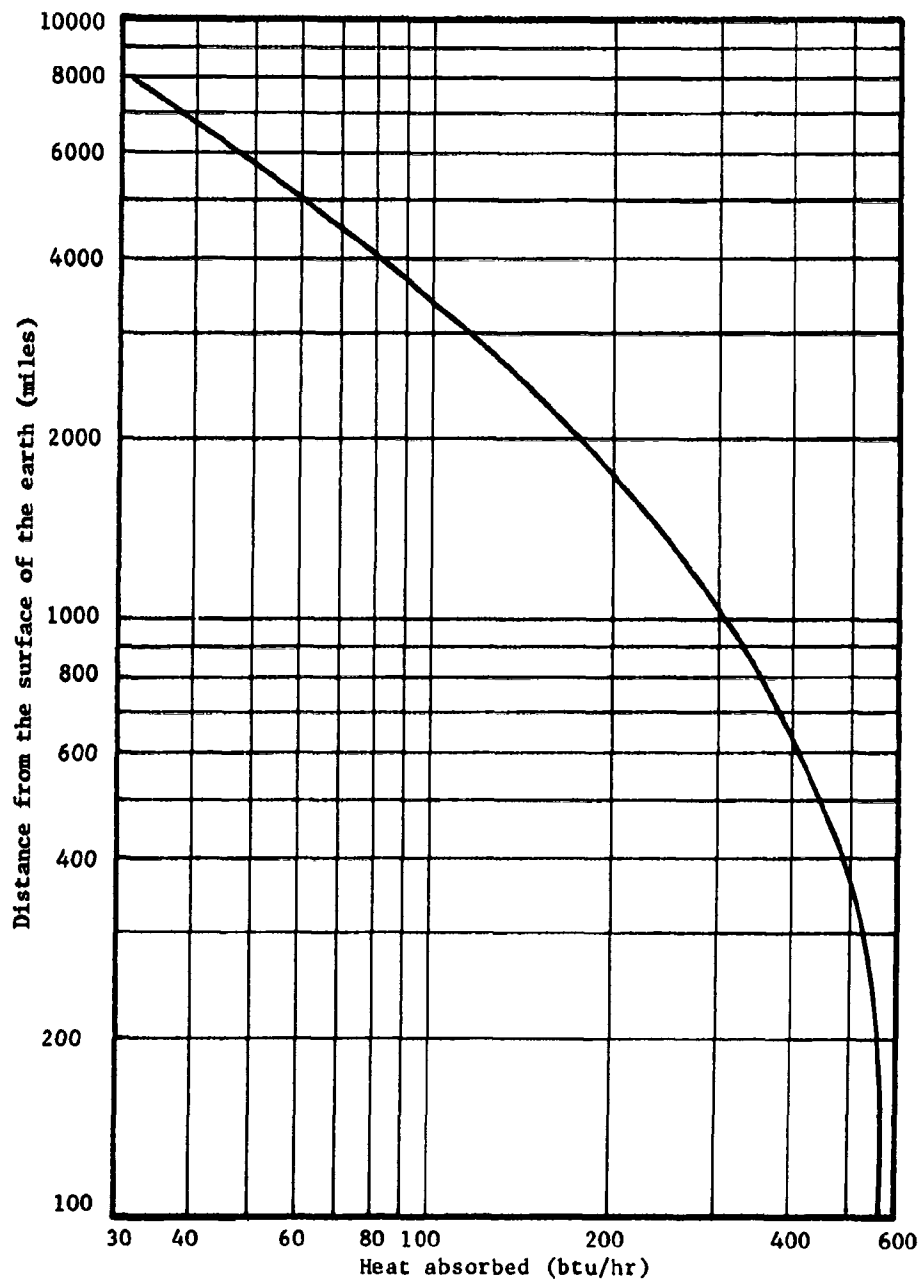


Figure 12. Variation of the total heat absorbed by the cylindrical model with respect to the distance from the surface of the earth for the earth's albedo.

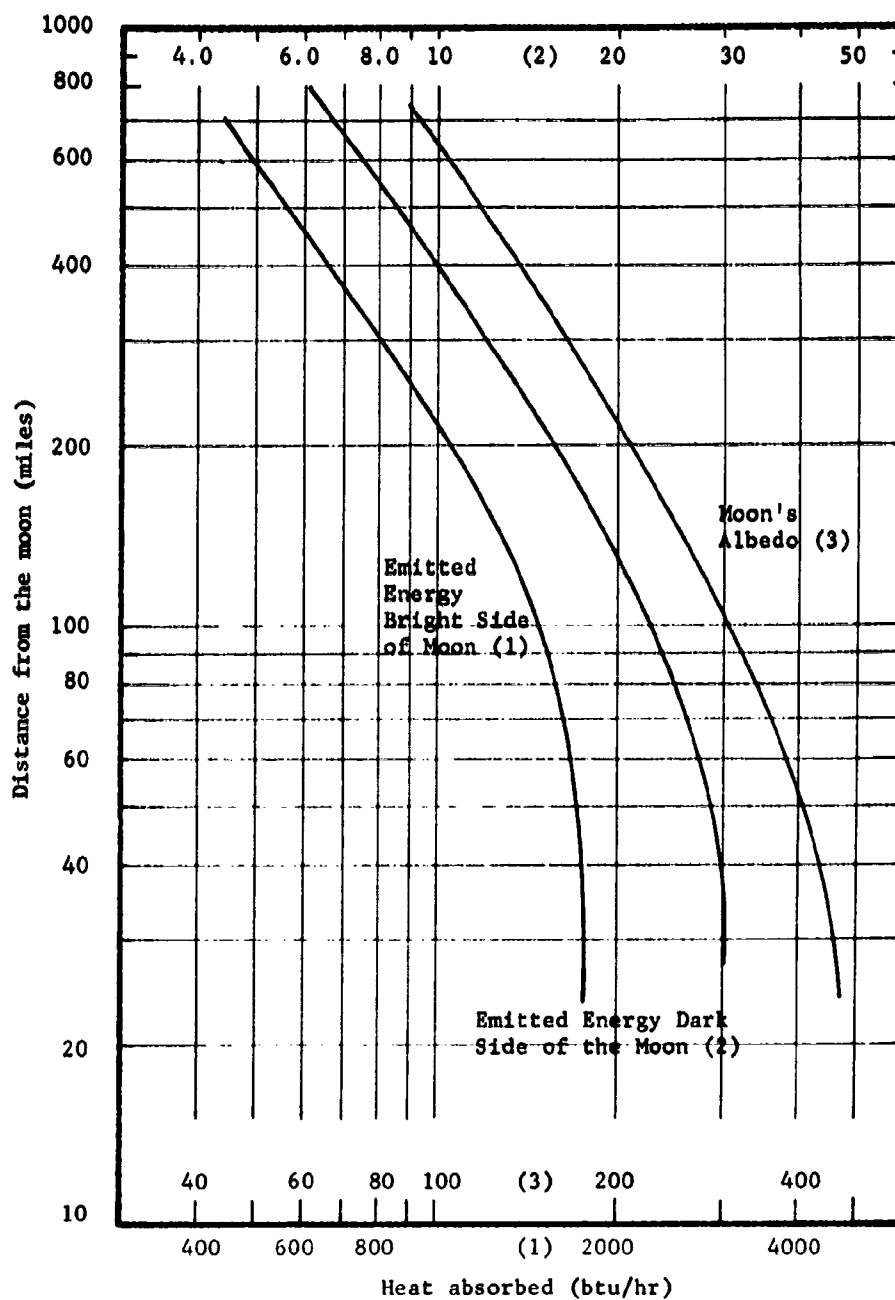
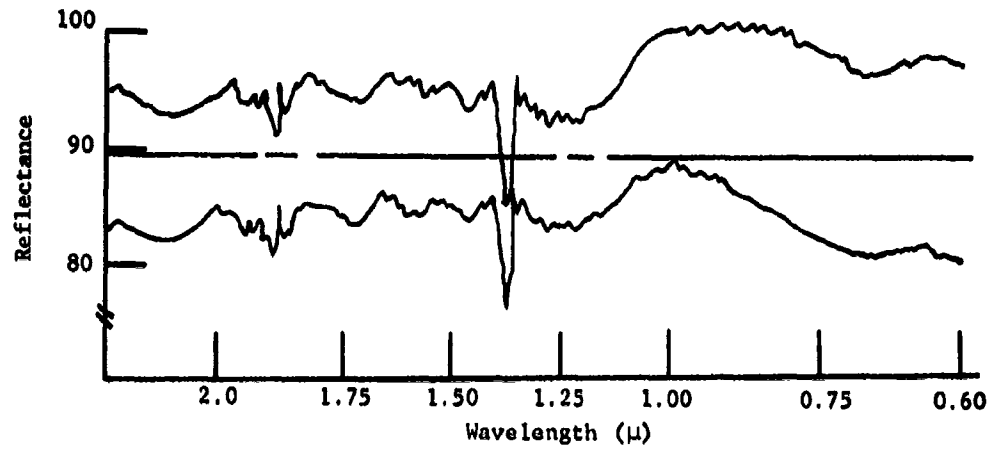
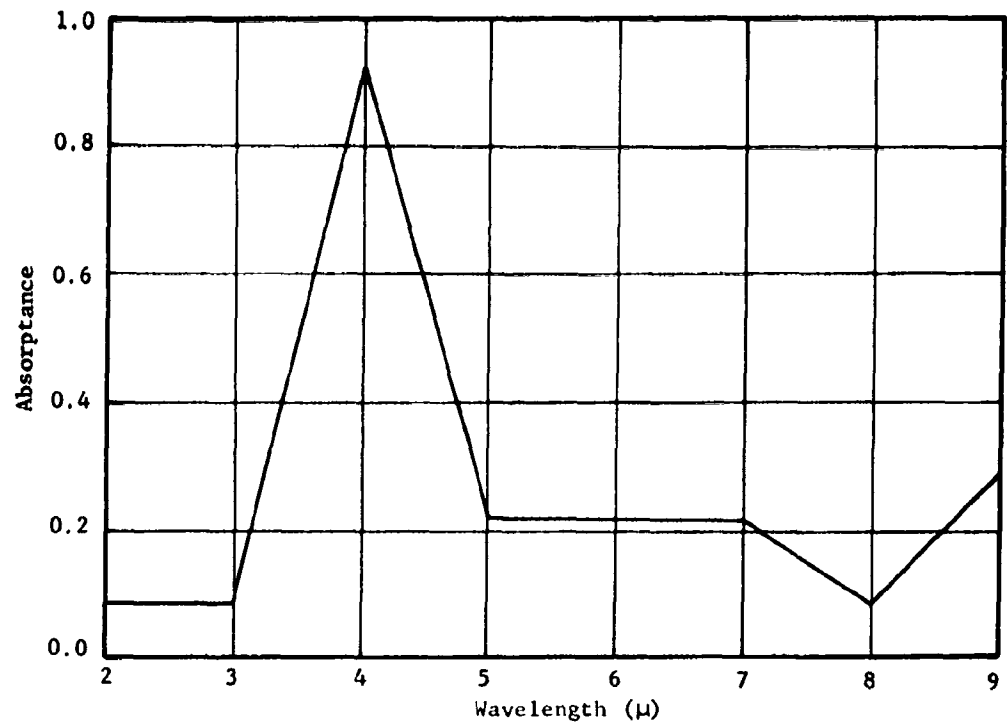


Figure 13. Variation of the heat absorbed due to the moon's emitted energy and albedo for the cylindrical model with respect to the distance of the model from the surface of the moon.



Average reflectance for aluminized nylon cloth.



Average absorbance for aluminized nylon cloth.

Figure 14. Average absorbance and reflectance for aluminized nylon cloth at different wavelengths.

TABLE 2
NEGATIVE MERT ASSUMED (RTU/MR) BY THE
CUMULATIVE MERT IN SPACE CONFIGURATION A

q_c	$Q(\text{Solar})$	$Q(\text{Black Space})$ as q_c varies from 1.0 to 0.05															
		1.0	0.9	0.8	0.7	0.6	0.5	0.4	0.3	0.2	0.16	0.12	0.1	0.05	0.05	0.1	0.6
1.0	2419	2830	2820	2826	2827	2826	2825	2824	2822	2821	2821	2820	2820	2820	2820	2820	2820
0.9	2827	2838	2837	2836	2835	2834	2833	2832	2830	2829	2829	2828	2828	2828	2828	2828	2828
0.8	2335	2345	2344	2343	2342	2341	2340	2338	2337	2337	2337	2336	2336	2336	2336	2336	2336
0.7	2043	2054	2053	2052	2051	2050	2049	2048	2046	2045	2045	2044	2044	2044	2044	2044	2044
0.6	1751	1762	1761	1760	1759	1758	1757	1756	1754	1753	1753	1753	1753	1753	1753	1753	1753
0.5	1460	1471	1470	1469	1468	1467	1466	1465	1463	1462	1462	1461	1461	1461	1461	1461	1461
0.4	1168	1179	1178	1177	1176	1175	1174	1173	1171	1170	1170	1169	1169	1169	1169	1169	1169
0.3	876	887	886	885	884	883	882	881	879	878	878	877	877	877	877	877	877
0.2	584	596	594	593	592	591	590	589	587	586	586	585	585	585	585	585	585
0.16	487	478	477	476	475	474	473	472	470	469	469	468	468	468	468	468	468
0.12	380	381	380	379	378	377	376	375	373	372	372	371	371	371	371	371	371
0.1	282	303	302	301	300	299	298	297	295	294	294	293	293	293	293	293	293
0.06	146	137	136	135	134	133	132	131	129	128	128	127	127	127	127	127	127

TABLE 3
RADIATIVE HEAT ABSORBED (BTU/HR) BY THE
CALIBRATED MODEL IN SPACE CONFIGURATION 8

Q(Emitted Solar Side of Moon) as ϵ_m Varies from 1.0 to 0.05															
ϵ_s	Q_{Solar}	Q_{Albedo}	1.0	0.9	0.8	0.7	0.6	0.5	0.4	0.3	0.2	0.16	0.12	0.1	0.05
1.0	2807	127	2876	2498	2161	1873	1606	1358	1070	803	535	428	321	208	134
0.9	2616	114	2683	2333	2026	1773	1552	1352	1104	817	549	448	335	222	148
0.8	2416	102	2480	2152	1875	1675	1500	1340	1132	905	637	538	423	310	206
0.7	2226	90	2278	2010	1775	1675	1500	1340	1132	905	637	538	423	310	206
0.6	2035	80	2066	1887	1720	1582	1465	1358	1227	1072	834	717	610	507	423
0.5	1844	70	1875	1720	1582	1465	1358	1227	1072	834	717	610	507	423	310
0.4	1654	60	1685	1544	1412	1300	1200	1112	1032	968	908	852	802	752	702
0.3	1463	50	1494	1372	1260	1160	1080	1012	958	908	852	802	752	702	652
0.2	1272	40	1303	1200	1100	1020	960	908	852	802	752	702	652	602	552
0.1	1081	30	1112	1020	940	880	828	784	744	708	672	640	608	576	544
0.05	890	20	921	840	770	718	672	632	596	564	532	504	476	448	420
0.04	799	15	830	750	680	628	584	544	508	476	448	420	392	364	336
0.03	708	10	739	660	590	538	494	454	418	386	358	330	302	274	246
0.02	617	5	648	570	500	448	404	364	328	296	268	240	212	184	156
0.01	526	0	557	480	410	358	314	274	238	206	178	150	122	94	66
0.005	435	0	466	390	320	268	224	184	148	116	88	60	32	4	0

TABLE 4
RELATIVE MEAT AMOUNTS (RTU/MS) AT THE
CHARACTERISTIC POINTS IN SPACE CONFIGURATION C

$Q(\text{Mean})$	$Q(\text{Mean})$ varies from 1.0 to 0.05															
	1.0	0.9	0.8	0.7	0.6	0.5	0.4	0.3	0.2	0.16	0.12	0.1	0.05	0.05	0.05	0.05
1.0	181	180	179	178	177	176	175	173	172	172	171	171	171	171	171	171
0.9	153	164	163	162	161	160	159	158	156	155	155	154	154	154	154	154
0.8	136	147	146	145	144	143	142	141	139	138	138	137	137	137	137	137
0.7	119	130	129	128	127	127	127	126	124	123	123	122	122	122	122	122
0.6	102	113	112	111	110	109	108	107	105	104	104	103	103	103	103	103
0.5	85	96	95	94	93	92	91	90	88	87	87	86	86	86	86	86
0.4	68	79	78	77	76	75	74	73	71	70	70	69	69	69	69	69
0.3	51	62	61	60	59	58	57	56	54	53	53	52	52	52	52	52
0.2	34	45	44	43	42	41	40	39	37	36	36	35	35	35	35	35
0.16	27	38	37	36	35	34	33	32	30	29	29	28	28	28	28	28
0.12	20	31	30	29	28	27	26	25	23	22	22	21	21	21	21	21
0.1	17	28	27	26	25	24	23	22	20	19	19	18	18	18	18	18
0.05	9	20	19	18	17	16	15	14	12	11	10	10	10	10	10	10

TABLE 5
RADIATIVE HEAT ABSORBED (WU/M²) BY THE
CYLINDRICAL WHEEL IN SPACE CONFIGURATION D

α_g	Q_{Solar}	Q_{Albedo}	$Q(\text{Irradiated Solar Side of Earth}) \text{ as } \phi_g \text{ varies from } 1.0 \text{ to } 0.05$													
			1.0	0.9	0.8	0.7	0.6	0.5	0.4	0.3	0.2	0.1	0.05	0.05	0.1	0.05
1.0	2007	897	1128	1085	1042	998	954	913	869	826	783	740	740	740	740	718
0.9	2016	627	1056	1015	972	928	886	843	798	756	713	669	629	629	629	608
0.8	2326	558	1074	1031	988	945	902	859	815	772	729	686	643	643	643	622
0.7	2015	468	819	876	833	790	747	704	660	617	574	531	531	531	531	510
0.6	1744	418	849	896	853	810	767	724	681	638	595	552	552	552	552	531
0.5	1454	348	779	826	783	740	697	654	611	568	525	482	482	482	482	461
0.4	1143	279	710	757	714	671	628	585	542	499	456	413	413	413	413	392
0.3	872	209	640	687	644	601	558	515	472	429	386	343	343	343	343	322
0.2	561	139	570	617	574	531	488	445	402	359	316	273	273	273	273	252
0.1	465	112	543	590	547	504	461	418	375	332	289	246	246	246	246	225
0.05	145	35	446	493	450	407	364	321	278	235	192	149	149	149	149	128

TABLE 6
RADIATIVE HEAT ABSORBED (BTU/HR) BY THE
CYLINDRICAL MODEL IN SPACE CONFIGURATION 2

α_{eff}	$Q(\text{Earth})$	$Q(\text{Black Space})$ and α_{eff} varies from 1.0 to 0.05															
		1.0	0.9	0.8	0.7	0.6	0.5	0.4	0.3	0.2	0.16	0.12	0.1	0.05			
		11.4	10.3	9.1	8.0	6.8	5.7	4.6	3.4	2.3	1.8	1.4	1.1	0.6			
1.0	431	648	441	440	439	438	437	436	434	433	433	432	432	432			
0.9	388	388	388	387	386	385	384	383	381	380	380	380	380	380			
0.8	345	356	355	354	353	353	351	350	348	347	347	346	346	346			
0.7	302	313	312	311	310	309	308	307	305	304	304	303	303	303			
0.6	259	270	269	268	267	266	265	264	262	261	261	260	260	260			
0.5	216	227	226	225	224	223	222	221	219	218	218	217	217	217			
0.4	173	183	182	181	180	179	178	177	175	174	174	173	173	173			
0.3	129	140	139	138	137	136	135	134	132	131	131	130	130	130			
0.2	86	97	96	95	94	93	92	91	89	88	88	87	87	87			
.16	69	80	79	78	77	76	75	74	72	71	71	70	70	70			
.12	52	63	62	61	60	59	58	57	55	54	54	53	53	53			
0.1	43	54	53	52	51	50	49	48	46	45	45	44	44	44			
.05	23	33	32	31	30	29	28	27	25	24	24	23	23	23			

TABLE 7 PAGE 1
HEAT ABSORBED BY THE CALIBRATIONS HEREIN
IN SPACE CONFIGURATION 7

Degrees	Orbit Time (minutes)	$\phi = 1.9$			$\phi = 0.9$			$\phi = 0.9$		
		Solar	Earth	Albedo Total	Solar	Earth	Albedo Total	Solar	Earth	Albedo Total
0	0	400	431	687	300	300	627	327	345	588
30	7	1000	431	1337	1026	300	1303	1420	345	1200
60	14	2715	431	2836	2446	300	2843	2174	345	2333
90	21	2804	431	3046	2616	300	3041	2226	345	2677
120	28	2715	431	2836	2446	300	2843	2174	345	2333
150	35	1000	431	1337	1027	300	1303	1420	345	1200
180	42	400	431	687	300	300	627	327	345	588
210	49	1000	431	2836	1027	300	1303	1420	345	1200
240	56	-	431	-	-	300	2843	-	345	1795
270	63	-	431	431	-	300	300	-	345	345
300	70	-	431	431	-	300	300	-	345	345
330	77	1000	431	2836	1027	300	1303	1420	345	1795
360	84	400	431	687	300	300	627	327	345	588
				1337			1303			1200

TABLE 7 CONTINUED
PAGE 2

Degrees	Orbit Time (minutes)	$\alpha - 0.7$			$\alpha - 0.6$			$\alpha - 0.5$		
		Solar	Earth	Albedo Total	Solar	Earth	Albedo Total	Solar	Earth	Albedo Total
0	0	284	302	488 1076	245	259	418 922	205	216	348 769
30	7	1266	302	488 2056	1045	259	418 1762	904	216	348 1468
60	14	1903	302	488 2693	1631	259	418 2306	1359	216	348 1923
90	21	2035	302	488 2825	1744	259	418 2421	1454	216	348 2018
120	28	1903	302	488 2693	1631	259	418 2306	1359	216	348 1923
150	35	1266	302	488 2056	1045	259	418 1762	904	216	348 1468
180	42	284	302	488 1076	245	259	418 922	205	216	348 769
210	49	1266	302	- 1568	1045	259	- 1344	904	216	- 1120
240	56	-	302	- 302	-	259	- 259	-	216	- 216
270	63	-	302	- 302	-	259	- 259	-	216	- 216
300	70	-	302	- 302	-	259	- 259	-	216	- 216
330	77	1266	302	- 1568	1045	259	- 1344	904	216	- 1120
360	84	284	302	488 1076	245	259	418 922	205	216	348 769

TABLE 7. CONTINUED
PAGE 3

Degrees	Orbit Time (minutes)	d=0.4			d=0.3			d=0.2		
		Solar	Earth	Albedo Total	Solar	Earth	Albedo Total	Solar	Earth	Albedo Total
0	"	164	172	279 615	123	129	209 461	82	86	139 307
30	7	723	172	279 1174	542	129	209 890	362	86	139 587
60	14	1087	172	279 1538	815	129	209 1153	544	86	139 769
90	21	1165	172	279 1614	872	129	209 1210	581	86	139 806
120	28	1087	172	279 1538	815	129	209 1153	544	86	139 769
150	35	723	172	279 1174	542	129	209 890	362	86	139 587
180	42	164	172	279 615	123	129	209 461	82	86	139 307
210	49	723	172	279 1174	542	129	209 890	362	86	139 587
240	56	-	172	- 172	-	129	- 129	-	86	- 86
270	63	-	172	- 172	-	129	- 129	-	86	- 86
300	70	-	172	- 172	-	129	- 129	-	86	- 86
330	77	723	172	279 1174	542	129	209 890	362	86	139 587
360	84	164	172	279 615	123	129	209 461	82	86	139 307

TABLE 7. CONTINUED.
PAGE 4

i.e. reas	Orbit Time (minutes)	$\alpha_{-0.16}$			$\alpha_{-0.12}$			$\alpha_{-0.1}$		
		Solar	Earth	Albedo Total	Solar	Earth	Albedo Total	Solar	Earth	Albedo Total
0	0	65	69	112 246	49	52	84 185	41	43	70 154
30	7	289	69	112 470	217	52	84 353	181	43	70 294
60	14	435	69	112 616	326	52	84 462	272	43	70 385
90	21	465	69	112 646	349	52	84 485	291	43	70 404
120	28	435	69	112 616	326	52	84 462	272	43	70 385
150	35	289	69	112 470	217	52	84 353	181	43	70 294
180	42	65	69	112 246	49	52	84 185	41	43	70 154
210	49	289	69	- 358	217	52	- 269	181	43	- 224
240	56	-	69	- 69	-	52	- 52	-	43	- 43
270	63	-	69	- 69	-	52	- 52	-	43	- 43
300	70	-	69	- 69	-	52	- 52	-	43	- 43
330	77	289	69	- 358	217	52	- 269	181	43	- 224
360	84	65	69	112 246	49	52	84 185	41	43	70 154

Table 1. Continued.
PAGE 5

Degrees	Orbit Time (minutes)	$\alpha = 0.05$		
		Solar	Earth	Albedo Total
0	0	21	22	45
30	7	91	22	35
60	14	136	22	148
90	21	146	22	35
120	28	156	22	193
150	35	91	22	35
180	42	21	22	20.1
210	49	91	22	35
240	56	-	22	22
270	63	-	22	22
300	70	-	22	22
330	77	91	22	22
360	84	21	22	113
				7.7

TABLE 3 PAGE 1
HEAT ABSORBED BY THE CYLINDRICAL MODEL
IN SPACE CONFIGURATION C

Decrease	Orbit Time (minutes)	N = 1.0		N = 0.9		N = 0.8							
		Solar Moon	Albedo Total	Solar Moon	Albedo Total	Solar Moon	Albedo Total						
0	0	409	2676	127	3212	368	2408	114	2890	327	2141	102	2570
30	10	1808	2676	127	4611	1627	2408	114	4149	1450	2141	102	3883
60	20	2718	2676	127	5521	2446	2408	114	4968	2174	2141	102	4417
90	30	2907	2676	127	5710	2616	2408	114	5138	2326	2141	102	4599
120	40	2718	2676	127	5521	2446	2408	114	4968	2174	2141	102	4417
150	50	1808	2676	127	4611	1627	2408	114	4149	1450	2141	102	3883
180	60	409	2676	127	3212	368	2408	114	2890	327	2141	102	2570
210	70	1808	265	-	2073	1627	239	-	1866	1450	212	-	1682
240	80	-	285	-	285	-	239	-	239	-	212	-	212
270	90	-	285	-	285	-	239	-	239	-	212	-	212
300	100	-	285	-	285	-	239	-	239	-	212	-	212
330	110	1808	285	-	2073	1627	239	-	1866	1450	212	-	1682
360	120	409	2876	127	3212	368	2408	114	2890	327	2141	102	2570

TABLE 8. CONTINUED
PAGE 2

Degrees	Orbit Time (minutes)	$\alpha = 0.7$		$\alpha = 0.6$		$\alpha = 0.5$					
		Solar	Albedo Total	Solar	Albedo Total	Solar	Albedo Total				
0	0	286	1873	89	245	1806	76	205	1338	64	1807
30	10	1266	1873	89	1085	1806	76	904	1338	64	2306
60	20	1903	1873	89	1631	1806	76	1359	1338	64	2761
90	30	2035	1873	89	1744	1806	76	1454	1338	64	2856
120	40	1903	1873	89	1631	1806	76	1359	1338	64	2761
150	50	1266	1873	89	1085	1806	76	904	1338	64	2306
180	60	286	1873	89	245	1806	76	205	1338	64	1807
210	70	1266	186	1452	1085	159	1244	904	133	1037	-
240	80	-	186	-	-	159	-	-	133	-	133
270	90	-	186	-	-	159	-	-	133	-	133
300	100	-	186	-	-	159	-	-	133	-	133
330	110	1266	186	-	1085	159	-	904	133	-	1037
360	120	286	1873	89	245	1806	76	205	1338	64	1807

TABLE 8. CONTINUED
PAGE 3

Degrees	Orbit Time (minutes)	$\lambda = -0.4$		$\lambda = -0.3$		$\lambda = -0.2$	
		Solar	Albedo	Solar	Albedo	Solar	Albedo
		Moon	Total	Moon	Total	Moon	Total
0	0	164	1070	51	1285	82	944
30	10	723	1070	51	1285	38	944
60	20	1067	1070	51	1285	38	944
90	30	1163	1070	51	1285	38	944
120	40	1067	1070	51	1285	38	944
150	50	723	1070	51	1285	38	944
180	60	164	1070	51	1285	38	944
210	70	723	106	51	1285	38	944
240	80	-	106	-	106	-	106
270	90	-	106	-	106	-	106
300	100	-	106	-	106	-	106
330	110	723	106	51	1285	38	944
360	120	164	1070	51	1285	38	944

TABLE 8 CONTINUED
PAGE 4

Degrees	Orbit Time (minutes)	$\alpha = 0.16$			$\alpha = 0.12$			$\alpha = 0.1$		
		Solar	Moon	Albedo Total	Solar	Moon	Albedo Total	Solar	Moon	Albedo Total
0	0	65	428	20 513	49	321	15 385	41	248	13 322
30	10	289	428	20 737	217	321	15 533	181	248	13 442
60	20	435	428	20 883	328	321	15 682	272	248	13 553
90	30	485	428	20 913	349	321	15 685	281	248	13 572
120	40	435	428	20 883	328	321	15 682	272	248	13 553
150	50	289	428	20 737	217	321	15 533	181	248	13 442
180	60	65	428	20 513	49	321	15 385	41	248	13 322
210	70	289	42	331	217	32	-	181	27	-
240	80	-	42	42	-	32	-	-	27	-
270	90	-	42	42	-	32	-	-	27	-
300	100	-	42	42	-	32	-	-	27	-
330	110	289	42	331	217	32	-	181	27	-
360	120	65	428	20 513	49	321	15 385	41	248	13 322

TABLE 2 CONTINUED
PAGE 5

Degrees	Orbit Plane Tilt (in degrees)	$\alpha = 0.05$		
		Polar	Mean	Albedo Total
0	0	21	134	7 162
30	10	91	134	7 233
60	20	136	134	7 277
90	30	145	134	7 286
120	40	136	134	7 277
150	50	91	134	7 233
180	60	21	134	7 162
210	70	91	13	- 184
240	80	-	13	- 13
270	90	-	13	- 13
300	100	-	13	- 13
330	110	91	13	- 164
360	120	21	134	7 162

space configuration A, for instance, find in TABLE 2 the appropriate value of $Q(\text{solar})$, 350 btu/hr, corresponding to α_s equal 0.12 in the column labeled $Q(\text{solar})$. Also, find the value of $Q(\text{black space})$, 1.4 btu/hr, in the column labeled $Q(\text{black space})$ corresponding to α_{bs} equal 0.12. Hence, the solar side of the space man absorbs heat at the rate of only 1.4 btu/hr. The total heat absorbed by the model is approximately 351 btu/hr. A similar procedure is used for configurations B, C, D, E, F and G. As a final example (other examples are given in Appendix V), the total heat absorbed by the model in configuration B when the absorptance and emittance are 0.12 is given in terms of $Q(\text{solar})$, $Q(\text{albedo})$ and $Q(\text{emitted})$. Selection of the appropriate absorbed heat terms from TABLE 3 shows that $Q(\text{solar})$, $Q(\text{albedo})$ and $Q(\text{emitted})$ are 350, 15 and 321 btu/hr, respectively, or the total heat absorbed relative to the solar side of the man is 350 btu/hr while the total heat absorbed on the moon side is 336 btu/hr. The total heat absorbed on both sides of the man is 685 btu/hr.

HYPOTHETICAL CHAMBER CONFIGURATIONS I, II, III AND IV

Chamber I properties are given as follows:

- (1) The effective radiation area of the chamber is 210 ft².
- (2) The internal chamber pressure is zero atmospheres.
- (3) The chamber walls are diffuse blackbody radiators.
- (4) There are no internal radiation sources present except the subject and the chamber walls.
- (5) The wall temperatures vary from 320 R to 950 R.
- (6) Any heat gained by the subject due to conduction is negligible.
- (7) A non-absorbing medium exists between the chamber walls and the subject.

The total amount of heat absorbed in btu/hr by the cylindrical model in chamber I is given in tabular and graphical form (see TABLE 9 and Figure 15) at wall temperatures ranging from 320 R to 950 R and for subject absorptances (ϵ) varying from 1.0 to 0.05. For an absorptance of 1.0, $Q(\text{absorbed})$ varies from 365 btu/hr at a wall temperature of 320 R to 28,345 btu/hr at a wall temperature of 950 R. For an absorptance of 0.05, $Q(\text{absorbed})$ varies from 18 btu/hr at a wall temperature of 320 R to 1375 btu/hr at a wall temperature of 950 R.

Chamber II is identical to chamber I except that the effective radiation area of the chamber is divided into two individual energy fields such that the temperatures of each field can be controlled separately from 320 R to 950 R. For instance, the temperature of the top half of the chamber can be a maximum value of 950 R while the wall temperature of the bottom half is a minimum of 320 R. The total heat absorbed by the cylindrical model in chamber II is given in tabular and graphical form in TABLE 10 and fig. 16 in terms of heat absorbed versus chamber wall temperature (320 R to 950 R) for subject absorptances varying from 1.0 to 0.05. For a subject absorptance of 1.0 $Q(\text{absorbed})$ varies from 183 btu/hr ($T_w = 320$ R) to 14,172 btu/hr ($T_w = 950$ R) while for a subject absorptance of 0.05, $Q(\text{absorbed})$ varies from 9 btu/hr ($t_w = 320$) to 709 btu/hr at a wall temperature of 950 R. Chamber II is, of course, identical to chamber I as long as the wall temperatures of each half of the chamber are the same.

Chamber III is identical to chamber I with the following exceptions:

- (1) The emittance and absorptance of the chamber walls are 0.94.

TABLE 9
RADIATIVE HEAT ABSORBED BY THE
CYLINDRICAL MODEL IN CHAMBER 1

wall Temp (R)	Heat Absorbed (Btu/hr)														
	Space Suit Absorptivity														
	1.0	0.9	0.8	0.7	0.6	0.5	0.4	0.3	0.2	0.16	0.12	0.1	0.05		
320	365	329	292	256	219	183	146	109	73	58	44	37	18		
350	522	470	418	365	313	261	209	156	104	84	63	52	26		
400	889	800	711	622	533	445	356	267	178	142	107	89	45		
450	1427	1284	1142	999	856	714	571	428	285	228	171	143	71		
500	2175	1938	1740	1522	1305	1088	870	652	435	348	261	218	108		
550	3134	2866	2547	2228	1910	1592	1274	955	637	509	382	318	159		
600	4510	4059	3608	3157	2706	2255	1804	1353	902	722	541	451	226		
650	6212	5591	4970	4348	3727	3106	2485	1864	1242	994	746	622	310		
700	8355	7520	6684	5849	5013	4178	3342	2507	1671	1337	1003	836	418		
750	11011	9910	8808	7708	6607	5506	4404	3303	2202	1762	1321	1101	550		
800	14254	12829	11403	9978	8552	7127	5702	4276	2851	2281	1710	1428	713		
850	18166	16349	14533	12716	10900	9083	7266	5450	3633	2807	2180	1816	907		
900	22832	20549	18266	15982	13700	11416	9133	6850	4566	3653	2740	2284	1142		
950	28345	25511	22676	19942	17007	14173	11338	8504	5689	4535	3401	2835	1372		

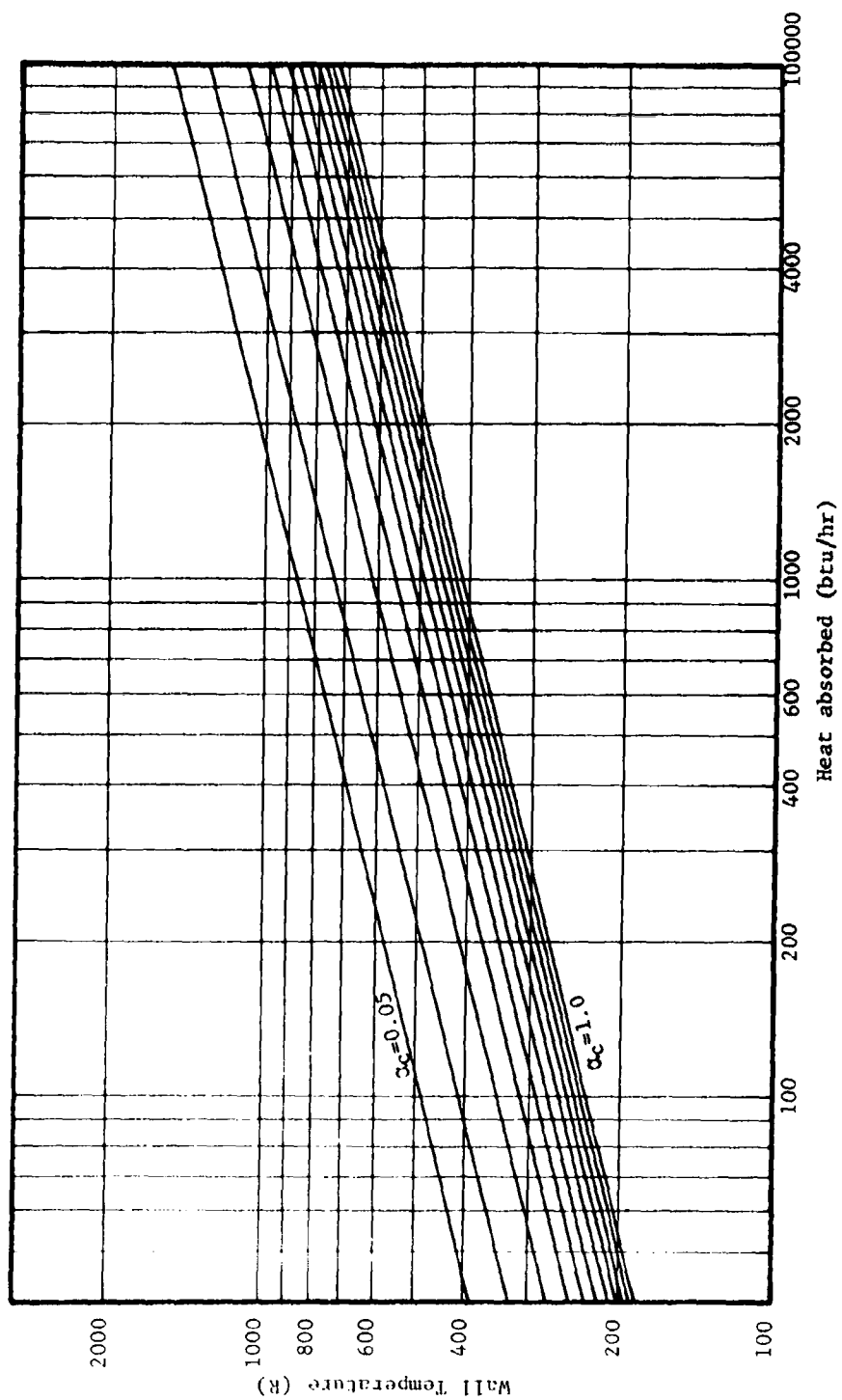


Figure 15. Total heat absorbed by the cylindrical model versus chamber I wall temperature.

TABLE 10
RADIATIVE HEAT ABSORBED BY THE
CYLINDRICAL MODEL IN CHAMBER II

Wall Temp (R)	Heat Absorbed (Btu/hr)													
	Space Suit Absorptivity													
	1.0	0.9	0.8	0.7	0.6	0.5	0.4	0.3	0.2	0.16	0.12	0.1	0.05	
320	183	164	146	128	110	91	73	55	37	29	22	18	9	
350	241	235	209	183	157	131	104	78	52	42	31	26	13	
400	445	401	356	312	267	223	178	134	89	71	53	45	23	
450	713	642	570	499	428	357	285	214	143	114	86	71	36	
500	1088	979	870	761	653	544	435	326	218	174	131	109	54	
550	1592	1433	1274	1114	955	796	637	478	318	255	191	159	80	
600	2255	2030	1804	1579	1353	1128	902	677	451	361	271	226	113	
650	3106	2796	2485	2174	1864	1553	1242	932	621	497	373	311	156	
700	4178	3780	3342	2924	2507	2089	1671	1253	836	668	501	418	209	
750	5505	4955	4404	3854	3303	2753	2202	1652	1101	881	681	531	276	
800	7125	6414	5702	4989	4278	3564	2851	2138	1425	1140	855	713	357	
850	9080	8172	7264	6356	5448	4540	3632	2724	1816	1453	1090	908	454	
900	11420	10278	9136	7994	6852	5710	4568	3426	2284	1827	1370	1142	571	
950	14172	12755	11338	9920	8503	7086	5669	4252	2834	2208	1701	1417	709	

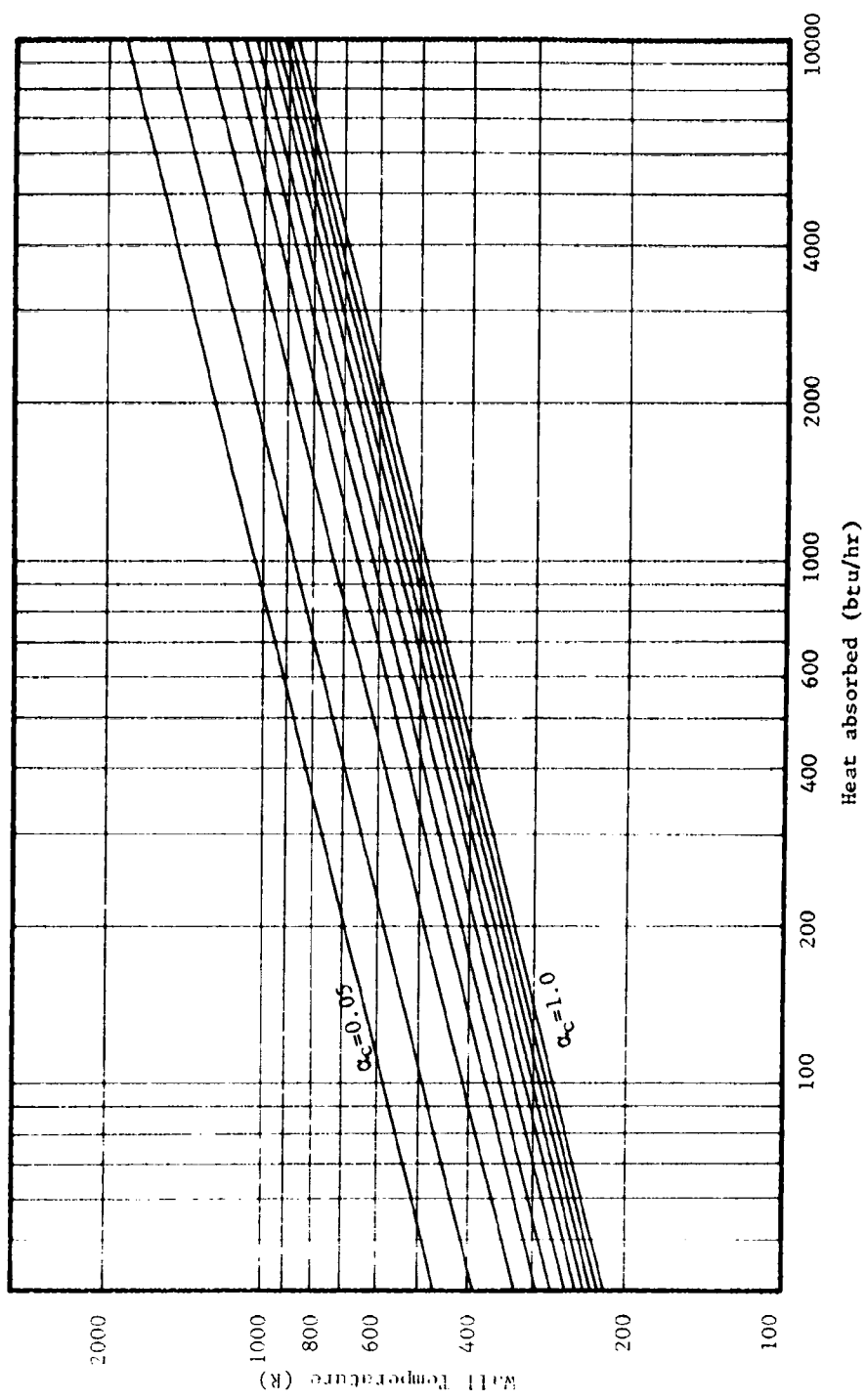


Figure 16. Total heat absorbed by the cylindrical model in chamber II versus the wall temperature of chamber II.

- (2) The internal chamber pressure is no longer a vacuum but varies from 1.0 to 0.01 atmospheres.

The total heat absorbed by the model in chamber III (see TABLE 11 and fig. 17) varies for a subject absorptance of 1.0 from 343 btu/hr at a wall temperature of 320 R to 26,643 btu/hr at a wall temperature of 950 R while for a subject absorptance of 0.05, $Q(\text{absorbed})$ varies from 17 btu/hr at a wall temperature of 320 R to 1332 btu/hr at a wall temperature of 950 R. Since the internal chamber pressure of chamber III exists between finite limits, the heat transferred by convection must also be determined in order to establish which of the two equations (5) or (7) page 13 is applicable for chamber III analysis. Specifically, natural convection film coefficients are given (see tables 12, 13 and 14) for various combinations of environmental and surface element temperatures at internal chamber pressures of 1.0, 0.1 and 0.01 atmospheres (see Appendices II and IV). The average film coefficients for natural convection over a horizontal cylinder at chamber pressures of 1.0, 0.1 and 0.01 atmospheres are 0.097, 0.03 and 0.0097 btu/hr ft², respectively. Thus, the average film coefficients in conjunction with the applicable area A and the applicable temperature difference ΔT yield the net heat gained or lost by convection. Furthermore, for any actual test the surface temperature of the subject must be known. However, a check of the effect of convection on the total amount of heat absorbed by the man can be obtained by the following analysis.

Suppose that at time equal zero the chamber III wall and air temperatures are 900 R and that the surface temperature of the space suit is 560 R. Dependent on the absorptance of the suit, $Q(\text{absorbed})$ due to radiation may assume values from 21,470 btu/hr to 1074 btu/hr and the heat transferred by convection is 660 btu/hr at 1.0 atmospheres, 198 btu/hr at 0.1 atmospheres and 66 btu/hr at 0.01 atmospheres. Furthermore, the ratio of $Q(\text{convection})/Q(\text{radiation})$ varies from 3.07% for α equal 1.0 to 61.4% for α equal 0.05 at a chamber pressure of 1.0 atmospheres (see fig. 18), and at chamber pressures of 0.1 and 0.01 atmospheres the per cent variation is 0.92% ($\alpha_c = 1.0$) to 18.4% ($\alpha_c = 0.05$) and 0.31% ($\alpha_c = 1.0$) to 6.14% ($\alpha_c = 0.05$), respectively. Similar curves are available for environmental temperatures of 700 R and 600 R (see fig. 19 and 20), but in each case the ratio of $Q(\text{convection})$ to $Q(\text{radiation})$ is practically the same as illustrated in the example. Thus, for environmental temperatures greater than the initial surface temperature of the space suit, convection is negligible at a chamber pressure of 0.01 atmospheres. Moreover, at a pressure of 0.1 atmospheres it is negligible for suits with an average absorptance greater than 0.3.

Suppose now that at time equal zero the surface temperature of the suit, T_s , and the air temperature in the chamber, T_a , are assumed to be 560 R and 400 R, respectively. Heat is now transferred from the subject to the surroundings at a greater rate than the subject receives heat. Furthermore, based on the average film coefficient, the instantaneous heat loss due to convection is 310 btu/hr at a chamber pressure of 1.0 atmospheres, 96.3 btu/hr at 0.1 atmospheres and 31 btu/hr at 0.01 atmospheres. The heat absorbed due to radiation varies from 837 btu/hr to 42 btu/hr at absorptances of 1.0 and 0.05, respectively. Thus, the instantaneous heat loss due to convection is of major importance when compared to heat absorbed

TABLE 11
RADIATIVE HEAT ABSORBED BY THE
CYLINDRICAL MODEL IN CHAMBER III

Wall Temp (K)	Heat Absorbed (Btu/hr)															
	Space Self Absorptivity															
	1.0	0.9	0.8	0.7	0.6	0.5	0.4	0.3	0.2	0.16	0.12	0.1	0.05			
320	343	309	274	240	206	172	137	104	80	56	42	34	17			
350	480	441	392	343	294	245	196	148	96	70	60	50	25			
400	837	753	670	586	502	419	335	250	167	134	100	84	42			
450	1342	1208	1074	939	805	671	537	402	268	214	160	134	67			
500	2045	1841	1636	1432	1227	1023	818	614	409	328	246	205	103			
550	2893	2584	2304	2005	1706	1407	1107	808	509	478	340	280	150			
600	4239	3815	3391	2967	2543	2120	1696	1272	846	678	506	434	212			
650	5639	5255	4671	4087	3503	2920	2336	1752	1168	934	700	584	282			
700	7154	6689	6203	5608	4712	3927	3142	2356	1571	1256	942	785	383			
750	10350	9315	8280	7245	6210	5175	4140	3104	2070	1656	1242	1035	513			
800	13399	12050	10719	9379	8039	6700	5360	4020	2680	2144	1608	1340	670			
850	17870	15363	13656	11949	10242	8535	6828	5121	3414	2732	2048	1707	854			
900	21470	18322	17176	15029	12882	10735	8588	6441	4284	3436	2576	2147	1074			
950	28643	23979	21314	18650	16086	13522	10857	7993	5329	4282	3108	2604	1332			

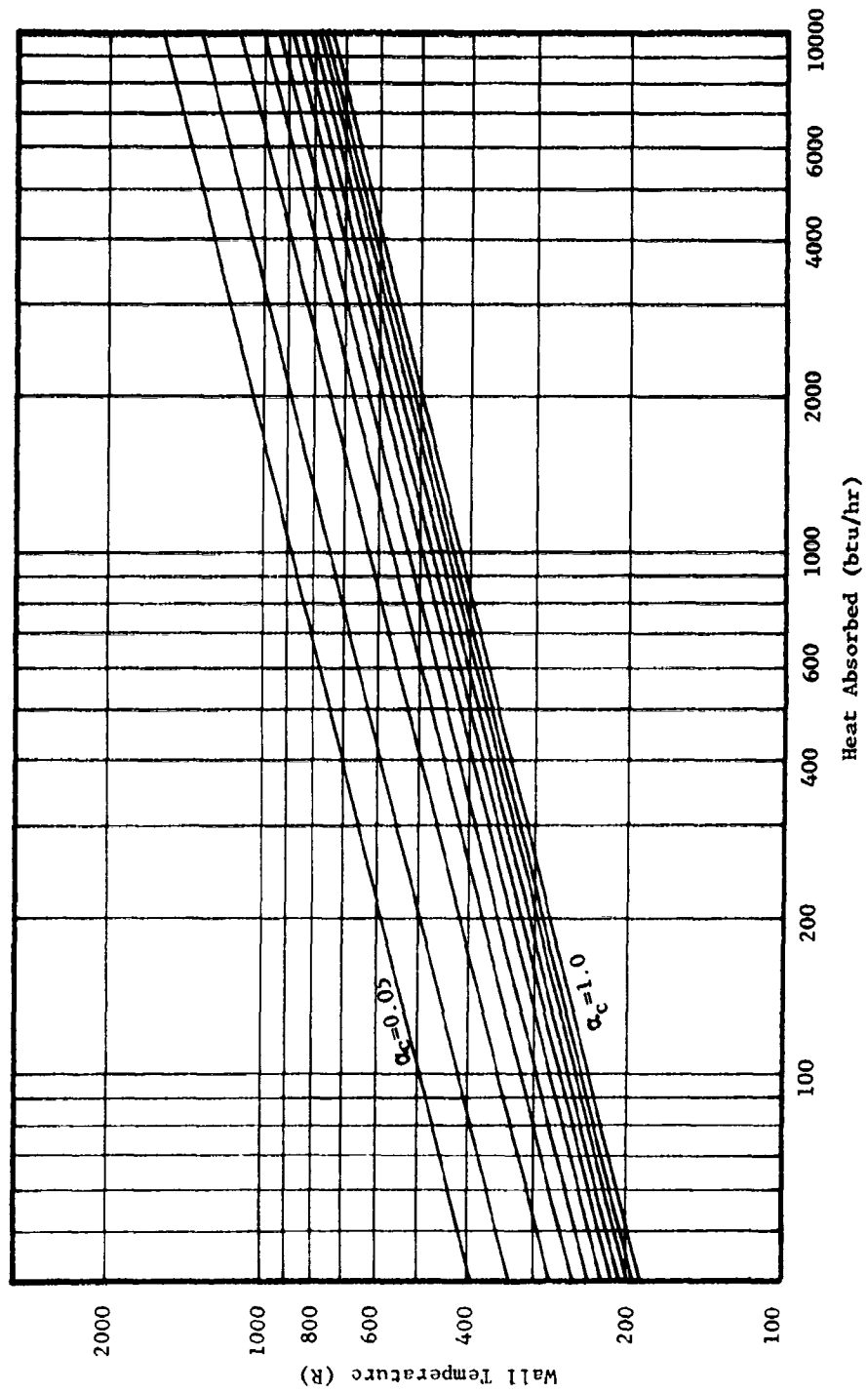


Figure 17. Total heat absorbed by the cylindrical model in chamber III versus the wall temperature of chamber III.

TABLE 12
NATURAL CONVECTION FILM COEFFICIENTS FOR FLOW
OVER A HORIZONTAL CYLINDER USING VARIOUS
ENVIRONMENTAL AND SURFACE TEMPERATURES AT A
BAROMETRIC PRESSURE OF 1.0 ATMOSPHERES

T(F)	Surface Temperature (T _s -F)								
	-50	-25	0	50	100	150	200	300	400
-50	0.000	0.071	0.085	0.100	0.110	0.120	0.126	0.138	0.147
-25	0.067	0.000	0.067	0.088	0.100	0.109	0.116	0.127	0.136
0	0.078	0.065	0.000	0.078	0.092	0.102	0.110	0.120	0.131
50	0.089	0.082	0.075	0.000	0.075	0.089	0.099	0.112	0.123
100	0.096	0.092	0.087	0.073	0.000	0.073	0.087	0.103	0.109
150	0.101	0.097	0.094	0.085	0.071	0.000	0.071	0.094	0.106
200	0.103	0.101	0.098	0.091	0.082	0.069	0.000	0.082	0.098
250	0.106	0.104	0.101	0.096	0.089	0.080	0.068	0.068	0.089
300	0.108	0.106	0.103	0.098	0.093	0.087	0.079	0.000	0.079
350	0.109	0.107	0.106	0.101	0.097	0.092	0.085	0.065	0.065
400	0.111	0.110	0.108	0.104	0.101	0.096	0.091	0.076	0.000
450	0.109	0.108	0.107	0.104	0.100	0.096	0.092	0.081	0.062

TABLE 13
NATURAL CONVECTION FILM COEFFICIENTS FOR FLOW
OVER A HORIZONTAL CYLINDER USING VARIOUS
ENVIRONMENTAL AND SURFACE TEMPERATURES AT
A BAROMETRIC PRESSURE OF 0.1 ATMOSPHERES

T(F)	Surface Temperature (T _s -F)								
	-50	-25	0	50	100	150	200	300	400
-50	0.000	0.023	0.027	0.032	0.036	0.038	0.040	0.044	0.047
-25	0.021	0.000	0.021	0.028	0.032	0.034	0.037	0.040	0.043
0	0.025	0.021	0.000	0.025	0.029	0.032	0.035	0.038	0.041
50	0.028	0.026	0.024	0.000	0.024	0.028	0.031	0.035	0.039
100	0.030	0.029	0.027	0.023	0.000	0.023	0.027	0.033	0.036
150	0.032	0.031	0.030	0.027	0.023	0.000	0.023	0.030	0.034
200	0.033	0.032	0.031	0.029	0.026	0.022	0.000	0.026	0.031
250	0.034	0.033	0.032	0.030	0.028	0.025	0.021	0.021	0.028
300	0.034	0.033	0.033	0.031	0.030	0.027	0.025	0.000	0.025
350	0.034	0.034	0.033	0.032	0.031	0.029	0.027	0.021	0.021
400	0.035	0.035	0.034	0.033	0.032	0.030	0.029	0.024	0.000
450	0.035	0.036	0.034	0.033	0.032	0.030	0.029	0.026	0.019

TABLE 14
NATURAL CONVECTION FILM COEFFICIENTS FOR FLOW
OVER A HORIZONTAL CYLINDER USING VARIOUS
ENVIRONMENTAL AND SURFACE TEMPERATURES AT A
BAROMETRIC PRESSURE OF 0.01 ATMOSPHERES

T(F)	Surface Temperature (T _s -F)									
	-50	-25	0	50	100	150	200	250	300	400
-50	0.000	0.007	0.009	0.010	0.011	0.012	0.013	0.014	0.015	0.016
-25	0.008	0.000	0.003	0.011	0.012	0.013	0.014	0.015	0.016	0.017
0	0.008	0.007	0.000	0.008	0.009	0.010	0.011	0.012	0.013	0.014
50	0.009	0.008	0.007	0.000	0.008	0.009	0.010	0.011	0.012	0.013
100	0.010	0.009	0.008	0.007	0.000	0.007	0.008	0.010	0.011	0.012
150	0.010	0.010	0.009	0.008	0.007	0.000	0.007	0.009	0.011	0.012
200	0.010	0.010	0.010	0.009	0.008	0.007	0.000	0.008	0.010	0.011
250	0.011	0.010	0.010	0.010	0.009	0.008	0.007	0.007	0.009	0.009
300	0.011	0.011	0.010	0.010	0.009	0.009	0.008	0.008	0.009	0.009
350	0.011	0.011	0.011	0.010	0.010	0.009	0.009	0.008	0.008	0.008
400	0.011	0.011	0.011	0.010	0.010	0.010	0.009	0.008	0.008	0.008
450	0.011	0.011	0.011	0.010	0.010	0.010	0.009	0.008	0.008	0.008

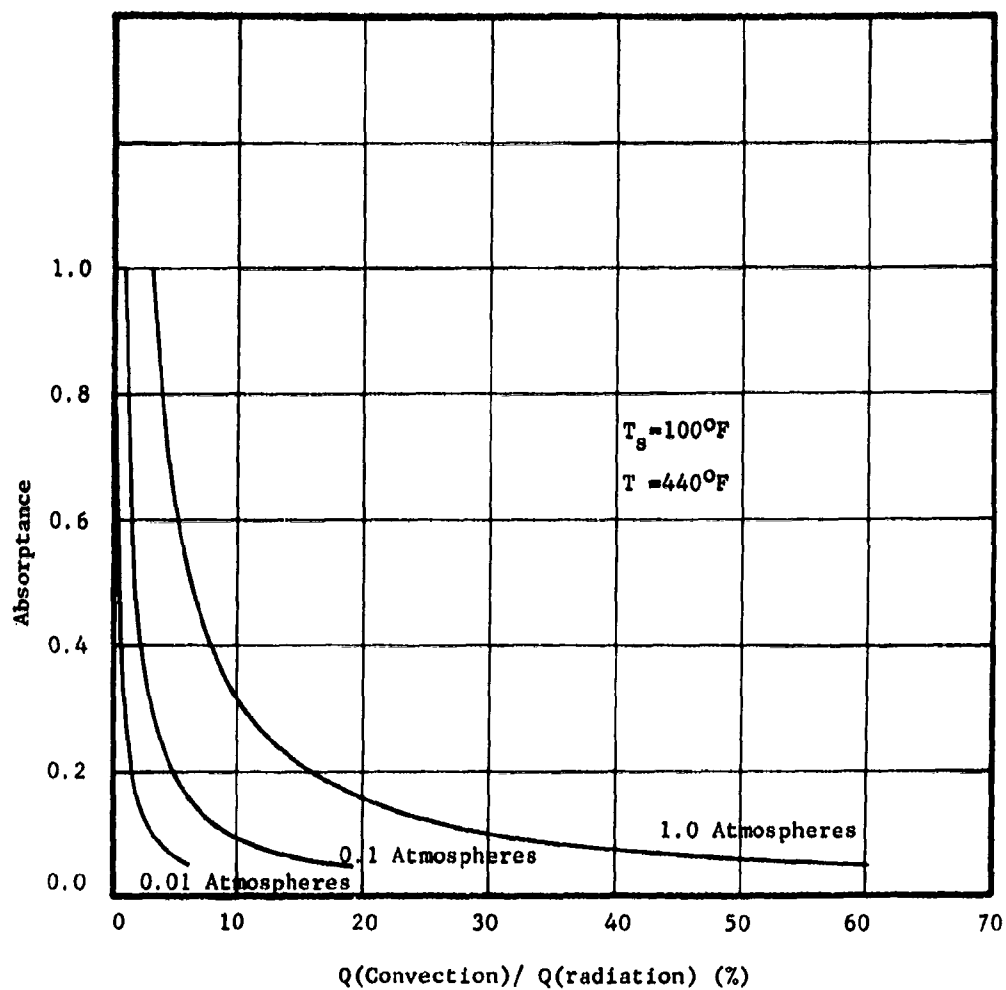


Figure 18. The ratio of the heat transferred by convection to the heat absorbed by radiation versus the absorptance of the space suit.

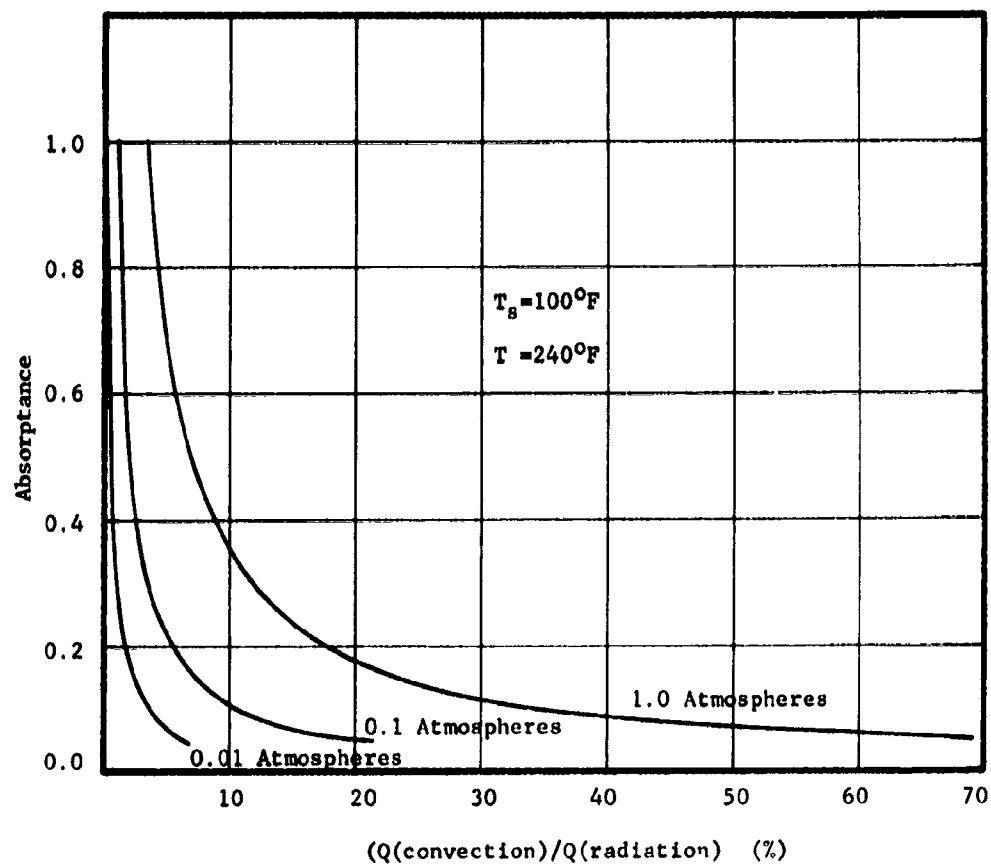


Figure 19. The ratio of the heat transferred by convection of the heat absorbed by radiation at chamber pressures of 1.0, 0.1 and 0.01 atmospheres versus space suit absorptance

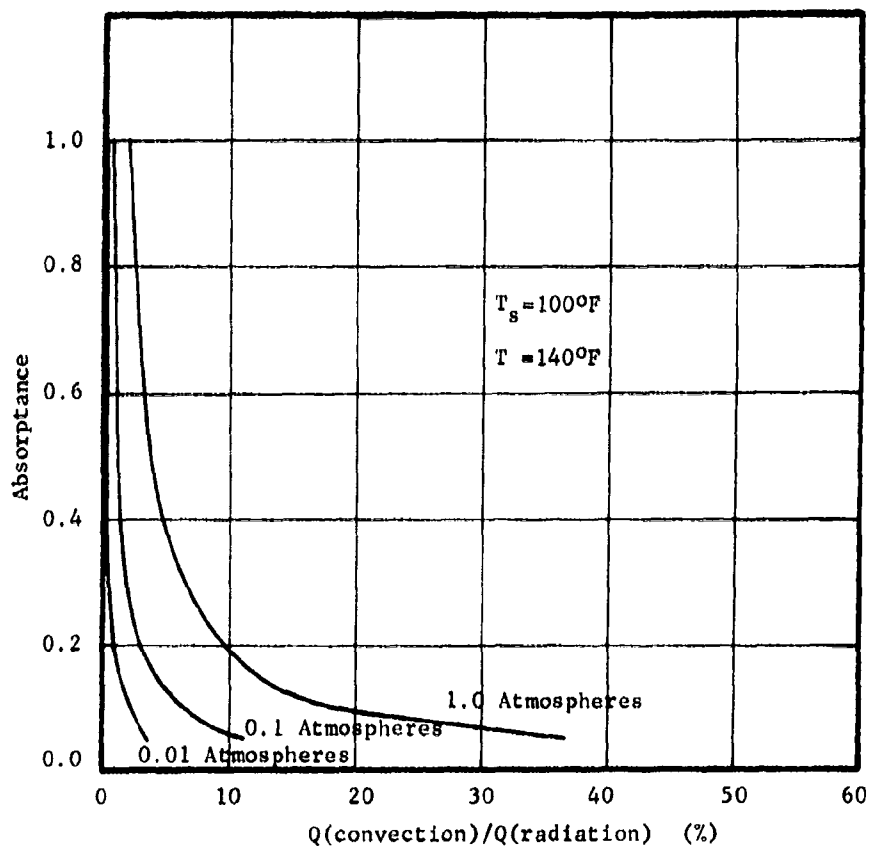


Figure 20. The ratio of the heat transferred by convection to the heat absorbed by radiation at chamber pressures of 1.0, 0.1 and 0.01 atmospheres versus space suit absorptance.

due to radiation. However, if the final surface temperature of the space suit approaches the temperature of the surrounding environment in a reasonably short period of time after the subject has been placed in the chamber, convection can be neglected at a chamber pressure of 0.01 atmospheres (see fig. 21). If the transient or step function is not approximated, convection cannot be neglected and the surface temperature of the space suit and the environmental temperature must be recorded so that equation 7, page 14 can be applied to the heat absorbed calculations. In conclusion, experimental tests are necessary in order to provide numerical results for environmental temperatures less than the initial space suit temperature.

Chamber IV is identical with chamber II with the following exceptions:

- (1) The emittance of the chamber walls is 0.094.
- (2) The internal chamber pressure is no longer a vacuum but varies from 1.0 to 0.01 atmospheres.

Also, all comments and assumptions which apply to the convection heat transfer analysis concerning chamber III apply to chamber IV, and the total heat absorbed by the model in chamber IV due to radiation is given in tabular form in Table 15 and in graphical form in fig. 22.

Two additional modified versions of chambers III and IV were also considered in the preliminary calculations. Specifically, chambers III and IV were modified by the addition of two 20" x 12" silica glass windows. However, calculations indicate that the effect of the glass windows on the overall chamber performance of the modified chambers when compared to chambers III and IV is negligible since silica glass is considered opaque at thermal wavelengths greater than 2.7μ .

The AMRL Facility. The overall properties of the chamber at the Aerospace Medical Research Laboratories are summarized as follows:

- (1) Upper wall and ceiling temperatures. 410 R to 910 R.
- (2) Lower wall and ceiling temperatures. 410 R to 910 R.
- (3) Air temperature. 410 R to 910 R.
- (4) Barometric Pressure. 760 mm of Hg to 20 mm of Hg.
- (5) Air Motion 0 - 800 fpm.
- (6) Humidity5 mm of Hg H₂O to 50 mm of Hg H₂O.

When the AMRL thermal chamber is compared with chambers I, II, III and IV the following variations are evident:

- (1) The effective temperature range of the AMRL chamber is 410 R to 910 R compared to 320 R to 950 R for chambers I, II, III and IV.

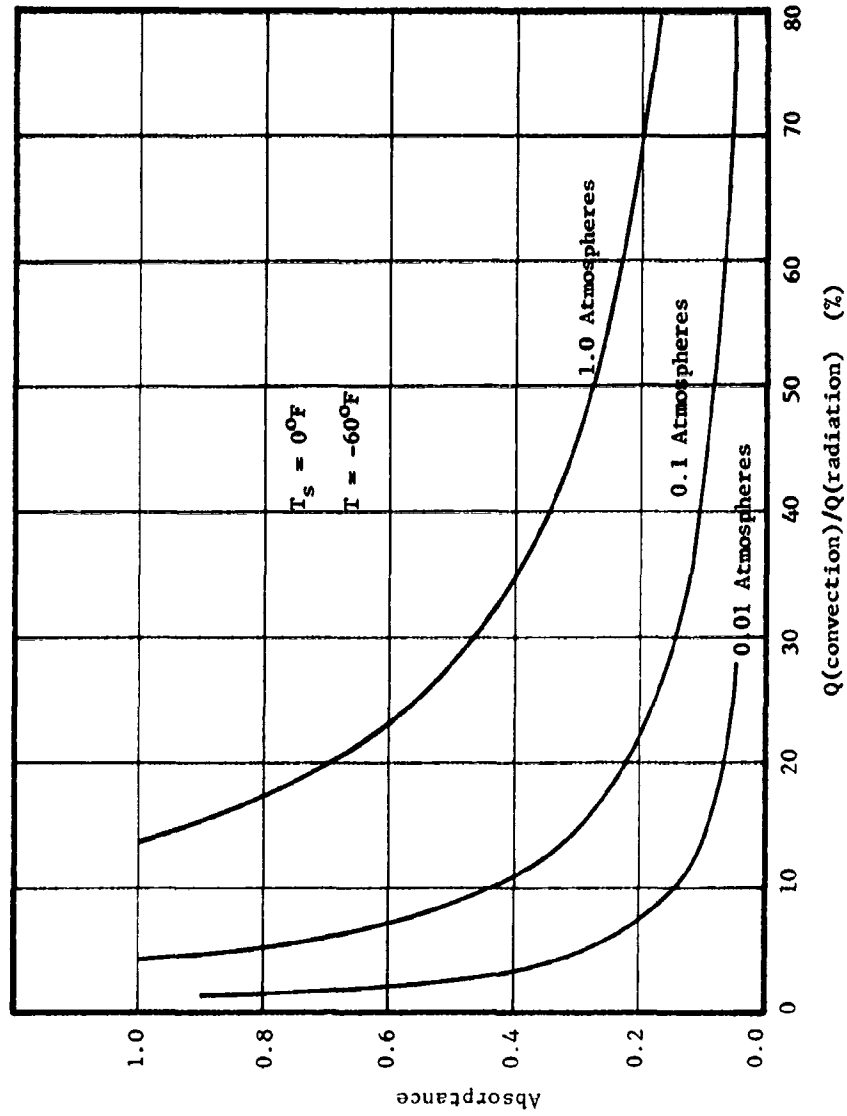


Figure 21. The ratio of the heat transferred by convection to the heat absorbed by radiation at chamber pressures of 1.0, 0.1 and 0.01 atmospheres versus space suit absorptance.

TABLE 15

RADIATIVE HEAT ABSORBED BY THE
CYLINDRICAL MODEL IN CHAMBER IV

Wall Temp (K)	Heat Absorbed (Btu/hr)													
	Space Salt Absorptivity													
	1.0	0.9	0.8	0.7	0.6	0.5	0.4	0.3	0.2	0.16	0.12	0.1	0.05	
320	172	155	138	120	103	86	69	52	34	26	21	17	9	
350	245	221	196	172	147	123	98	74	49	39	29	25	12	
400	418	376	334	293	251	209	167	125	84	67	50	42	21	
450	671	604	537	469	403	336	268	201	134	107	80	67	34	
500	1022	920	818	716	613	511	409	307	204	164	123	102	51	
550	1497	1347	1198	1048	898	749	599	449	299	239	180	150	75	
600	2120	1906	1686	1484	1272	1080	848	636	424	339	254	212	106	
650	2920	2628	2336	2044	1752	1460	1168	876	584	467	350	282	146	
700	3927	3534	3142	2749	2356	1964	1571	1178	785	628	471	383	196	
750	5175	4658	4140	3623	3105	2588	2070	1553	1035	828	621	518	259	
800	6696	6028	5359	4690	4019	3350	2680	2010	1340	1072	804	670	335	
850	8535	7682	6828	5975	5121	4268	3414	2561	1707	1366	1024	854	427	
900	10735	9642	8588	7514	6441	5368	4294	3220	2147	1716	1288	1073	537	
950	13322	11990	10658	9325	7993	6661	5329	4000	2664	2131	1599	1332	666	

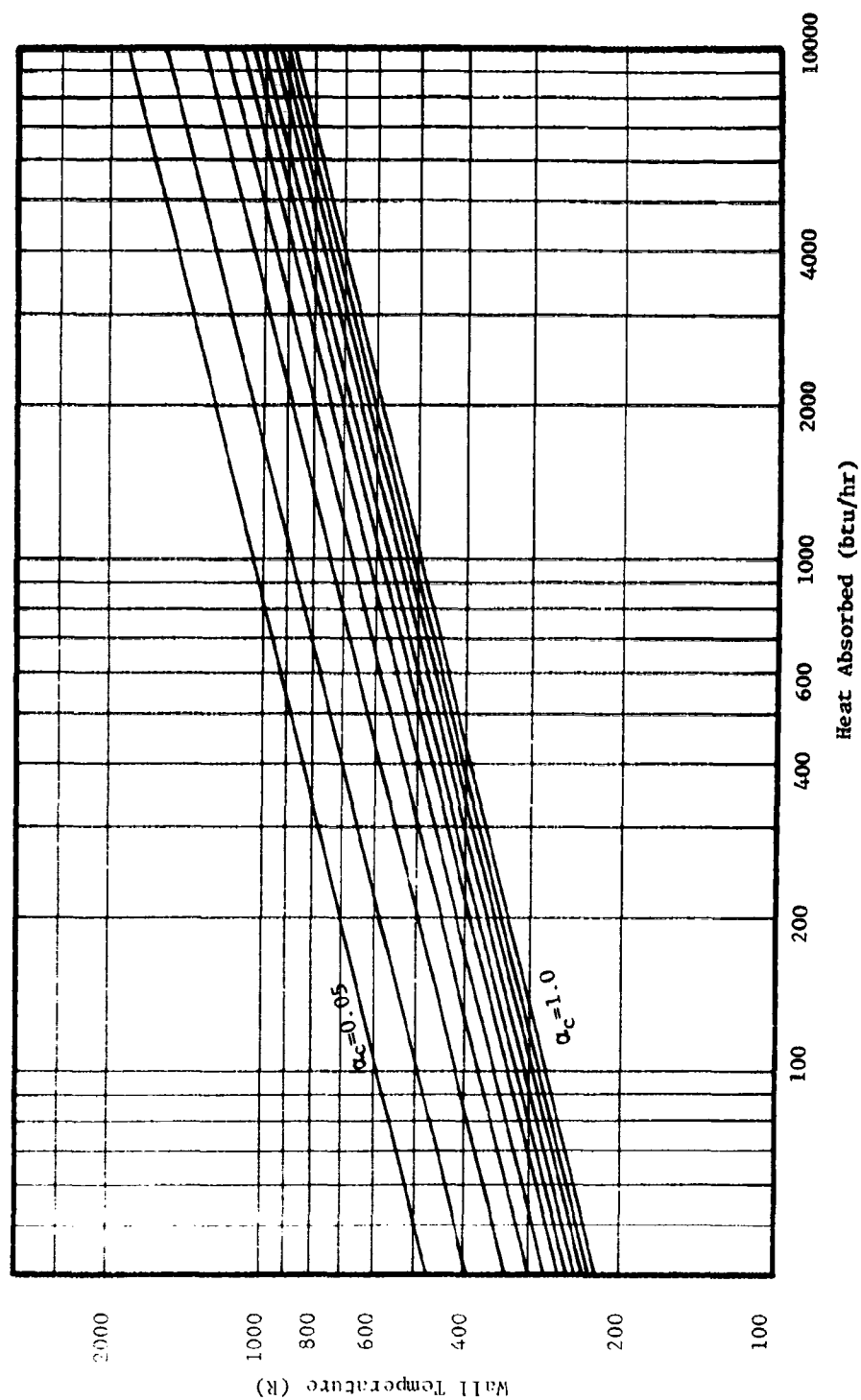


Figure 22. The total heat absorbed by the cylindrical model in chamber IV versus the wall temperature of chamber IV.

(2) The lower pressure limit for chambers I and II is zero atmospheres and for chambers III and IV is 7.6 mm of Hg compared to 20 mm of Hg for the AMRL chamber.

(3) Dry air is assumed for chambers III and IV

If items (2) and (3) are neglected, the only differences between chambers III and IV and the AMRL chamber are the effective temperature ranges for each case.

COMPARISON OF SPACE CONFIGURATIONS A, B, C, D AND E WITH CHAMBER CONFIGURATION III

Due to the amount of graphical and tabular data involved, only one comparison of space configurations A, B, C, D and E with one chamber configuration III, is presented as a guide for the interpretation of all numerical calculations. Space configurations F and G are not compared with chamber III since space configurations B and D are special cases of F and G. To recapitulate, the heat loads absorbed by the model in space configurations A, B, C, D and E are given in Tables 2, 3, 4, 5 and 6. The heat absorbed by the model in chamber III is given in figure 17 and Table 11. Since the results of the heat absorbed calculations for both space and chamber configurations are given for various space suit absorptances ranging from 1.0 to 0.05, one obvious method of comparison is to superimpose the results of the space calculations on the chamber calculations. Specifically, the results of space configurations A, B, C, D and E in terms of heat absorbed by the cylindrical model in btu/hr are superimposed on the results of the chamber III calculations which are, also, in terms of heat absorbed (btu/hr) by the model as the chamber III wall temperatures vary from 320 R to 950 R (see fig. 23, 24, 25, 26 and 27).

For a specific example consider the comparison of the heat absorbed by the cylindrical model in chamber III with the heat absorbed by the model in space configuration A (see fig. 23 and the supplementary information page 76).

The intersections of the vertical lines (heat absorbed by the model in space configuration A) and the slanted lines (heat absorbed by the model in the chamber) defines all possible points required for determining the equivalent chamber temperatures for simulating the space condition. Specifically, the minimum temperature required is 263 R and the maximum temperature is 1150 R. Note that for a greybody radiator the required chamber simulation temperature is 550 R for all suit absorptances.

The temperature range of chamber III varies from 320 R to 950 R. However, since the temperature range of the AMRL chamber varies from 410 R to 910 R, these two temperatures (410 R and 910 R) are used as the boundary limits for the comparison of chamber III with the space configurations. Moreover, models of space suits with surface properties that yield results which fall within the closed loop marked by the heavy unbroken line can be simulated directly in chamber III. For instance, if the suit absorptance is 0.9, the chamber can be used for direct simulation of space configuration A as α_c varies from 1.0 to 0.16.

Comparison of the heat absorbed by the cylindrical model in chamber III with the heat absorbed by the model in space configuration B is given in fig. 24 in which the space configuration results are again superimposed on the chamber configuration results. α_{me} is the suit

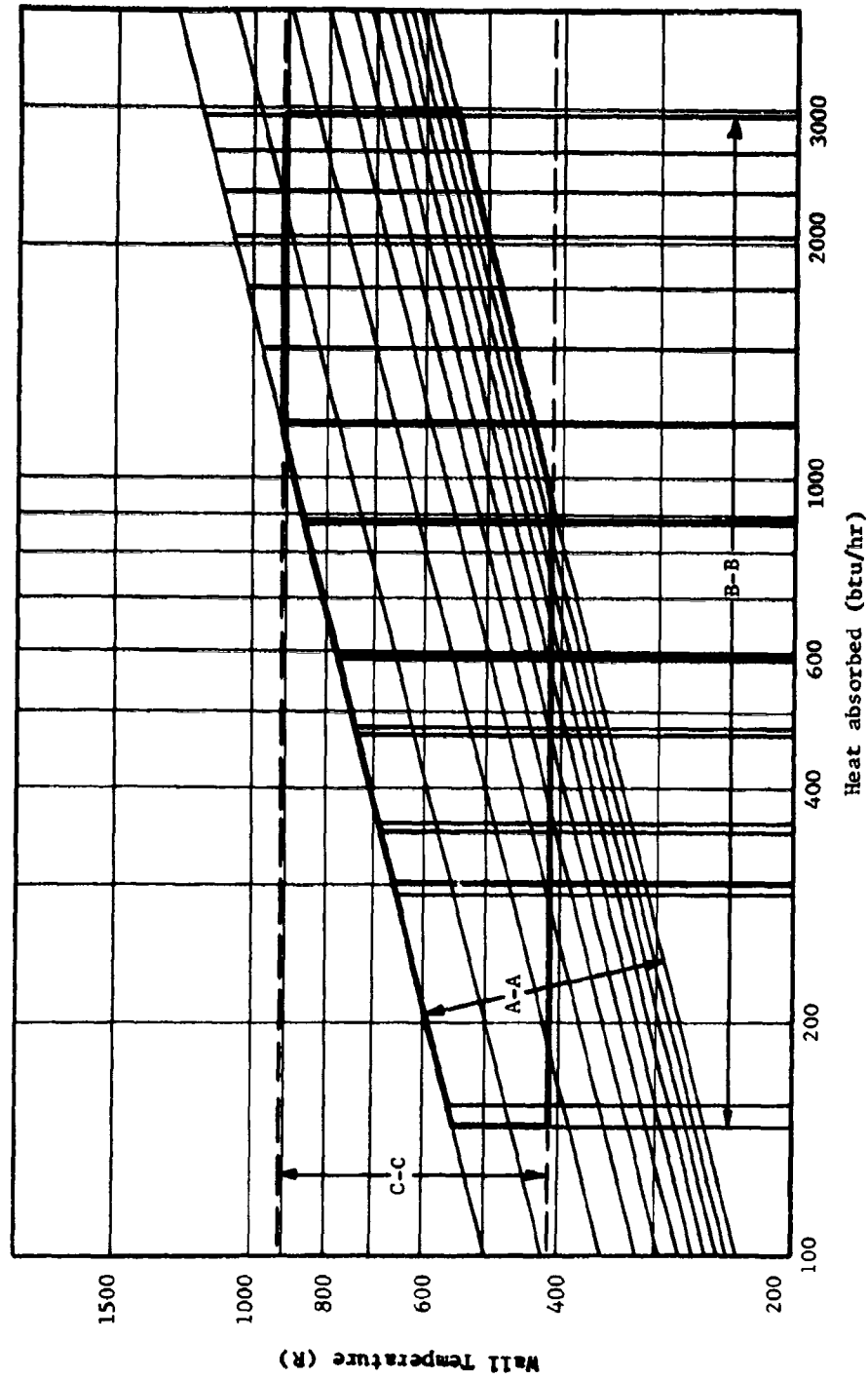
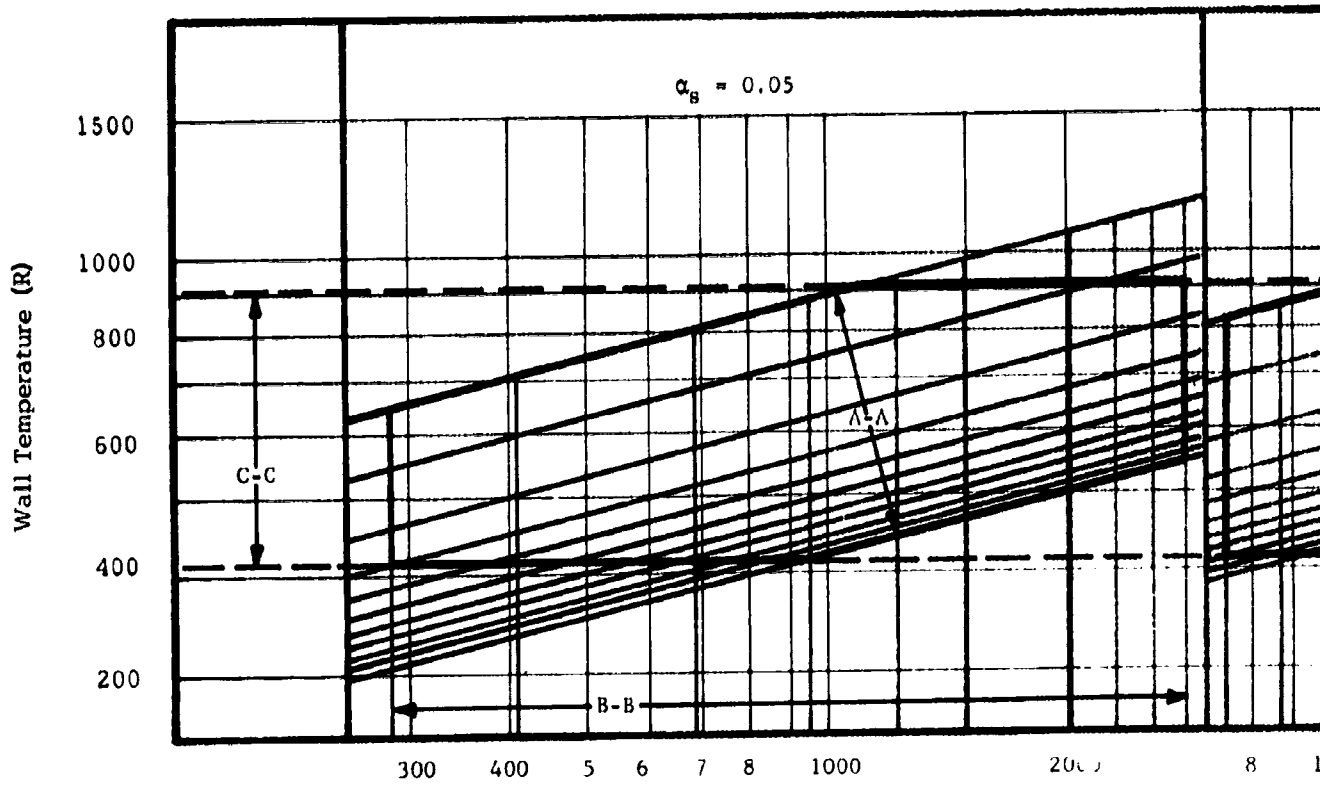


Figure 23. Comparison of the heat absorbed by the cylindrical model in chamber III with the heat absorbed by the model in space configuration A.



1

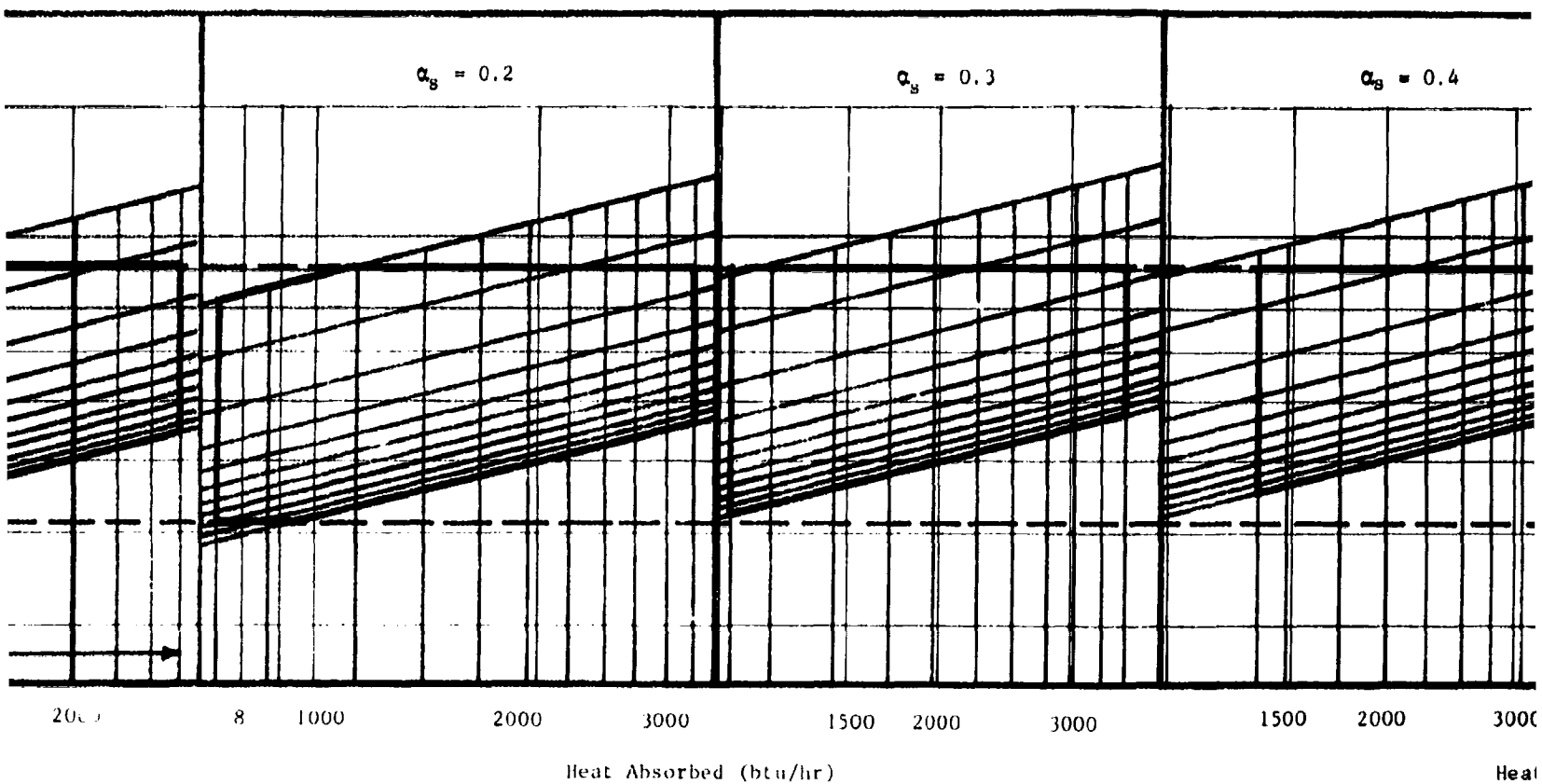


Figure 24. Comparison of heat absorbed in chamber for different space configurations.

2

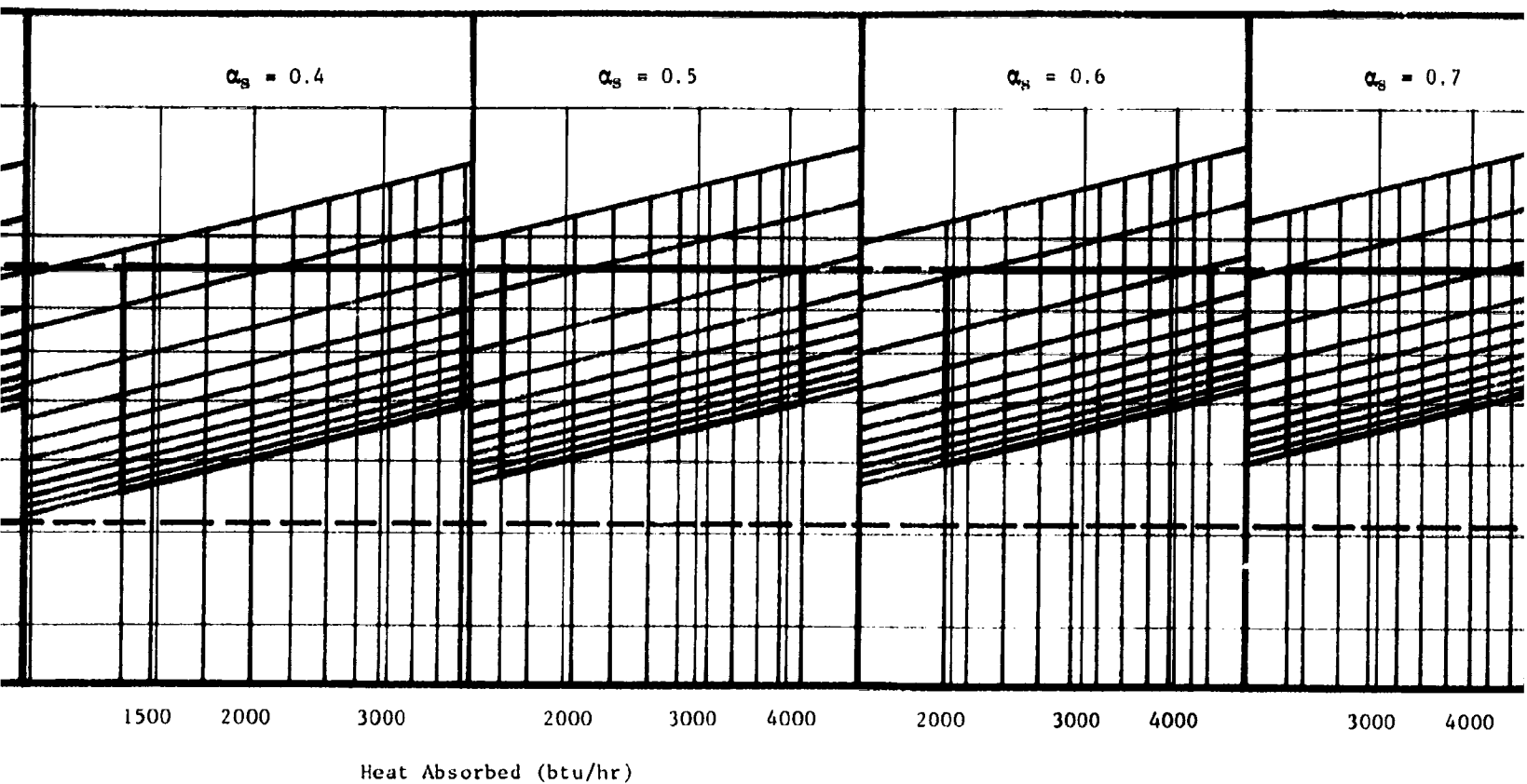
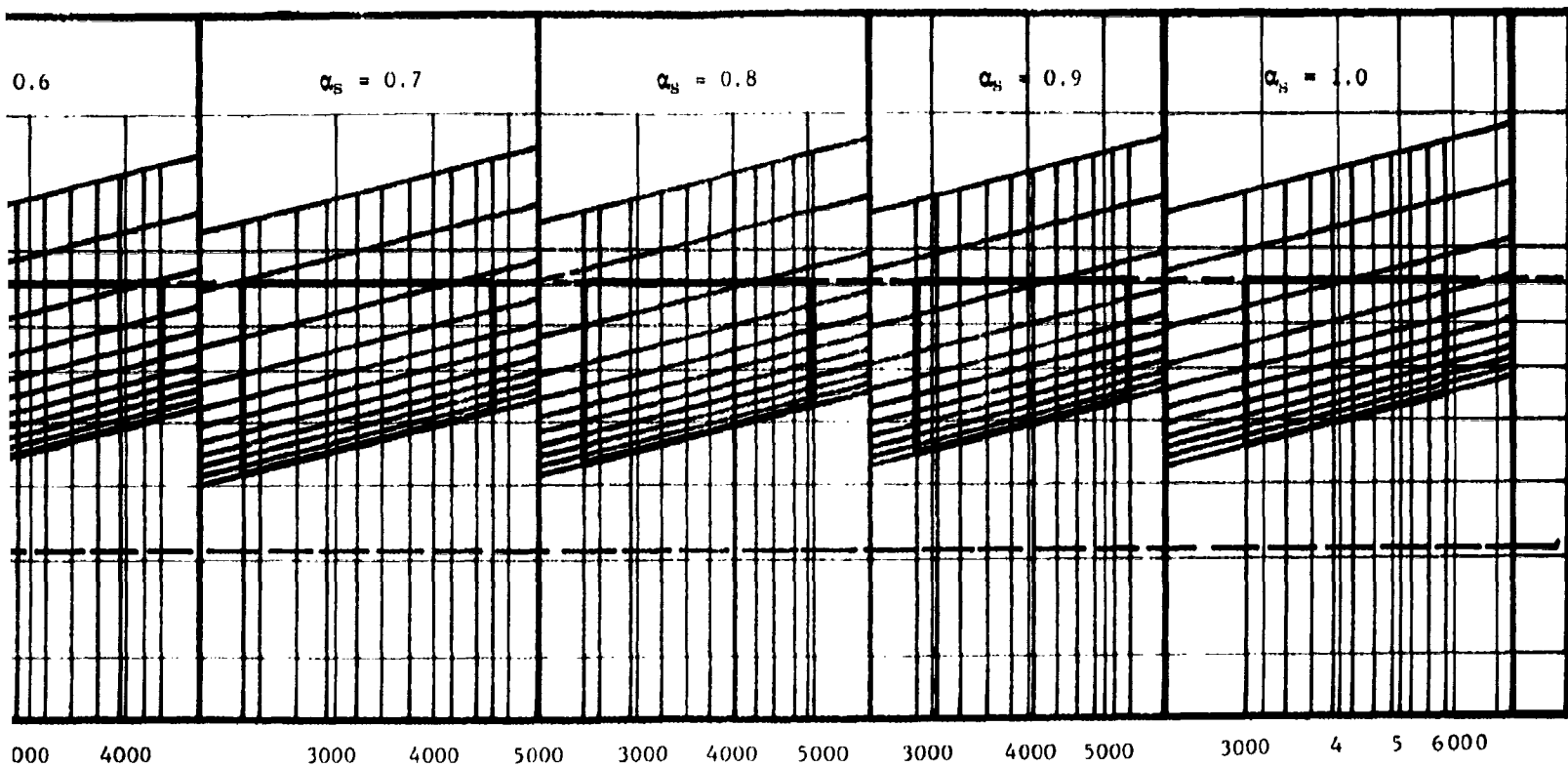


Figure 24. Comparison of the heat absorbed by the cylindrical model in chamber III with the heat absorbed by the model in space configuration B.



4

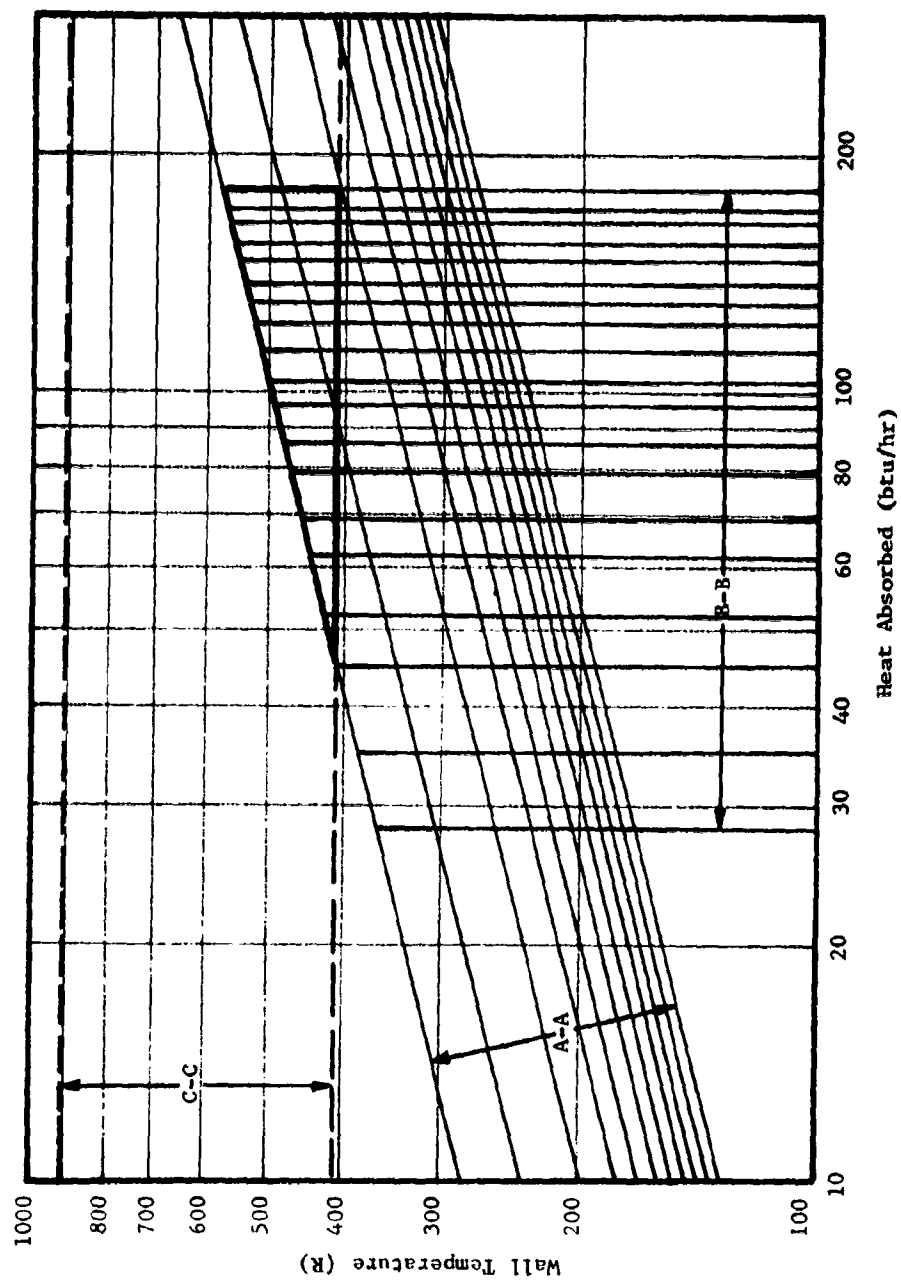


Figure 25. Comparison of the heat absorbed by the cylindrical model in chamber III with the heat absorbed by the model in space configuration C.

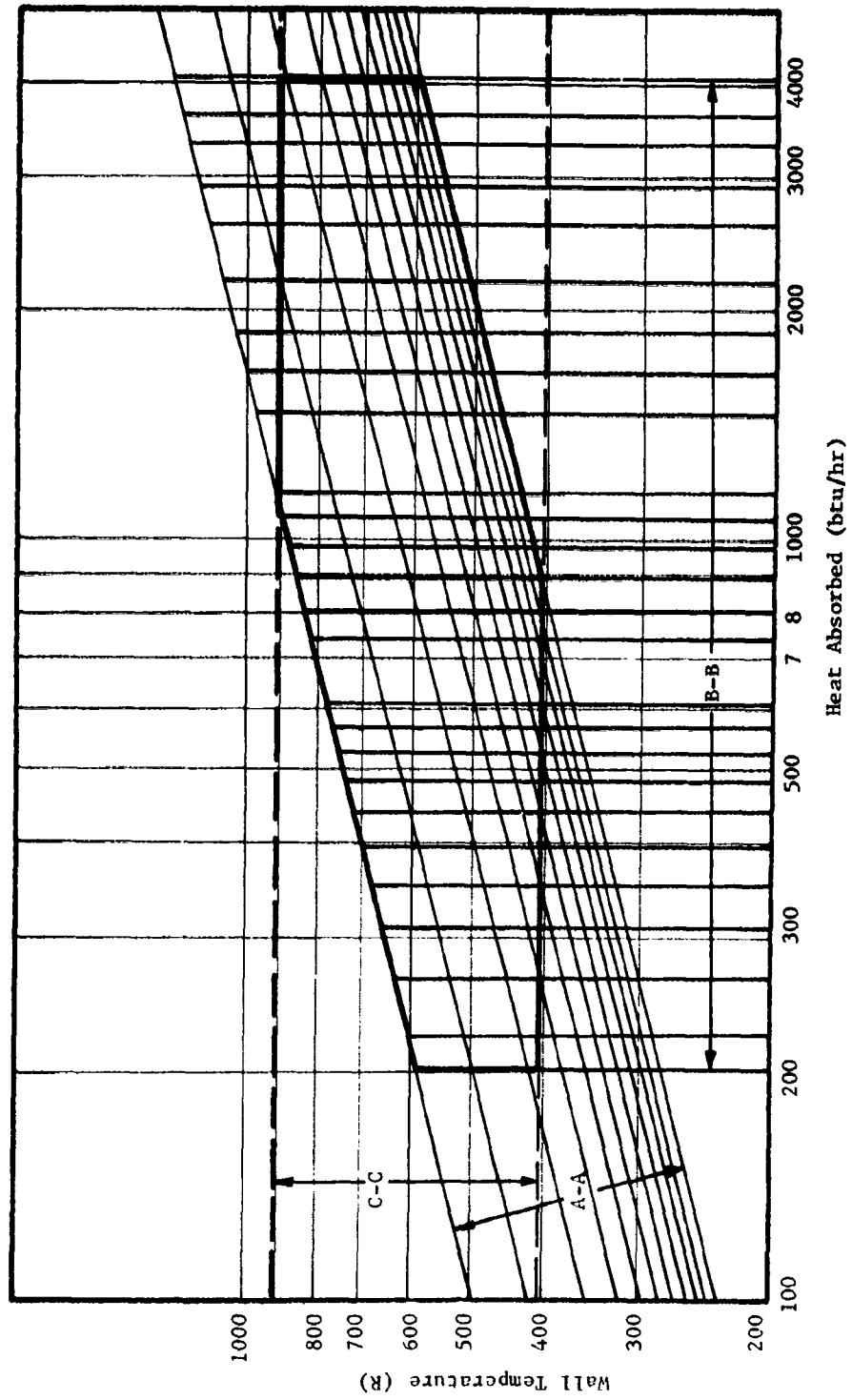


Figure 26. Comparison of the heat absorbed by the cylindrical model in chamber III with the heat absorbed by the model in space configuration D.

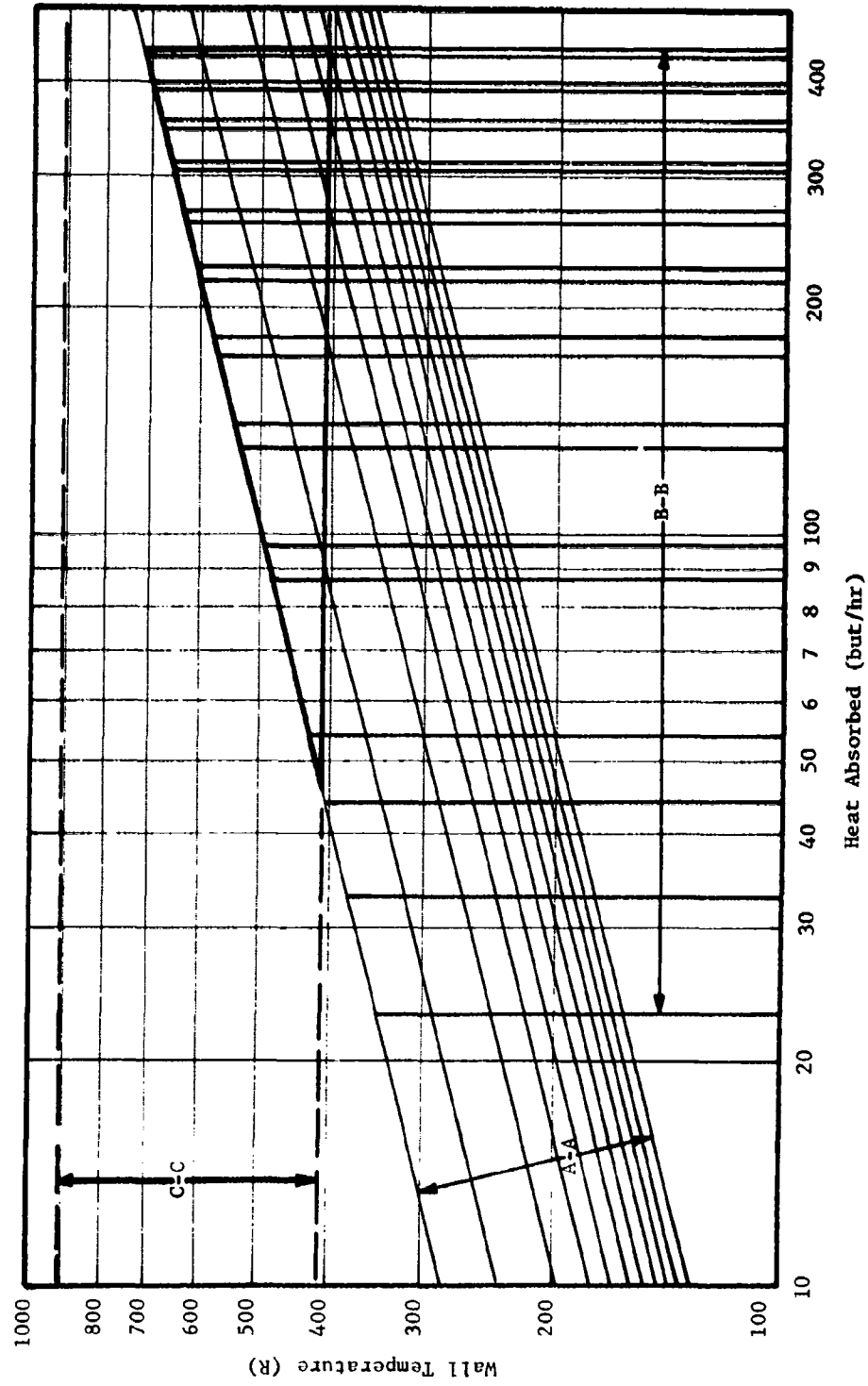


Figure 27. Comparison of the heat absorbed by the cylindrical model in chamber III with the heat absorbed by the model in space configuration E.

SUPPLEMENTARY AID

For Figures 23, 24, 25, 26 and 27

1. α_s is the space suit absorptance based on the sun as the thermal energy source.
2. α_{bs} is the space suit absorptance based on the black space environment as the thermal energy source.
3. α_{me} is the space suit absorptance based on the moon as the thermal energy source.
4. α_{ee} is the space suit absorptance based on the earth as the thermal energy source.
5. The absorptance of the suit based on the sun and the earth's and moon's albedos as thermal energy sources is the same for all three cases.
6. α_c is the space suit absorptance based on the thermal chamber as the thermal energy source.
7. The temperature limits of the AMRL chamber are 410 R to 910 R and are designated on each figure as (C-C).
8. The temperature limits of hypothetical chamber III are 320 R to 950 R.
9. The vertical straight lines (B-B on each figure) denote the heat absorbed by the cylindrical model for the given space configuration as the appropriate absorptance (α_{bs} , α_{me} or α_{ee}) varies from 1.0 to 0.05.
10. The slanted straight lines (A-A on each figure) denote the heat absorbed by the cylindrical model in chamber III as the space suit absorptance (α_c) varies from 1.0 to 0.05 as follows: 1.0, 0.9, 0.8, 0.7, 0.6, 0.5, 0.4, 0.3, 0.2, 0.1 and 0.05.
11. All points obtained by the intersection of the vertical and slanted straight lines which fall within the closed loop marked by the heavy unbroken line can be simulated in the AMRL chamber.
12. REFER TO FIGURE 24: Each segment labeled α_s (1.0), α_s (0.9), α_s (0.8), α_s (0.7), α_s (0.6), α_s (0.5), α_s (0.4), α_s (0.3), α_s (0.2), α_s (0.1) and α_s (0.05) represents the heat absorbed by the model for each appropriate value of α_s .
13. REFER TO FIGURE 24: The vertical lines represent the variation in the heat absorbed for each value of α_{me} as α_s varies from 1.0 to 0.9 to 0.8 to 0.7 to 0.6 to 0.5 to 0.4 to 0.3 to 0.2 to 0.1 to 0.05.

14. REFER TO FIGURE 24; For each segment the slanted lines (A-A) represent the heat absorbed by the model while the model is in the thermal chamber as the space suit absorptance α_s varies from 1.0 to 0.9 to 0.8 to 0.7 to 0.6 to 0.5 to 0.4 to 0.3 to 0.2 to 0.1 to 0.05.

absorptance based on the energy spectrum of the moon's emitted energy. α_s varies from 1.0 to 0.05 and the absorptance of the suit as a function of wavelength is the same for the incident solar energy and the moon's albedo. However, at each value of α_s , α_{me} varies from 1.0 to 0.05. Thus, in order to prevent overlapping values for the heat absorbed as α_s and α_{me} vary from 1.0 to 0.05, the superimposed results are presented in segments for each value of α_s from 1.0 to 0.05 as α_{me} varies from 1.0 to 0.5. Again, the vertical lines denote the variation in heat absorbed by the model in the thermal chamber as α_c varies from 1.0 to 0.05, and the intersection of these lines defines all possible points required for determining the equivalent chamber temperatures. Specifically, for simulating space configuration B the minimum temperature required is 305 R while the maximum temperature required is 1370 R. As before, cylindrical models with surface properties that fall within the closed loop marked by the heavy unbroken line can be simulated directly in chamber III.

The heat absorbed by the model in space configurations C and E are given in figures 25 and 27 as α_m and α_{bs} vary from 1.0 to 0.05. The intersections of the vertical and slanted lines in the closed loop denote values which can be simulated in the chamber. For instance, for space configuration C if α_m and α_{bs} are 1.0 and α_c is 0.10, the required chamber temperature for simulating the space condition is 485 R.

Finally, the heat absorbed by the cylindrical model in space configuration D is superimposed on the heat absorbed calculations for chamber configuration III (see fig. 26) as α_s , α_{ee} and α_c vary from 1.0 to 0.05. α_{ee} is the absorptance of the model based on the energy spectrum of the earth's emitted energy, and all points obtained by the intersection of the vertical and slanted lines which fall within the closed loop can be simulated in chamber III.

If the AMRL chamber approximates a greybody radiator with a wall absorptance and/or emittance of at least 0.94 and convection is negligible, chamber III as outlined above is identical to the AMRL chamber. Thus, all conditions which fall within the closed loops can be simulated in the AMRL facility. Consequently, human tolerance to the space conditions which can be simulated is simply a matter of experimentation. However, other methods must be employed in addition to actual experimentation to determine the human tolerance time to the space conditions which fall outside the temperature range of the AMRL chamber.

Is it theoretically possible to conduct human experimentation in ventilated space suits under less than space equivalent conditions and extrapolate the results to a specific space condition?

Extrapolation is defined as:

To infer from the observed trend of a variable, values of that variable beyond the observation range.

In other words if a definite trend of the variable, tolerance time, can be recorded as a function of chamber wall temperature, extrapolation is in order. Moreover, since tolerance time is a function of the temperature of the hot and cold environments, it is necessary to investigate extrapolation beyond the hot (positive) and cold (negative) environmental limits of the AMRL chamber. One rule of thumb states that extrapolation is applicable for values 50% greater than the difference between the norm and the maximum experimental values.

Consider the positive chamber environmental limit of 910 R as applied to the comparison of space configurations A, B, C, D and E with chamber III or the AMRL chamber. The maximum temperature required is 1360 R or a temperature 450 R greater than the maximum chamber temperature. Assume a reference environment at a temperature of 560 R. It is suggested that between 560 R and 910 R a definite trend can be established between chamber wall temperature and tolerance time with a sufficient number of experimental tests. In this case extrapolation to at least 1100 R is acceptable.

Consider the negative chamber environmental limit of 410 R. The minimum temperature required is 150 R. As before, assume a reference environment at a temperature of 560 R. It seems doubtful that a trend between tolerance time and wall temperature can be established between 410 R and 560 R which will provide extrapolative data, unless at the lower temperatures tolerance to the cold environment is due to localized cooling such as cold hands or feet.

In conclusion the AMRL thermal chamber is inadequate for simulating or extrapolating to a specific space condition where the maximum chamber temperature required is greater than 1100 R. Furthermore, using strictly "the rule of thumb", the extrapolation limit of the negative environment is 360 R. Based on these results, a more optimum set of chamber properties are:

- (1) Minimum chamber temperature 320 R .
- (2) Barometric pressure pressure at 300,000 ft
above the earth.
- (3) Greybody chamber walls with an absorptance and/or emittance
of 0.94 or greater.
- (4) Dry air inside the chamber.

SUMMATION OF MAJOR CONCLUSIONS

- (1) Greybody environments with an emittance and/or absorptance of 0.94 or greater approximate blackbody radiators.
- (2) Convection is negligible at a chamber pressure of 0.01 atmospheres for chamber environmental temperatures greater than the initial surface temperature of the space suit.
- (3) Experimental tests are necessary in order to determine if convection is negligible for chamber environmental temperatures less than the initial space suit temperature.
- (4) The AMRL chamber is identical to chambers III and IV if convection heat transfer is neglected and dry air is assumed for the AMRL chamber and chambers III and IV.
- (5) The extrapolation limit for the AMRL chamber's positive environment is 1100 R.
- (6) The extrapolation limit for the AMRL chamber's negative environment is 360 R.
- (7) A more optimum set of AMRL chamber properties are:
 - a. Minimum chamber temperature 320 R.
 - b. Maximum chamber temperature 1100 R.
 - c. Barometric pressure , pressure at
300,000 ft above
the earth.
 - d. Greybody chamber walls with an absorptance and/or emittance
of 0.94 or greater.
 - e. Dry air inside the chamber.
- (8) All points which can be simulated directly in the AMRL chamber are given graphically in fig. 23, 24, 25, 26 and 27.
- (9) Four specific examples of particular space suits as applied to chamber configurations I, II, III and IV and space configurations A, B, C, D, E, F and G are given in Appendix V.

RECOMMENDATIONS

I. The present calculations should be continued as follows:

- (1) Repeat all calculations for space configurations A, B, C, D, E, F and G in which the presence of a space vehicle is not neglected.
- (2) Expand the calculations to include, for example, space men on the surface of the moon and orbits of Venus and Mars.
- (3) Repeat all calculations with a more sophisticated space man model such as the model illustrated in fig. 28.
- (4) Expand the orbit analysis to include specific launch times (hour, day, month, year) and to include different types of circular orbits ranging from polar to equatorial orbits.
- (5) Repeat all orbit calculations for various elliptical orbits.

II. The method of solution should be up-dated as follows:

- (1) Instead of selecting two distinct suit absorptances α_s and α_h determine experimentally the relationship between α and the source wavelength for given space suit materials so that solutions of all calculations by computer methods will provide results based on the actual space suit properties.
- (2) Determine the absorptance and emittance of the AMRL facility as a function of wavelength. This will, of course, confirm or deny the use of the graybody assumption used in this report.
- (3) Determine the time required for the surface temperature of the space suit to attain the environmental chamber temperature. This will give an indication of whether convection is really negligible.
- (4) Repeat all calculations using the results of items (1), (2) and (3)

III. Conduct experimental tests based on the present calculations relating human tolerance time to specific AMRL chamber conditions and to the space conditions which can be simulated in the AMRL chamber.

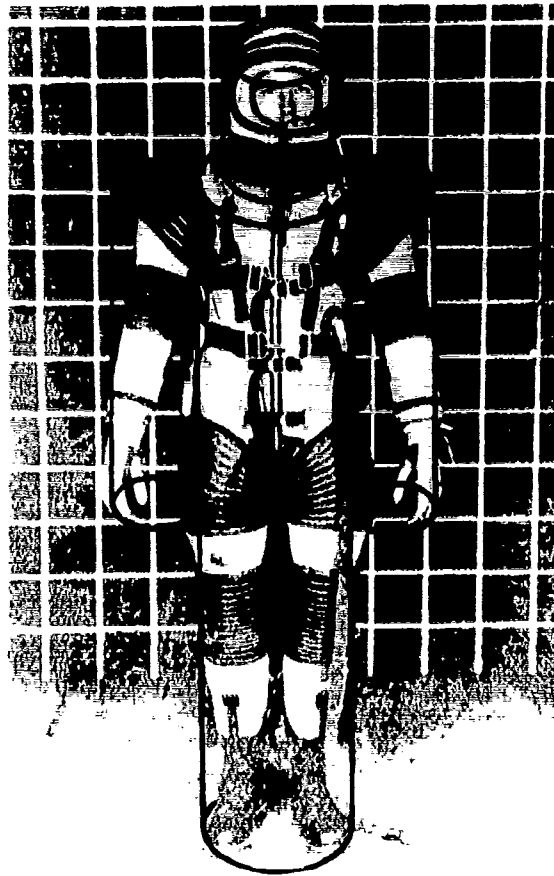


Figure 28. Space man model based on a system of cylinders.

REFERENCES

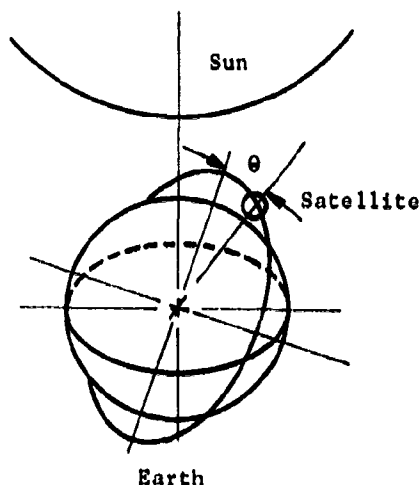
1. Belasco, N., A Design Study for Protective Suits for Space Flight Operations, ASC Technical Report 61-389, Life Support Systems Laboratory, Aerospace Medical Laboratory, Wright-Patterson Air Force Base, Ohio, August 1961.
2. Berman, A.I., The Physical Principles of Astronautics, John Wiley and Sons, Inc., New York, N.Y., 1961.
3. Binder, R. C., Advanced Fluid Mechanics, Prentice-Hall, Inc., Englewood Cliffs, N.J., 1958.
4. Birkebak, R.C., and J.P. Hartnett, "Measurement of the Total Absorptivity for Solar Radiation of Several Engineering Materials," Trans ASME, Vol 80, pp 373-378, February 1958.
5. Boelter, L.M.K., V.H.Cherry, H.A. Johnson, R.L. Martinelli, Heat Transfer Notes, University of California Press, 1946.
6. Brown, W. S., C.C. Pitts, and G. Leppert, "Forced Convection Heat Transfer from a Uniformly Heated Sphere," Trans ASME, Vol 84, pp 131--140, May 1962.
7. Camack, W.G., and D.K. Edwards, "Effective of Surface Thermal Radiation Characteristics on the Temperature Control Problem in Satellites," Surface Effect on Space Craft Material, John Wiley and Sons, Inc., New York, N.Y., 1960.
8. Cambel, A.B., and Jennings, B.H., Gas Dynamics, McGraw-Hill Book Co., New York, N.Y., 1958.
9. Carlson, L.D., "Maintaining the Thermal Balance in Man," 1962 IRE International Convention Board, Part 9.
10. Carlson, L.D., "Temperature," Annual Review of Physiology, Vol 24, 1962.
11. Carslaw, H.S., and J.C. Jaeger, Conduction of Heat in Solids, Oxford at the Clarendon Press, 1948.
12. Correale, J.V., and Guy, W.W., "Space Suits," Space World, Nov-Dec. 1963.
13. Chambre, P.L., "Nonlinear Heat Transfer Problems," Journal of Applied Physics, Vol 30, pp 1683-1989, Nov. 1959.
14. Cramer, K. R., and Irvine, Jr., Analysis of Nonuniform Suit Temperatures for Space Suits in Orbit, WADC Technical Report MRL-TDR-62-8, Wright Air Development Center, Wright-Patterson Air Force Base, Ohio, March 1962.

15. Cunningham, F.G., "Power Input to a Small Flat Plate from a Diffusely Radiating Sphere, with Application to Earth Satellites," NASA TN D-710, 1961.
16. Dunkle, R.V., "Thermal Radiation Tables and Applications," ASME Transactions, pp 549-552, May 1954.
17. Dunkle, R.V., "Configuration Figures for Radiant Heat Transfer Calculations Involving People," Trans ASME, Sept. 1962.
18. Dusenberre, G.M., Numerical Analysis of Heat Flow, Mc-Graw-Hill Co. Inc., New York, N.Y., 1949.
19. Dwinnell, J.H., Principles of Aerodynamics, McGraw-Hill Book Co., Inc, New York, N.Y., 1949.
20. Dzhasybekova, E.K., X.M. Kazacheriski, and A.V. Kharitonov, "Determination of the Earth's Albedo," Astron Zh, Vol 37, pp 131-134, 1960.
21. Haltiner, G.J., and F.L. Martin, Dynamical and Physical Meteorology, McGraw-Hill Book Co., Inc., New York, N.Y., 1957.
22. Englohm, G., and R.J. Baschiere, Thermal Transport and Radiative Properties of Fibrous Structural Materials, ASD Technical Report 62-180, Aeronautical Systems Division, Wright-Patterson Air Force Base, Ohio, Nov. 1962.
23. Handbook of Geophysics, The MacMillan Co., New York, N.Y., 1960.
24. Harrison, T.R., Radiation Pyrometry and its Underlying Principles of Radiant Heat Transfer, John Wiley and Sons, Inc., New York, N.Y., 1960.
25. Hovanessian, S.A., "On the Solution of the Diffusion Equation with a Heat Source," Trans ASME, Vol 84, pp 312-316, Nov. 1962.
26. Iberall, A.S., "Human Body as an Inconstant Heat Source and its Relation to Clothes Insulation," Trans ASME, Vol 82, pp 96-102, 1960.
27. Jakob, M., Heat Transfer Volume II, John Wiley and Sons, Inc., New York, N.Y., 1960.
28. Jakob, M., and G.A. Hawkins, Elements of Heat Transfer, John Wiley and Sons, Inc. New York, N.Y., 1959.
29. Kaufmann, W.C., "Human Tolerance Limits for Thermal Environments of Aerospace," AMRL Memorandum M-27, February 1963.
30. Kreith, F., Radiation Heat Transfer for Spacecraft and Solar Power Plant Design, International Textbook Co., Scranton, Pennsylvania, 1962.
31. Kreith, F., Principles of Heat Transfer, International Textbook Co., Scranton, Pennsylvania, 1958.

32. Kuiper, G.P., The Earth as a Planet, University of Chicago, 1960.
33. Livingston, W.A., Jr., Outer Space Environment Models for Use With Space Vehicle Simulators, AMRL Technical Report MRL-TDR-62-40, Aerospace Medical Research Laboratories, Wright Patterson Air Force Base, Ohio, May 1962.
34. McCutchan, J.W., "The Prediction of Human Thermal Tolerance when Using a Ventilating Garment With an Anti-Exposure Suit," Journal of Heat Transfer, Vol 82, pp 96-102, 1960.
35. Newell, H.E., Jr., High Altitude Rocket Research, Academic Press, Inc., New York, N.Y., 1953.
36. Pai, S., Introduction to the Theory of Compressible Flow, D.VanNostrand Co., Inc. Princeton, New Jersey, 1959.
37. Prian, V.D., "Orbital Simulator," The Journal of Environmental Sciences, pp 13-17, October 1963.
38. Schlichting, H., Boundary Layer Theory, McGraw-Hill Book Co., Inc., New York, 1960.
39. Schmidt, C.M., and H.J. Hanawalt, "Skin Temperature of a Satellite," Jet Propulsion, Vol 27, pp 1079-1083, 1957.
40. Schneider, P.J., Conduction Heat Transfer, Addison-Wesley Publishing Co., Inc., Cambridge, Massachusetts, 1955.
41. Sparrow, E.M., J.L. Gregg, J.V.Szel and P. Manas, "Analysis, Results and Interpretation for Radiation Between Some Simply Arranged Gray Surfaces," Trans ASME, Vol 83, pp 207-214, May 1961.
42. Stair, R., and R. Johnston, "Ultraviolet Spectral Radiant Energy Reflected from the Moon," J. Res. National Bureau Standards, Vol 51, pp 81-84, August 1953.
43. Stall, A.M., "The Role of the Skin in Heat Transfer," Trans ASME, Vol 82, pp 239-241, August 1960.
44. Stolz, G., Jr., "Numerical Solutions to an Inverse Problem of Heat Conduction for Simple Shapes," Trans ASME, Vol 82, pp 20-25, Feb 1960.
45. Teifel, V.G., "The Difference in the Spectral Properties of the Areas on the Lunar Surface," Soviet Astronomy, AJ(NY), Vol 3, pp 955-959, May-June 1960.

APPENDIX I

Approximate orbit analysis (ref. 30). The geometry of an earth-sun-satellite system is illustrated below.



The angle τ is defined as the angle between the plane of the satellite orbit and the earth's terminator. The angular position of the satellite in its orbit is denoted by θ such that the noon position or the point of the orbit nearest the sun is given by the value $\theta = 0$.

The angle at which the satellite enters the earth's shadow is given by the expression

$$\theta_s = \frac{\sin^{-1} \frac{\sin(\cos^{-1} \frac{R}{r})}{\sin \tau}}{\sin \tau} + 90^\circ$$

where R is the radius of the earth and r is the distance from the center of the earth to the satellite. For a circular orbit, the time required for 1 orbit is

$$t = \frac{2\pi r}{V_s}$$

where V_s is defined as

$$V_s = \left(g \frac{R^2}{r} \right)^{\frac{1}{2}}$$

The time spent in the earth's shadow is

$$t_s = \frac{\tau^2/3}{R/g} \left\{ 1 - \frac{1}{90} \sin^{-1} \left[\frac{\sin(\cos^{-1} \frac{R}{r})}{\sin \tau} \right] \right\}$$

APPENDIX II

Properties of Dry Air at Low Pressure (ref. 23, ref. 28, ref. 35)

- I. Thermal conductivity--According to Jakob, thermal conductivity k is a function of pressure below 1 mm of Hg for heavy gases and below 20 mm of Hg for light gases (hydrogen and helium) otherwise k is independent of pressure and is a function of temperature only.
- II. Viscosity--From the kinetic theory of gases it is shown that the coefficient of viscosity μ is defined as follows (ref. 5).

$$\mu = \frac{1.051}{3} \frac{m v}{\sqrt{2} \pi \sigma^2 (1 + D/T)}$$

m - molecular mass

v - random velocity

σ - diameter of the molecules

D - constant depending on the gas

T - absolute temperature

From this equation it is seen that viscosity is independent of pressure. Refer to figure 29 for the variation of density, specific heat, Prandtl number, dynamic viscosity and thermal conductivity of dry air with air temperature.

TABLE 16
SPECIFIC HEAT OF DRY AIR AT VARIOUS
PRESSURES AND TEMPERATURES

Temp	Pressures				
(R)	.01 atm	.1 atm	.4 atm	.7 atm	1 atm
360	.2344	.2395	.2398	.2364	.2404
450	.2396	.2396	.2398	.2400	.2401
540	.2400	.2400	.2401	.2403	.2404
630	.2408	.2408	.2409	.2410	.2411
720	.2420	.2421	.2421	.2422	.2423
810	.2438	.2438	.2438	.2439	.2439
900	.2459	.2459	.2459	.2460	.2460
990	.2483	.2484	.2484	.2484	.2484

TABLE 17
DENSITY OF DRY AIR AT VARIOUS
PRESSURES AND TEMPERATURES

Temp	Pressures				
(R)	.01 atm	.1 atm	.4 atm	.7 atm	1 atm
360	.001102	.01102	.0441	.0773	.1104
450	.0008810	.00882	.0353	.0617	.0882
540	.000735	.00735	.0294	.0514	.0735
630	.000630	.00630	.0252	.0441	.0630
720	.000551	.00551	.0220	.0386	.0551
810	.00049	.00490	.0198	.0343	.0490
900	.00044	.00441	.0178	.0308	.0441
990	.00040	.00401	.0160	.0280	.0401

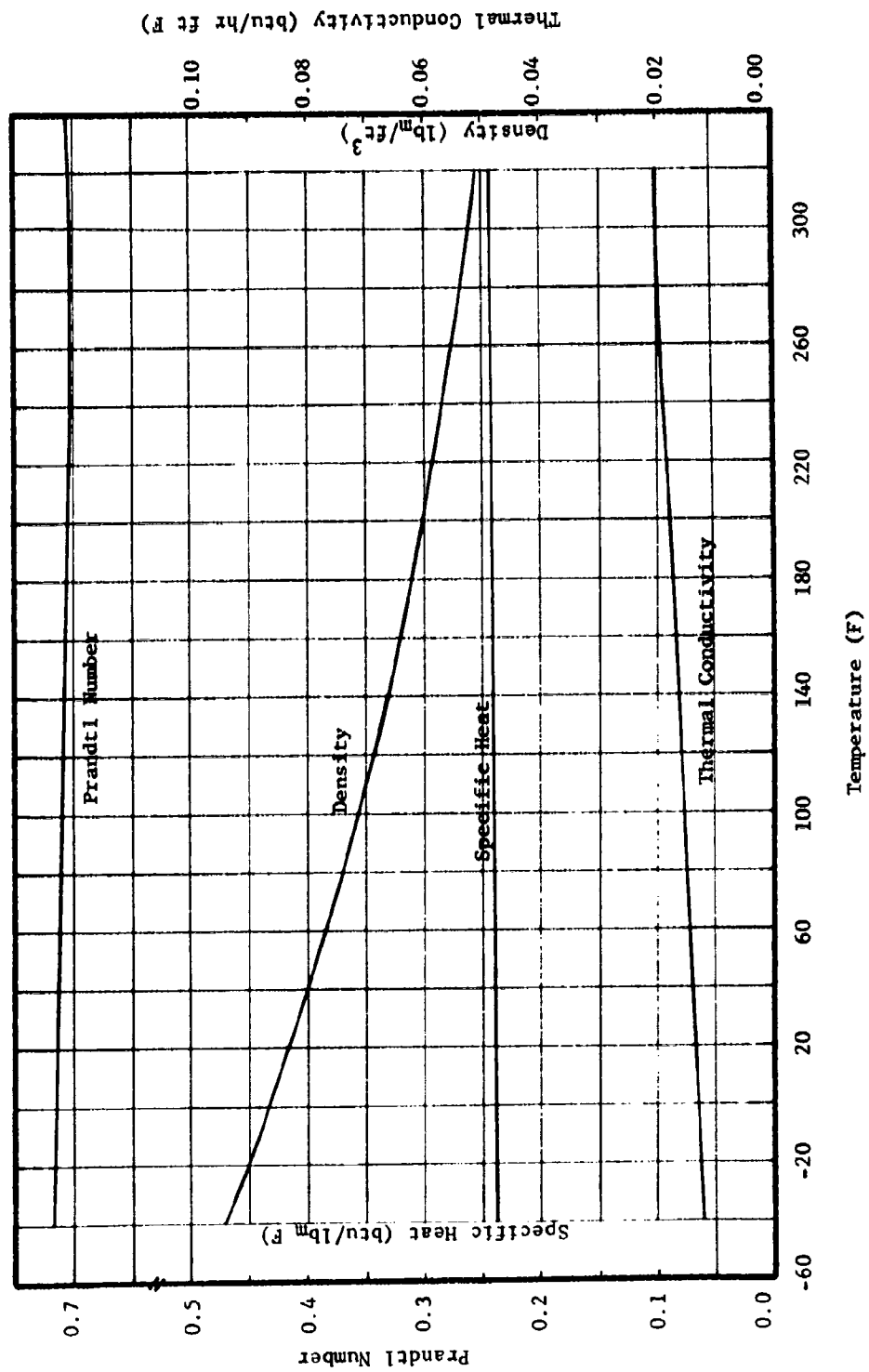


Figure 29. Properties of dry air at atmospheric pressure.

APPENDIX III

Subject: Integration of the following equation.

$$E = c_1 \int_0^{\infty} \frac{d\lambda}{\lambda^5 (e^{c_2/\lambda T} - 1)} \quad (a)$$

Let $x = \frac{c_2}{\lambda T}$

Revise equation (a) as follows

$$E = c_1 \int_0^{\infty} \frac{\lambda^{-5} (\lambda^{-2} d\lambda)}{(e^{c_2/\lambda T} - 1)}$$

$$d(\lambda^{-1}) = -\lambda^{-2} d\lambda$$

thus

$$c_1 \int_0^{\infty} \frac{\lambda^{-3} (\lambda^{-2} d\lambda)}{e^{c_2/\lambda T} - 1} = -c_1 \int_{\infty}^0 \frac{(\frac{1}{\lambda})^3 d(\frac{1}{\lambda})}{e^{c_2/\lambda T} - 1} \quad (b)$$

The differential and the limits of integration are in terms of $1/\lambda$.

$$\frac{T^4 c_2^4}{c_2^3 T^3 c_2 T} = 1 \quad (c)$$

Reverse the limits on equation (b) and multiply equation (a) by equation (c).

$$E = \frac{c_1 T^4}{c_2^4} \int_0^{\infty} \frac{(\frac{c_2}{\lambda T})^3 d(\frac{c_2}{\lambda T})}{e^{c_2/\lambda T} - 1} \quad (d)$$

However, $x = c_2/\lambda T$ and the limits of integration are in terms of x . Thus, equation (d) can be revised as follows:

$$E = \frac{c_1}{c_2^4} \left[\int_0^{\infty} \frac{x^3 dx}{e^x - 1} \right] T^4 \quad (e)$$

Since
$$e^x - 1 = \left(\frac{e^{-x}}{e^{-x}} \right) = \frac{e^{-x}}{1 - e^{-x}} = e^{-x} + e^{-2x} + e^{-3x} + \dots + e^{-nx}$$

equation (e) becomes

$$E = \frac{C_1}{C_2^4} \left[\int_0^\infty x^3 e^{-x} dx + \int_0^\infty x^3 e^{-2x} dx + \int_0^\infty x^3 e^{-3x} dx + \dots \right] T^4 \quad (f)$$

$$\int_0^\infty x^n e^{-ax} dx = \frac{n!}{a^{n+1}}$$

if n is a positive integer and $a > 0$ (ref. 24). n is 3, thus equation (f) is revised as follows:

$$E = \frac{C_1}{C_2^4} \left[\frac{3!}{1^4} + \frac{3!}{2^4} + \frac{3!}{3^4} + \dots + \frac{3!}{\infty^4} \right] T^4$$

and since $3! = 6$

$$E = \frac{6C_1}{C_2^4} \left[1 + \frac{1}{2^4} + \frac{1}{3^4} + \dots + \frac{1}{\infty^4} \right] T^4$$

$$E = \frac{6C_1}{C_2^4} \left[\sum_{n=1}^{\infty} \frac{1}{n^4} \right] T^4 \quad \sum_{n=1}^{\infty} \frac{1}{n^4} = \frac{\pi^4}{90}$$

Thus,

$$E = \sigma T^4$$

where

$$\sigma = \frac{6C_1}{C_2^4} \left[\sum_{n=1}^{\infty} \frac{1}{n^4} \right]$$

or

$$\sigma = \frac{6C_1}{C_2^4} \frac{\pi^4}{90} = \frac{C_1}{C_2^4} \frac{\pi^4}{15}$$

APPENDIX IV

THERMAL BOUNDARY LAYERS IN NATURAL FLOW

The equations describing two dimensional fluid flow are (ref. 3, ref. 38):

$$\frac{\partial(\rho u)}{\partial x} + \frac{\partial(\rho v)}{\partial y} = 0 \quad (a)$$

$$\rho(u \frac{\partial u}{\partial x} + v \frac{\partial u}{\partial y}) = \mu \frac{\partial^2 u}{\partial y^2} - \frac{dP}{dx} + \rho g_x \beta (T - T_\infty) \quad (b)$$

$$\rho g c_p (u \frac{\partial T}{\partial x} + v \frac{\partial T}{\partial y}) = k \frac{\partial^2 T}{\partial y^2} + \mu \left(\frac{\partial u}{\partial y} \right)^2 + u \frac{\partial P}{\partial x} \quad (c)$$

$$\frac{P}{\rho} = g R T \quad \mu = \mu(T) \quad (d)$$

For incompressible flow ($\rho = \text{constant}$) and for constant viscosity, equation a, b, c and d reduce to

$$\frac{\partial u}{\partial x} + \frac{\partial v}{\partial y} = 0 \quad (e)$$

$$\rho(u \frac{\partial u}{\partial x} + v \frac{\partial u}{\partial y}) = \mu \frac{\partial^2 u}{\partial y^2} - \frac{dP}{dx} + \rho g_x \beta (T - T_\infty) \quad (f)$$

$$\rho g c_p (u \frac{\partial T}{\partial x} + v \frac{\partial T}{\partial y}) = k \frac{\partial^2 T}{\partial y^2} + \mu \left(\frac{\partial u}{\partial y} \right)^2 \quad (g)$$

which gives three equations for u, v and T.

Natural flow of a gas over a flat plate, cylinder, etc., is defined as flow which is generated by density gradients created by temperature differences. These flows, of course, exhibit a boundary layer structure dependent on the viscosity and thermal conductivity of the fluid.

Schlichting shows that for a vertical hot plate equation (e), (f) and (g) reduce to

$$\frac{\partial u}{\partial x} + \frac{\partial v}{\partial y} = 0 \quad (h)$$

$$u \frac{\partial u}{\partial x} + v \frac{\partial u}{\partial y} = \frac{\mu}{\rho} \frac{\partial^2 u}{\partial y^2} + g \frac{T_w - T_\infty}{T_\infty} \Theta \quad (i)$$

$$u \frac{\partial \Theta}{\partial x} + v \frac{\partial \Theta}{\partial y} = \frac{k}{\rho c_p} \frac{\partial^2 \Theta}{\partial y^2} \quad (j)$$

where

$$\Theta = \frac{T - T_\infty}{T_w - T_\infty}$$

He further shows

$$\mathcal{I}''' + 3\mathcal{I}\mathcal{I}'' - 2\mathcal{I}'^2 + \Theta = 0$$

$$\Theta'' + 3 N_{PR} \mathcal{I} \Theta' = 0$$

if

$$u = \frac{\partial \psi}{\partial y} \quad v = -\frac{\partial \psi}{\partial x} \quad \eta = \frac{cy}{(x)^{1/4}} \quad \psi = 4\nu C x^{3/4} \mathcal{I}(\eta)$$

$$C = \left[\frac{g(T_w - T_\infty)}{4\nu^2 T_\infty} \right]^{1/4} \quad u = 4\nu x^{1/2} C^2 \mathcal{I}'$$

$$v = \nu C x^{-1/4} (\eta \mathcal{I}' - 3\mathcal{I})$$

where $\Theta(\eta)$ is the temperature distribution. The boundary conditions are

$$\left. \begin{array}{l} \mathcal{I} = \mathcal{I}' = 0 \\ \Theta = 1 \end{array} \right\} \eta = 0 \quad \left. \begin{array}{l} \mathcal{I}' = 0 \\ \Theta = 0 \end{array} \right\} \eta = \infty$$

The solutions of these equations for various values of the Prandtl number are given on page 333 of Schlichting's Boundary Layer Theory. Moreover, the quantity of heat transferred per unit time and area from the plate to the fluid is

$$q(x) = -K \left(\frac{\partial T}{\partial y} \right)_0 = -K C x^{-1/4} \left(\frac{d\theta}{d\eta} \right)_0 (T_w - T_\infty)_0$$

since

$$\left(\frac{d\theta}{d\eta} \right)_0 = -0.508 \quad N_{Pr} = 0.733 \quad \text{The total heat}$$

transferred by a plate of length L and width b is

$$Q_T = b \int_0^L q(x) dx = \frac{4}{3} (0.508) b L^{3/4} C K (T_w - T_\infty)$$

or

$$Q_{\text{total}} = b K N_m (T_w - T_\infty)$$

$$\text{where } N_m = 0.677 C L^{3/4}$$

or

$$N_m = 0.478 N_{gr}^{1/4}$$

$$N_{gr} = \frac{g L^3 (T_w - T_\infty)}{v^2 T_\infty}$$

These calculations are for a heated vertical flat plate; however, Schlichting points out that motion due to natural convection around a horizontal circular cylinder has been treated in a similar manner by R. Hermann. Namely, for $P = 0.7$ the mean heat transfer coefficient N_m is $0.372 N_{gr}^{1/4}$ where N_{gr} is based on the cylinder diameter. Actual measurements in air show that

$$N_m = 0.395 N_{gr}^{1/4}$$

APPENDIX V

For specific comparisons of space configurations A, B, C, D, E, F and G with chamber configurations I, II, III and IV, some stipulation must be made concerning the thermal radiation properties of space suits. Therefore, the following special cases are cited:

SPECIAL CASE (1) Graybody Radiator (ref. 1)

$$\alpha_s = 0.12$$

$$\alpha_h = 0.12$$

SPECIAL CASE (2) Aluminized Nylon Cloth (ref. 22)

$$\alpha_s = 0.16$$

$$\alpha_h = 0.30$$

SPECIAL CASE (3) Polished Aluminum Surface (ref. 30)

$$\alpha_s = 0.3$$

$$\alpha_h = 0.05$$

SPECIAL CASE (4) (Ref. 12)

$$\alpha_s = 0.1$$

$$\alpha_h = 0.05$$

Tables 2, 3, 4, 5 and 6 give the total heat loads for the model in space configurations A, B, C, D and E for various values of space suit absorptivity.

Sample Problem: Determine the total heat absorbed by the cylindrical model in space configuration A (table 2) for special case (1). Select from the column labeled α_s the applicable space suit absorptivity of 0.12. Select from the row labeled α_{hs} the applicable space suit absorptance of 0.12. The intersection of the row corresponding to $\alpha_s = 0.12$ and the column corresponding to $\alpha_{hs} = 0.12$ gives 351 btu/hr, the total heat absorbed by the model in the given space configuration. Thus, the total heat loads absorbed by the model in space configurations A, B, C, D and E are selected from tables 2, 3, 4, 5 and 6 as illustrated above and summarized in table 18. For an illustration, configuration F (Special case 1) is given in table 19, in which $Q(\text{solar})$, $Q(\text{earth})$ and $Q(\text{albedo})$ are given as a function of orbit time.

Equivalent chamber temperatures for the four special cases, space configurations A, B, C, D and E, are determined as follows:

TABLE 18
RADIATIVE HEAT ABSORBED BY THE CYLINDRICAL MODEL
IN SPACE CONFIGURATIONS A, B, C, D AND E FOR SPECIAL
CASES (1), (2), (3) AND (4)

Space Configuration	Total Heat Absorbed (Btu/hr)			
	Special Case (1)	Special Case (2)	Special Case (3)	Special Case (4)
A	301	470	877	203
B	685	1388	1044	438
C	21	30	52	20
D	485	706	1103	383
E	53	72	130	44

TABLE 19
SPECIAL CASE 1P; EARTH ORBIT ANALYSIS

Time (minutes)	Solar (Btu/hr)	Earth (Btu/hr)	Albedo (Btu/hr)	Subtotal (Btu/hr)	Total (Btu/hr)
0	49	52	84	136	185
7	217	52	84	136	383
14	326	52	84	136	468
21	349	52	84	136	485
28	326	52	84	136	468
35	217	52	84	136	383
42	49	52	84	136	185
49	217	52	-	52	269
56	-	52	-	52	52
63	-	52	-	52	52
70	-	52	-	52	52
77	217	52	-	52	269
84	49	52	84	136	185

Select one of the chamber configurations, for instance, chamber III. The heat absorbed by the model in chamber III is given in figure 17. Select the appropriate value of heat absorbed from table 18 and superimpose this value, say 351 but/hr, on figure 17. Follow the vertical line which describes 351 btu/hr to the point where it crosses the applicable space suit absorptivity, say 0.12. The equivalent chamber temperature is read directly from figure 17 and is 548 R.

Specifically, the equivalent chamber temperatures for the four special cases using space configurations, A, B, C, D and E are given in table 20. The equivalent chamber temperatures required for chambers I and III to simulate the given space conditions fall within the actual operating limits of these chambers except for configurations C(1) and C(2). For chambers II and IV configurations B(1), B(2), B(4) and D(4) can be simulated directly. Considering the AMRL facility, chamber configurations A(1), A(2), A(3), A(4), B(1), B(2), B(3), B(4), C(3), D(1), D(2), D(3), D(4) and E(3) can be simulated directly if the upper and lower chamber wall temperatures are maintained at the same value. If the upper and lower wall temperatures are varied similar to chamber IV, space configurations B(1), B(2), B(4) and D(1), D(2), D(4) can be simulated directly.

TABLE 20
EQUIVALENT CHAMBER TEMPERATURE FOR SPACE CONFIGURATIONS
A, B, C, D AND E

Space Configuration	Equivalent Chamber Temperature (R)			
	I	II	III	IV
A (1)	540	640 0	548	680 0
(2)	480	580 0	470	580 0
(3)	548	1000 0	880	1010 0
(4)	648	780 0	680	780 0
B (1)	640	640 638	648	680 640
(2)	582	580 630	600	585 640
(3)	578	1000 670	900	1005 640
(4)	710	780 640	780	775 685
C (1)	288	312 0	288	315 0
(2)	232	288 0	238	270 0
(3)	416	480 0	420	500 0
(4)	328	382 0	328	380 0
D (1)	583	640 508	600	680 510
(2)	510	580 480	520	585 470
(3)	882	1000 720	900	1005 730
(4)	685	780 570	700	775 580
E (1)	337	400 0	340	400 0
(2)	343	340 0	280	345 0
(3)	528	680 0	530	640 0
(4)	400	470 0	400	480 0

APPENDIX VI

SUMMATION OF ASSUMPTIONS

1. Greybody thermal environments with $\alpha = \epsilon$ for at least values of 0.94 and greater approximate blackbody radiators.
2. A man in a space suit in any one of the space configurations will move about, turn around, etc., in an attempt to prevent overheating or cooling of his body in such a manner that the average rate of thermal radiation on the space suit is constant.
3. The spectral distribution of the earth's and the moon's albedo is the same as the sun's incident energy.
4. The earth approximates a blackbody radiator at a temperature of 450 R.
5. At the sub-solar position the moon is a blackbody radiator at a temperature of 710 R.
6. The dark side of the moon is a blackbody radiator at a temperature of 210 R.
7. The earth's albedo is 0.4 ± 0.1 .
8. The moon's albedo is 0.073.
9. A cylindrical model of a 50th percentile "suited" man is used for all calculations.
10. The presence of a space capsule is neglected for all calculations for the heat absorbed by the model in the applicable space configuration.
11. Black space calculations are neglected for space configurations B, D, F and G.
12. The bulk of the thermal radiation incident on the space man falls into two categories:
 - (1) Thermal radiation wavelengths less than 4μ .
 - (2) Thermal radiation wavelengths greater than 4μ .
13. Absorbed heat loads are calculated for values of average absorptance α_s based the short wavelength radiation and α_h based on the higher wavelength radiation.
14. For environmental temperatures greater than the initial surface temperature of the space suit, convection is negligible at a chamber pressure of 0.1 atmospheres.

15. The AMRL chamber is a greybody radiator with a wall absorptance and/or emittance of 0.94 or greater.
16. The air pressure inside the AMRL chamber can be reduced to a point (at least .01 atmospheres) where convection heat transfer is negligible.